JPRS L/10684

26 July 1982

USSR Report

SPACE

(FOUO 3/82)

FBIS FOREIGN BROADCAST INFORMATION SERVICE

NOTE

JPRS publications contain information primarily from foreign newspapers, periodicals and books, but also from news agency transmissions and broadcasts. Materials from foreign-language sources are translated; those from English-language sources are transcribed or reprinted, with the original phrasing and other characteristics retained.

Headlines, editorial reports, and material enclosed in brackets [] are supplied by JPRS. Processing indicators such as [Text] or [Excerpt] in the first line of each item, or following the last line of a brief, indicate how the original information was processed. Where no processing indicator is given, the information was summarized or extracted.

Unfamiliar names rendered phonetically or transliterated are enclosed in parentheses. Words or names preceded by a question mark and enclosed in parentheses were not clear in the original but have been supplied as appropriate in context. Other unattributed parenthetical notes within the body of an item originate with the source. Times within items are as given by source.

The contents of this publication in no way represent the policies, views or attitudes of the U.S. Government.

APPROVED FOR RELEASE: 2007/02/09: CIA-RDP82-00850R000500080058-5

JPRS L/10684

26 July 1982

USSR REPORT

SPACE

(FOUO 3/82)

CONTENTS

MANNED MISSION HIGHLIGHTS

UDC 551.501.71:551.510.61:551.524.7

RESULTS OF INVESTIGATION OF REFRACTION DURING THIRD EXPEDITION IN 'SALYUT-6' ORBITAL STATION

Moscow IZVESTIYA AKADEMII NAUK SSSR: FIZIKA ATMOSFERY I OKEANA in Russian Vol 17, No 11, Nov 81 (manuscript received 3 Feb 81) pp 1123-1133

[Article by G.M. Grechko, A.S. Gurvich, V.A. Lyakhov, S.A. Savchenko and S.V. Sokolovskiy, Institute of Physics of the Atmosphere, USSR Academy of Sciences]

[Text] On the basis of measurements of distortions in the shape of the solar disk during observations made through the atmosphere from space, the authors obtain estimates of variations in refraction. They show that refractive attenuation of light intensity is subject to variations that are several times greater than the average value. On the basis of measurements of refraction, they obtain vertical profiles of density and temperature disturbances in the atmosphere at altitudes of 5-25 km.

Observations made by the first crew of the "Salyut-6" orbital station (OS) showed that refraction in the Earth's atmosphere leads not only to oblateness of the images of the Sun and Moon, but also to the appearance of perturbations--"steps"--on the edge of a heavenly body's visible disk. The amplitude of these perturbations can be so great as to result in a gap in the image. Most interesting was the fact that these severe refractive perturbations were observed not in the layer of atmosphere nearest the ground (which would not have been unexpected [1]), but at levels right up to several altitudes of the uniform atmosphere. This means that the analysis of refraction phenomena during observation of a heavenly body near the horizon must allow not only for the regular decrease in air density with altitude, but also the presence of perturbations existing in the real atmosphere.

On the basis of quantitative processing of the data that were obtained [2,3], as well as a qualitative analysis [4], it was possible to construct a unified picture of refraction phenomena manifested during observations of the Sun and Moon through the real atmosphere from space. The results of these investigations were not only a basis for explaining the previously mentioned effects from a unified viewpoint, but also indicated new possible ways for using refraction phenomena to investigate the atmosphere's structure on the basis of observations of extraterrestrial sources from on board spacecraft.

As the next stage of the investigation of atmospheric refraction, it was necessary to obtain not individual, random photographs of the most characteristic effects, but

series of sequential photographs that overlap in altitude and, in connection with this, improve the resolution in the photographs by choosing better exposure times and photographic materials and improving the optics. After the preliminary work was done, this assignment was given to the third crew on the "Salyut-6" OS, and in this article we present several of the photographs taken on this expedition and the results obtained by processing them.

The third crew of the "Salyut-6" OS photographed the Sun and Moon above the horizon, using a lens with a focal length of 0.5 m, NR-20 film and an exposure time of 1/500 s. The distance ℓ from the OS along the tangent to the Earth's surface was $\sim 2 \cdot 10$ km^3. Figure 1 [omitted] consists of two series of photographs (negatives) of the Sun, each of which was taken during a single setting of the Sun. The outlines of all photographs of the Sun and Moon, which were obtained with an angular resolution of $5 \cdot 10^{-5}$, differ strongly from those calculated on the basis of the model of a standard atmosphere [5], in which only regular oblateness is seen. In the photographs we see the characteristic deformations caused by refraction as steps of greater or smaller size. As a rule, these deformations are maximal in sections of the outline having a 45° inclination to the horizon. The largest deformations in the form of steps are basically symmetrical on the left and right halves of the images, although the fine details do not coincide. All of this indicates that the corresponding refraction perturbations are caused by horizontally layered irregularities in the distribution of the refractive index; thus, the visible displacements of different points in the image occurs basically along the vertical. Such irregularities can play a large role in the distant tropospheric propagation of ultrashort waves [6]. It is also important to note that in many cases the outline deformations have a quasiperiodic structure, which is particularly noticeable (for example) in photographs NR-2-16 and NR-3-17 and -18. This makes it possible to assume that observed deformations of this type are the manifestation of a system of internal waves. Radar investigations of the atmosphere on meter wavelengths also indicate the presence of severaly anisotropic irregularities in the refractive index at altitudes of 8-16 km [7].

The photographs taken of the Sun give the values of the angles of atmospheric refraction on a certain scale. The quantitative processing of the series of photographs was carried out in order to derive from them large-scale variations in the vertical density and temperature profiles and to evaluate the variations in the intensity of a signal from an extraterrestrial point source caused by refraction.

In order to determine the variations in the refractive index's vertical profile on the basis of measurements of refraction angles, in this work it is assumed that in some neighborhood of the perigee of the rays, the atmosphere is spherically symmetrical and that refractive index n depends only on the distance (r) from the origin of coordinates (the center of the Earth). Naturally, this approximation does not encompass all the details that are manifested in the photographs to some degree or another. However, it can be assumed that such an approach does not lead to substantial distortion of the largest details in the vertical structure of air density.

Let us impose a system of angular coordinates on the photographs, using ϕ and χ to designate the zenith and azimuth angles, respectively, of a ray at the observation point. Angle ϕ is read from the local vertical, while angle χ is read from the plane passing through the center of the Sun and the local vertical. Let the outline of the Sun's visible image be described by the equation $\chi = \pm\tau(\phi - \phi_1)$, where ϕ_1 is

the direction of a ray to the Sun's lower edge. Let us designate as ψ the zenith angle of a ray in the case where there is no atmosphere; in connection with this, the outline of the Sun's image would be described by the circumference equation $\psi = \psi_0 \pm (d^2/4 - \chi^2)$, where ψ_0 = direction to the center of the Sun, d = angular diameter of the Sun. Considering that the refraction angle is $\varepsilon = \phi - \psi$, we can write

$$\varepsilon(\varphi)=\varphi-\psi_0\mp[d^2/4-\tau^2(\varphi-\varphi_1)]^{1/2}. \quad (1)$$

Function $\varepsilon(\phi)$, determined in this manner according to the shape of the outline of the Sun's visible image, is known with accuracy up to that of the two constants ϕ_1 and ψ_0, which--generally speaking--can be computed if the relative positions of the Sun, Earth and OS are known at the moment of photographing. However, the surveying was done manually and the photographic equipment was not oriented rigidly relative to the station. Consequently, this method of computing constants ϕ_1 and ψ_0 could not be used. Therefore, in this article we used a method for determining ϕ_1 and ψ_0 according to the Sun's visible vertical dimension d', the theoretical possibilities of which are discussed in [8].

Let us determine the value of ϕ_1 by solving the equation

$$\varepsilon(\varphi_1)-\varepsilon(\varphi_1+d')=d-d', \quad (2)$$

where function $\bar{\varepsilon}(\phi)$ is calculated for a standard atmosphere and a known OS altitude. Let us determine the value of ψ_0 by requiring fulfillment of the natural condition

$$\int_{\varphi_1}^{\varphi_1+d'} [\varepsilon(\varphi)-\bar{\varepsilon}(\varphi)]\,d\varphi=0. \quad (3)$$

When using conditions (2) and (3), it was assumed that observed deviations of refraction from the standard values are small.

Henceforth, instead of ϕ we will use the value of a ray's sighting parameter p = = R sin ϕ, where R is the OS's radius. It should be mentioned here that determining ϕ_1 with the help of (2) essentially ties it not to the sighting parameter's absolute value p_1 = R sin ϕ_1, but to the difference p_1 - a, where a is the Earth's radius. Actually, function $\bar{\varepsilon}(p)$ that is used for the tie-in is computed by the formula

$$\varepsilon(p)=-2p\int_p^\infty \frac{d\ln\bar{n}(x)}{dx}\frac{dx}{(x^2-p^2)^{1/2}}, \quad (4)$$

where x = rn(r). Since refractive index $\bar{n}$ is actually known as a function of altitude z = r - a, function $\bar{\varepsilon}(p)$ (as determined by (4)) depends implicitly on the value of a in such a manner that difference p_1 - a (that is, the rays' altitudinal tie-in, for all practical purposes) proves to only very slightly sensitive to latitudinal variations in the Earth's radius and errors in determining the OS's altitude that are of the same order of magnitude [8]. Besides this, in [8] it is shown that when recovering small-scale density profile perturbations on the basis of measurements of refraction perturbations, a change (within reasonable limits) in the average profile's parameters leads to altitudinal displacements in the small-scale irregularities within limits of $\pm$0.5 km, with small deviations in their shape and amplitude. Among the shortcomings of this tie-in method, we should include the impossibility of determining density variations on scales corresponding to the visible vertical angular size of the Sun.

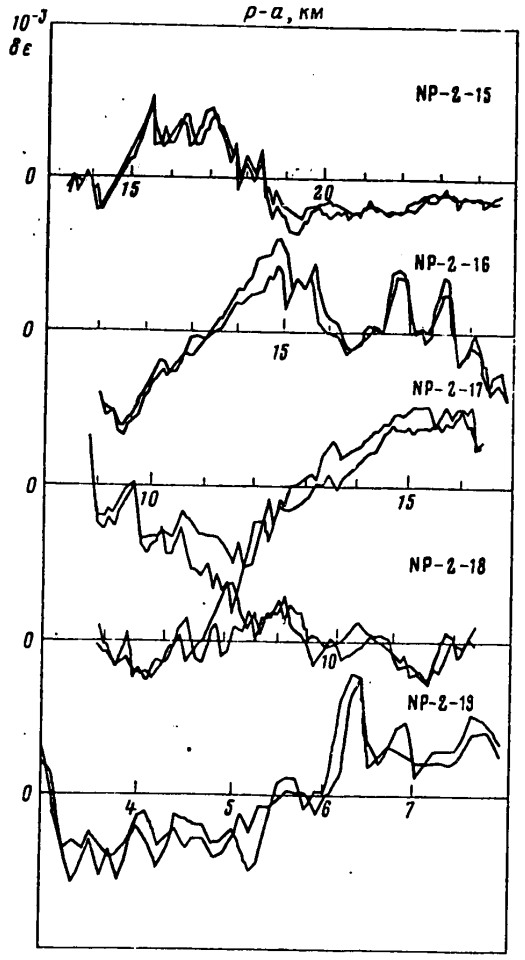

Figure 2. Results of measurements of refraction on the left and right sides of photographs in the NR-2 series.

Figure 2 shows the results of determining refraction variations $\delta\varepsilon(p) = \varepsilon(p) - \bar{\varepsilon}(p)$ for each photograph in the NR-2 series in Figure 1. The functions $\delta\varepsilon(p)$, as computed for the left and right edges of the image, are plotted in the graphs. For the greatest values of p - a (> 22 km), refraction variations are basically the result of errors in the measurement of the shape of the outline of the Sun's image, mainly because of washout of the edge of the image. The refraction distortions are manifested quite clearly at lower altitudes and the differences in fine details between the left and right sides become noticeable. If we take into consideration the fact that the distance between the perigees of the rays connecting the observation point and the ends of the Sun's horizontal diameter is about 20 km, this makes it possible to make a rough estimate of the horizontal dimension of the irregularities in the refractive index.

Using the same scale, in Figure 3 we plotted variations in refraction as computed for all the photographs in each series. So as not clutter up the figure, we used

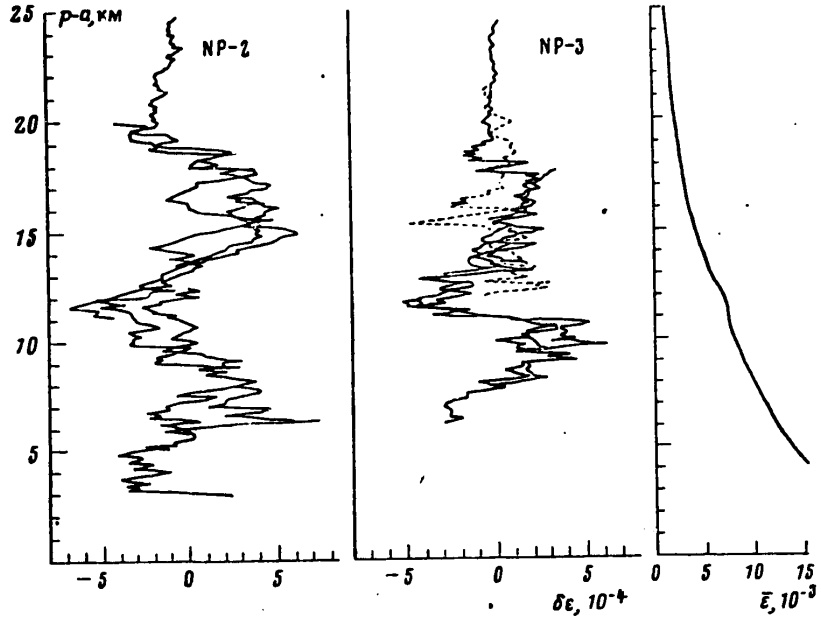

Figure 3. Results of measurements of refraction based on photographs in series NR-2 and NR-3.

the data obtained by processing the left side of each photograph. Comparing Figures 2 and 3, it is obvious that the difference between the variations in refraction, as determined for different photographs in sensing sections that do not overlap as far as altitude is concerned, is greater than for the two sides of a single picture, since the distance between the sensing rays at the same altitude is less at a single moment of time for each of the photographs than for different photographs (as a result of the OS's motion). However (as can also be seen in the graphs in Figure 2), it is worthy of note that the largest-scale changes in refraction in individual photographs basically match each other (photograph NR-3-17 is an exception). In order to show how the deviations of refraction from its standard altitudinal dependence are correlated, in Figure 3 we also give the theoretical refraction values for the standard model of the atmosphere. By comparing the variations in refraction with its standard pattern, it is possible to conclude that the relative changes are sufficiently great so that they can be recorded and used to obtain information about the state of the atmosphere, which was already obvious from the distortions of the outline of the Sun's visible image.

The functions $\delta\varepsilon(p)$ that were obtained on the basis of the processing of the photographs give a visual representation of the actually existing refraction perturbations in the atmosphere. In order to evaluate the magnitude of refraction perturbations having different vertical scales, the $\delta\varepsilon(p)$ functions that were measured for each photograph were smoothed by sliding averaging with respect to some interval of values of sighting parameter Δp. The root-mean-square deviation σ_ε of the original $\delta\varepsilon(p)$ functions from the smoothed ones $\delta\varepsilon(p,\Delta p)$ was then computed:

$$\sigma_\varepsilon^2 = \int_{p_1+\Delta p/2}^{p_2-\Delta p/2} [\delta\varepsilon(p) - \delta\varepsilon(p,\Delta p)]^2 dp/(p_2-p_1-\Delta p), \quad (5)$$

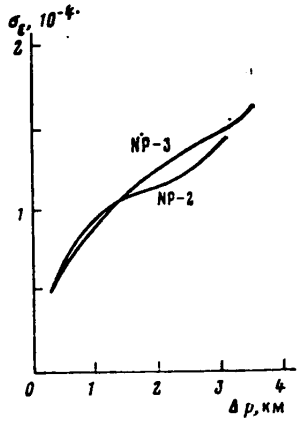

Figure 4. Function $\sigma_\varepsilon(\Delta p)$ for photographs in series NR-2 and NR-3.

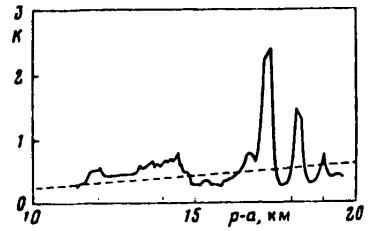

Figure 5. Function K(p) for photograph NR-2-16.

where p_1 and p_2 are the minimum and maximum values, respectively, of the sighting parameter for which function $\delta\varepsilon(p)$ was measured. Figure 4 depicts two functions $\sigma_\varepsilon(\Delta p)$, each of which was averaged for all the photographs in one series. The curve in Figure 4 corresponding to series NR-2 has a bending point, which may indicate the presence of some characteristic scale of refraction perturbations on the order of approximately 2 km. The root-mean-square deviation of the refraction perturbations corresponding to this scale is about 10^{-4} rad.

On the basis of the measurements that were made, it is possible to evaluate the refractive changes in the power of the signal received on board the spacecraft from the extraterrestrial source during observations through the atmosphere. It is necessary to have such estimates in order to make the correct choice of the parameters of the equipment used to study the atmosphere by the radio-occultation method [10]. Ignoring horizontal refraction, we can write refractive attenuation coefficient K for an infinitely remote source as

$$K(p)=|1-ld\varepsilon/dp|^{-1}. \qquad (6)$$

In order to calculate K(p) with the help of (6), it is necessary to differentiate the experimentally determined function $\varepsilon(p)$. In order to improve the stability of the obtained result, the experimental data in which the values of ε were obtained with a step $\Delta p = 0.1$ km were smoothed by sliding averaging with respect to the interval $\Delta p = 0.5$ km and the smoothed result was used to calculate coefficient K(p). The graph in Figure 5, in which the results of the calculation of K(p) for photograph NR-2-16 are presented as an example, shows that the changes in signal power can exceed 100 percent. This is obviously the bottom estimate, since the calculation of K(p) on the basis of the smoothed function $\varepsilon(p)$ leads to understatement of the values of K. If the variations in ε are so great that they result in interruption of the image, interference pulses that are the result of multiray propagation will also be observed during the reception of the monochromatic signal.

The mentioned change in signal power because of refraction variations is a cause of variations in the shining of stars and planets when they are observed through the atmosphere from on board spacecraft [9] that is different from the one discussed in [11]. The data obtained about the structure of irregularities in the refractive index and the estimates of the variations in refractive attenuation can be useful when investigating planetary atmospheres on the basis of observations from Earth of changes in the amplitude and frequency of the radio signal during occultation of automatic interplanetary stations [12] or the shining of stars as they move behind

planets [13]. The data obtained in this work also indicate that it is necessary to allow for refractive attenuation when investigating atmospheric transparency on the basis of observations from spacecraft. Significant variations in refraction can lead to a noticeable redistribution of the light field's intensity in the atmosphere itself, which--naturally--can affect the results of observations of aerosol scattering.

After the dependence of refraction on the sighting parameter has been determined on the basis of photographs, in an approximation of a spherically symmetrical atmosphere it is possible to proceed to the recovery of the refractive index's vertical profile [8].

Refraction $\varepsilon(p)$ and the refractive index $n(r)$ are related by the integral relationship

$$\varepsilon(p)=-2p\int_p^\infty \frac{d\ln n(x)}{dx}\frac{dx}{(x^2-p^2)^{1/2}}, \tag{7}$$

where $x = rn(r)$. When the variables are replaced ($x^2 = u$, $p^2 = v$) in equation (7), the result is an integral equation of the Abel type [14]:

$$\frac{\varepsilon(v)}{2\sqrt{v}}=-\int_v^\infty f(u)\frac{du}{\sqrt{u-v}} \tag{8}$$

relative to the unknown function $f(u) = d \ln n/du$. It is not difficult to write a formal solution of Abel's equation, and since in the future we will need the refractive index instead of function $f(u)$, by omitting the intermediate calculations let us write the expression that is derived for it, having returned to the old variables:

$$n(x)=\exp\left[\frac{1}{\pi}\int_x^\infty \frac{\varepsilon(p)}{(p^2-x^2)^{1/2}}dp\right], \quad \varepsilon=\varepsilon+\delta\varepsilon. \tag{9}$$

Mathematically, the solution of equation (8) for $f(u)$ is a poorly stipulated problem. However, since $n(u)$ is derived as the result of integrating function $f(u)$, in the final account the determination of $n(x)$ from equation (8) on the basis of measurements of $\varepsilon(p)$ is a mathematically correct problem that is not difficult to verify by using the definition in [15] and formula (9). The solution of (9) gives the values of refractive index n as a function of $x = rn(r)$, and the conversion to a dependence on altitude $z = r - a$ presents no difficulties. In order to calculate $n(x)$ on the basis of measured function $\varepsilon(p)$ with the help of (9), the integration interval was divided into two parts: $x < p_{max}$ and $x > p_{max}$, where p_{max} is the maximum value of the sighting parameter for which $\delta\varepsilon(p)$ can be determined from the photographs. For the calculations, experimental data were used for $x < p_{max}$, while the model of the standard atmosphere was used for $x > p_{max}$. Since refraction diminishes exponentially with altitude, the error from this replacement is sunstantial only in the upper part of the recovered profile of $n(x)$.

As the original experimental material, we used the functions $\delta\varepsilon(p)$ shown in Figure 6, which were obtained by averaging for all the photographs in each series (except for NR-3-17) and encompass a correspondingly large interval of altitude values. Recovery of the refractive index values on the basis of the averaged function $\delta\varepsilon(p)$

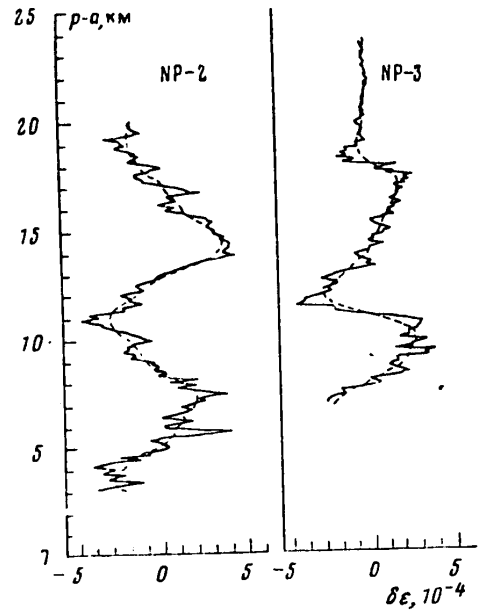

Figure 6. Averaged results of refraction measurements.

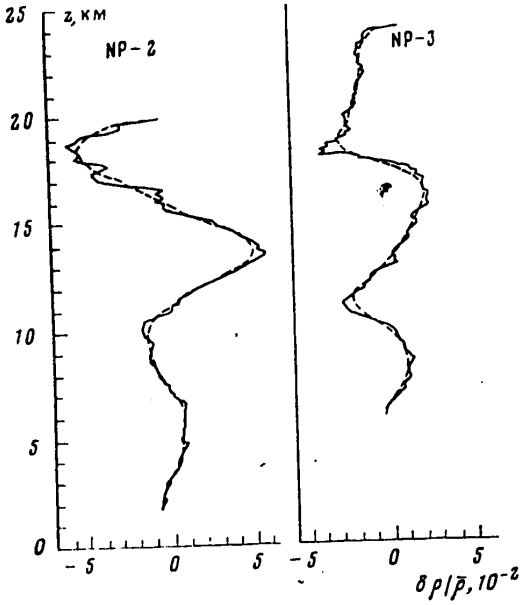

Figure 7. Results of recovery of density profiles.

made it possible (to a certain degree) to allow for refraction variations in the upper layers of the atmosphere for which there would not have been data if each photograph had been used separately. In addition to this, the conversion to averaged functions $\delta\varepsilon(p)$ apparently reduces the effect of irregularities not allowed for in the model of the spherically symmetrical atmosphere. The method used to tie in the rays results in a situation where refraction variations with a vertical scale greater than the difference in the altitudes of the perigees of the rays from the ends of the Sun's vertical diameter turn out not to be allowed for to a certain degree.

In the optical band, the refractive index of air depends only on density ρ [16]:

$$n = 1 + c\rho \qquad (10)$$

and, consequently, $\delta n = c\delta\rho$, while for light on wavelength 0.7 μm, $c = 2.25 \cdot 10^{-4} \cdot \text{kg}^{-1} \cdot \text{m}^3$. In order to obtain a more visual idea of the recovery of meteorological elements on the basis of measurements of refraction, Figure 7 depicts the dependences of the relative variations in density on altitude for the two series of photographs presented in Figure 1. In order to demonstrate with the experimental material the correctness of the mathematical problem of recovering the refractive index's (density's) vertical profile on the basis of measurements of variation in refraction, in Figure 7 we present the variations in $\delta\rho/\bar{\rho}$, calculated both on the basis of function $\delta\varepsilon(p)$ that was determined from the experiment with a step $\Delta p = 0.1$ km (solid line) and the same function that had been preliminarily smoothed by sliding averaging in the interval $\Delta p = 1.5$ km (broken line). A comparison of these two curves shows that the presence of small-scale variations in function $\delta\varepsilon(p)$ does not lead to variability in the results of the recovery of $\delta n(z)$, thereby confirming the mathematical correctness of the problem.

If function $\rho(z)$ is known, by using the equations of state of an ideal gas and static equilibrium, it is not difficult to also obtain the dependence of temperature T

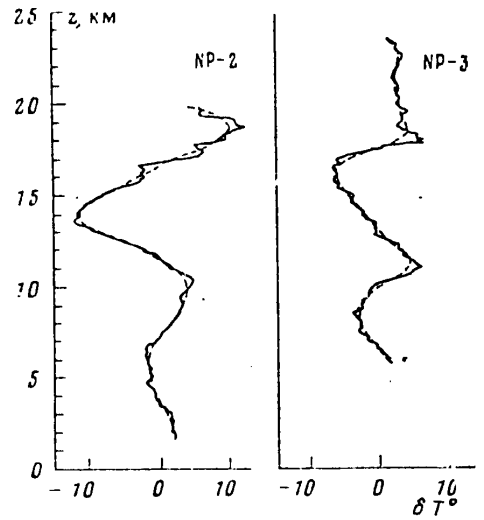

Figure 8. Results of recovering temperature profiles.

on altitude:

$$T(z)=\frac{Mg}{R\rho(z)}\int_{z}^{\infty}\rho(z')dz',\quad \rho=\bar{\rho}+\delta\rho, \tag{11}$$

where g = gravitational acceleration; M = = molecular weight of air; R = universal gas constant. Figure 8 depicts the altitudinal pattern of temperature variations $\delta T(z) = T(z) - \overline{T}(z)$. as calculated on the basis of variations in the altitudinal profiles of air density $\delta\rho(z)$ that were obtained from refraction measurements.

The results of calculations of variations in the vertical density and temperature profiles that we have presented indicate convincingly the extensive possibilities for using refraction phenomena for remote probing of the atmosphere. The use of the Sun and Moon as extensive sources, followed by the simultaneous registration of the positions of several stars, will make it possible to study the spatial features of atmospheric refraction. One of the first problems will be to explore the possibility of distinguishing the averaged vertical profiles of meteorological elements against a background of comparatively small-scale variations, which is a matter of interest for meteorological purposes. Investigations of the variations will apparently make it possible to study complex wave processes, the following of which in the atmosphere still presents considerable difficulty when using ground facilities. Improvement of the resolution of refraction measurements will make it possible to obtain information about the atmosphere at high altitudes and change over to the remote observation of turbulence in the troposphere.

In conclusion, the authors wish to thank A.M. Obukhov for his constant attention and their colleagues for their assistance in preparing for and conducting these investigations.

BIBLIOGRAPHY

1. Minnart, M., "Svet i tsvet v prirode" [Light and Color in Nature], Moscow, Izdatel'stvo "Nauka", 1969, 344 pp.

2. Grechko, G.M., Gurvich, A.S., Romanenko, Yu.V., Savchenko, S.A., and Sokolovskiy, S.V., "Vertical Structure of the Temperature Field in the Atmosphere, Based on Observations of Refraction From the 'Salyut-6' Orbital Station," DOKL. AN SSSR, Vol 248, No 4, 1979, pp 828-831.

3. Grechko, G.M., Gurvich, A.S., Romanenko, Yu.V., Sokolovskiy, S.V., and Tatarskaya, M.S., "Layered Structure of the Temperature Field in the Atmosphere, Based on Measurements of Refraction From the 'Salyut-6' Orbital Station," IZV. AN SSSR: FAO, Vol 17, No 2, 1981, pp 115-122.

4. Grechko, G.M., and Romanenko, Yu.V., "On the Horizontal Irregularity of the Earth's Atmosphere's Brightness Field," in "Issledovaniya atmosferno-opticheskikh yavleniy s borta orbital'noy nauchnoy stantsii 'Salyut-6'" [Investigations of Optical Atmospheric Phenomena From the "Salyut-6" Orbital Scientific Station], Tartu, 1979, pp 122-132.

5. Cameron, W.S., Glenn, J.H., Carpenter, M.S., and O'Keefe, J.A., "Effect of Refraction on the Setting Sun as Seen From Space in Theory and Observation," ASTRON. J., Vol 68, No 5, 1963, pp 348-351.

6. Vvedenskiy, B.A., editor, "Dal'neye troposfernoye rasprostraneniye UKV" [Distant Tropospheric Propagation of Ultrashort Waves], Moscow, Izdatel'stvo "Sovetskoye radio", 1965, 415 pp.

7. Gage, K.S., and Green, J.L., "Evidence for Specular Reflection From Monostatic VHF Radar Observations of the Stratosphere," RADIO SCI., Vol 13, No 6, 1978, pp 991-1001.

8. Sokolovskiy, S.V., "On Recovering Perturbations in the Density Profile in the Atmosphere on the Basis of Measurements of Refraction From an Artificial Earth Satellite," IZV. AN SSSR: FAO, Vol 17, No 6, 1981, pp 574-580.

9. Grechko, G.M., Gurvich, A.S., and Romanenko, Yu.V., "Structure of Density Irregularities in the Stratosphere, Based on Observations From the 'Salyut-6' Orbital Station," IZV. AN SSSR: FAO, Vol 16, No 4, 1980, pp 339-344.

10. Lusignan, B., Modrell, G., Morrison, A., Pomalaza, J., and Unger, S.G., "Sensing the Earth's Atmosphere With Occultation Satellites," PROC. IEEE, Vol 57, No 4, 1969, pp 458-467.

11. Kan, V., "On Evaluating Density Variations in the Stratosphere on the Basis of Observations of the Flickering of Stars," IZV. AN SSSR: FAO, Vol 17, No 8, 1981, pp 755-757.

12. Kliore, A., Levi, G.S., Cain, D.L., Fjeldbo, G., and Rassool, S.J., "Atmosphere and Ionosphere of Venus From the Mariner-V S-Band Radio Occultation Measurement," SCIENCE, Vol 158, No 3809, 1967, pp 1683-1688.

13. Veverka, J., Wasserman, L.H., Elliot, J., Sagan, C., and Liller, W., "The Occultation of β-Scorpii by Jupiter," ASTRON. J., Vol 79, No 1, 1974, pp 73-84.

14. Yutteker, E.T., and Vatson, D.N., "Kurs sovremennogo analiza" [Course in Contemporary Analysis], Moscow, Izdatel'stvo "Fizmatgiz", Vol 2, 1963, 515 pp.

15. Tikhonov, A.N., and Arsenin, V.Ya., "Metody resheniya nekorrektnykh zadach" [Methods for Solving Incorrect Problems], Moscow, Izdatel'stvo "Nauka", 1979, p 16.

16. "Spravochnik po geofizike" [Handbook on Geophysics], Moscow, Izdatel'stvo "Nauka", 1965, 571 pp.

11746
CSO: 1866/37

LIFE SCIENCES

UDC: 613.693+612.3

SPACE GASTROENTEROLOGY: TROPHOLOGICAL ESSAYS

Moscow KOSMICHESKAYA GASTROENTEROLOGIYA: TROFOLOGICHESKIYE OCHERKI in Russian 1981 (signed to press 30 Jun 81) pp 4-7, 11-12

[Annotation, foreword by Academician O. G. Gazenko and table of contents from book "Space Gastroenterology: Trophological Essays" by Konstantin Vladimirovich Smirnov and Aleksandr Mikhaylovich Ugolev, Department of Physiology, USSR Academy of Sciences, Izdatel'stvo "Nauka", 2400 copies, 278 pages]

[Text] This book defines the subject and methods of a new direction of space biology and medicine, space gastroenterology. For the first time, the results of investigations of the digestive organs, obtained from clinical and physiological examination of cosmonauts, who were crew members aboard the Soyuz series spacecraft and Salyut-Soyuz orbital complexes, were synthesized and analyzed. There is comprehensive discussion of the findings from studies of the digestive system of animals flown aboard biological earth satellites of the Cosmos series. Model studies established the functional phenomenology of the human and animal digestive system with exposure to hypokinesia and accelerations; there was demonstration of adaptability to the onboard diet of cosmonauts; some mechanisms of digestive organ reactions to spaceflight factors are discussed. In the final part, the prospects of development of space gastroenterology are discussed. This book is intended for specialists in the field of space biology and medicine, clinical and theoretical gastroenterology, physicians, biologists and physiologists. Tables 7, figures 87, references cover 37 pages.

Foreword

Among the problems of space biology and medicine, physiology of nutrition and digestion had remained in the shadows until recently. However, as the flights into space are changing into man's existence under unique ecological conditions for increasing periods of time, problems of nutrition and digestion are growing increasingly important and, to some extent, limiting. When the first space flights were planned and even made, most attention was given to the so-called technological aspect of organizing man's nutrition. It appeared that the main difficulties consisted of finding the most suitable means of taking meals under weightless conditions, making up rations, preserving foods, heating them, etc. As time passed, many of these problems were resolved, although some require further refinement. At the same time, it was found that man's

reactions to spaceflight conditions and factors involved changes in different aspects of metabolism. Moreover, these metabolic changes acquire importance to a man's general condition, his tolerance of stress situations and work capacity.

The practice of manned spaceflights put to space biology and medicine the task of comprehensive study of the digestive system which, as we know, is the active apparatus of metabolism in the body, a system through whose multifaceted function there is not only hydrolysis and transport of nutrients, but correction of metabolism.

The extensive data accumulated by researchers, both during space flights and in ground-based laboratory studies, require systematization and analysis. For this reason, it should be considered quite valid for a fundamental survey to be published on matters of space gastroenterology.

We cannot help but experience much satisfaction with the fact that this book was published in our country and written by scientists who participated in our joint work for many years. We should like to stress in particular the unquestionable timeliness and novelty of the monograph. The main material in this book is original. The research dealing with the effects of spaceflights on functioning of the human and animal digestive system is really unique. The monograph has not only applied value, but is of great importance to theoretical gastroenterology.

There is no need to specially introduce the authors of this work, who have been long known as major specialists in their field. It should be stressed that collaboration between laboratories of the Institute of Biomedical Problems, USSR Ministry of Health, and Institute of Physiology imeni I. P. Pavlov, USSR Academy of Sciences, is an excellent example of combining applied and basic research, which has already benefited practice and enriched gastroenterology with basic information.

We hope that the book will be useful to a wide range of specialists in space biology and medicine, physiologists and gastroenterologists. Since the work being offered to the attention of readers is the first attempt at an overview in this branch of science, while this area of research is developing rapidly and quite successfully on its own, it is hoped that there will be a need for another analysis and generalization of accumulated data after some time.

Contents Page

10,657
CSO: 1866/81

UDC: 612.821.6+613.693

FORMATION OF COMPLEX BEHAVIOR SKILLS IN ALBINO RATS AFTER EXPOSURE TO ARTIFICIAL GRAVITY ABOARD 'COSMOS-936' BIOSATELLITE

Moscow ZHURNAL VYSSHEY NERVNOY DEYATEL'NOSTI IMENI I. P. PAVLOVA in Russian Vol 31, No 3, May-Jun 81 (manuscript received 12 May 80) pp 564-569

[Article by N. N. Livshits, Z. I. Apanasenko, M. A. Kuznetsova and Ye. S. Meyzerov, Moscow]

[Text] Our objective here was to study the behavioral distinctions of albino rats during formation of complex labyrinth skills at the relatively long term (18-24 days) after landing of the biosatellite, aboard which artificial gravity was created. The flight conditions and centrifuge parameters for creating artificial gravity were described in the article by Ye. A. Il'in et al. [2]. In addition, problem solving in the mazes we used required rather fine spatial orientation. Both these factors (complicating the tasks and increased demands of spatial orientation) increased the sensitivity of the method to changes due to the effects of accelerations and angular velocities related to creation of artificial gravity.

Methods

The work was done with the same rats as in experiments with the use of relatively simple maze problems. The arbitrary designations of groups, information about distribution of animals in them and characteristics of factors are listed in Table 1.

By the time this study was conducted, there was complete normalization of alimentary excitability of the animals and it could not have an appreciable effect on the results.

Test problems were presented to the animals in two different mazes.

On the 18th-22d day after landing, we developed in the rats the skill of finding food in the maze, which precluded the possibility of retracing a previously traveled route. The maze was proposed in 1971 by S. Lachman [9], and it consisted of a starting compartment, viewing platform and three lanes giving off from it, closed by doors that prevented return to the viewing platform.

Table 1. Experimental conditions

Exposure conditions		Group designation	Rats per group	Acceleration, G	Angul. veloc., rad	Scope of experiments
On Cosmos-936	Stationary	FW_3	5	0	0	Complete (all methods)
	Centrifuge (r = 320 mm)	FC_2	5	1	5.3	Same
Mock-up on earth	Stationary	SW_3	5	1	0	Same
	Centrifuge (r = 320 mm)	SC_2	4	1.4	5.3	Reduced (only for HNA)
	(r = 98 mm)	C_2^0	4	1.1	5.3	Complete (all methods)
Vivarium	Main group	VC	6	1	0	Same
	Additional group	VC_a	18	1	0	Partial (one-third of methods)
	Intact group (without implanting sensors)*	VC_i	9	1	0	Reduced (only for HNA)

*Temperature sensors were implanted in the abdominal cavity of animals in the other groups.

During the experiment, the animal was given feed only when it first went in a passage. A second appearance in the same passage was considered a mistake and no food reinforcement was used. The experiment continued until the rat had been in all three passages. If the rat did not move from the starting place for 3 min or remained motionless on the viewing platform, it was considered to have refused to "solve" the proposed problem. The experiment was stopped if there were three successive refusals. It was considered that the rat "did not solve" the problem in such an experiment.

During the experiment, we recorded the number of correct and wrong runs, number of refusals and time spent by the rat to pass from the starting compartment into a passage.

Another rather complex maze, which was developed in our laboratory, was used on the rats on the 23d and 24th days after the flight. The system of passages, locked and unlocked doors, open gates and dead-ends enabled the animals to reach their goal over several possible routes. On each of these days, the maze test was used three times. We recorded the number of refusals to solve the problem, distance of the route used and time spent to travel it from the starting compartment to the additional feeding place. The length of the route was determined by the number of working units ("steps") of the maze that were traversed. Each "step" was 10 cm in size and the optimum variant of the route consisted of 10 "steps."

All of the results were submitted to statistical processing using the criterion proposed by N. A. Plokhinskiy [7] for comparing two regression series.

Results and Discussion

Analysis of our data revealed that development of the behavior algorithm in Lachman's maze was easier for the groups of animals that were not rotated on the centrifuge. Animals flown on the biosatellite showed virtually no difference from either the main vivarium or mock-up control (not submitted to rotation).

Difficulty in developing this skill was observed only in centrifuged animals.

The number of tests in which the animals coped well with their problem was appreciably smaller in the FC_2, SC_2 and C_2^0 groups than in the FW_3, VC ($P<0.05$) and SW_3 groups ($P<0.01$; Table 2).

Table 2. Mean parameters of rat behavior throughout period of working in Lachman maze

Parameters	Control				Flight experiment	
	Animal groups					
	VC	SW_3	SC_2	C_2^0	FW_3	FC_2
Experiments (%) in which problem was solved	79	100	62	69	85	45
Time spent to enter into passage from starting point, s	31	49	42	46	30	67

The most serious disturbances were noted in animals submitted to rotation in flight. The changes in this parameter were the most marked in this group, although the differences between them and C_2^0 and SC_2 were unreliable.

Table 3. Mean parameters of rat behavior in Lachman maze in experiments where problem was not solved

Parameters	Control		Flight experim.	
	Animal groups			
	SC_2	C_2^0	FW_3	FC_2
Number of attempts at solving problem	7	4	5.8	3.5
Failures (%) of these attempts	55	70	48	82

The FC_2 group of animals spent reliably more time ($P<0.05$) on choosing a passage in each run than all other groups (Table 2).

The same animals were also notable for less activity in attempting to cope with their task. They presented fewer attempts at solving the problem (Table 3), although this was unreliable, and moreover most of them failed; failure of such attempts occurred in appreciably fewer instances in other groups of animals. The differences for this criterion from SC_2 and FW_3 groups were reliable with $P<0.01$ and from C_2^0 with $P<0.05$.

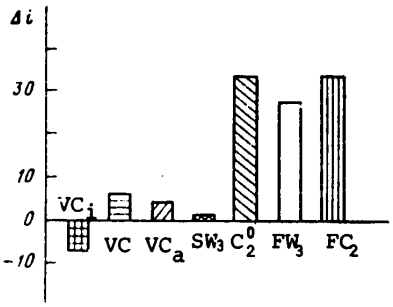

Figure 1.
Change in number of failures in the complicated maze on 2d experimental day, as compared to 1st, %. Group designations are the same as in Table 1

The group of animals exposed to angular velocity (C_2^0) on the ground had considerably less difficulty in the Lachman maze. They solved the presented problem in an appreciably higher percentage of cases (differences from the FC_2 group are unreliable) and manifested somewhat greater activity in trying to solve it. Although they made just as few attempts in the experiment with unsolved problem as the FC_2 group, as we have already mentioned, they failed in a reliably lower percentage of cases.

Among the animals submitted to centrifuging, the SC_2 group had the least difficulty in assimilating the proposed algorithm. They showed virtually no difference from the C_2^0 group with regard to number of tests where the problem was solved. However, they differed from both groups described above in that they displayed considerably more activity in attempting to solve the problem. In the experiments with unsolved problem, more attempts were made at solving it, and they ended with failure in an appreciably smaller number of cases. The differences in number of failures were reliable with $P<0.05$, as compared to the C_2^0 group and $P<0.01$, as compared to the FC_2 group.

Analysis of rat behavior in the complex maze revealed that it was the most difficult for the FC_2 and C_2^0 groups of animals.

Table 4. Mean parameters of performance of different groups of animals in complicated maze

Parameters	Experimental groups					
	VC	FW_3	FC_2	SW_3	SC_2	C_2^0
Failures, %	2,8	13,3	36,7	0	0	41,7
Number of steps	62,6	95,2	137,0	86,6	84,8	103,8
Time, s	63,4	128,3	201,0	81,1	78,1	131,0

As can be seen in Table 1, expressly these animals refused to solve the problem much more often, they chose the longest route to their goal and spent more time on it. The changes in the FC_2 group of rats were more significant than in C_2^0. The former animals differed from the main vivarium control group for all three of the above-mentioned parameters ($P<0.001$ in all cases). The differences from the control were unreliable in the C_2^0 group for length of route and time, but this group of rats refused to solve the problem more often than all others ($P<0.001$).

The animals in the FW_3 group presented poorer behavior parameters in the complex maze than the control ($P<0.01$ for distance and time). However, the changes were

less significant (particularly in number of failures) and were manifested at a later time than in the FC_2 group. No appreciable differences from the control were demonstrated in the SW_3 and SC_2 groups for any of the tested parameters ($P>0.05$).

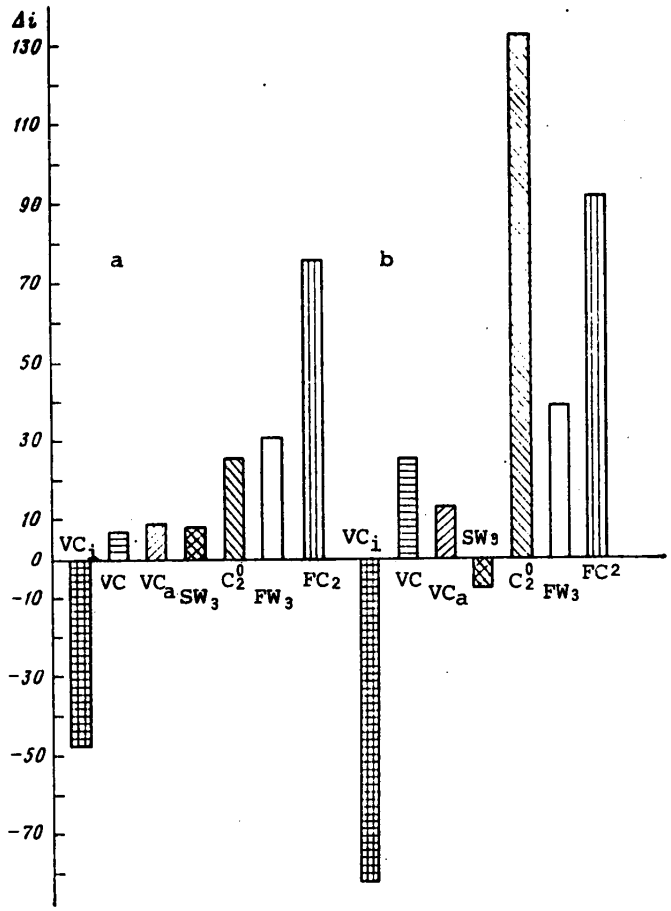

Figure 2. Changes in number of "steps" (a) and time (b) of passage through complex maze on 2d experimental day, as compared to the 1st. Group designations are the same as in Table 1.

It should also be noted that virtually all of the animals, with the exception of the intact control group--VC_i--failed to perfect skill in solving the problem in the complex maze during the experiment. As a rule, the parameters were worse on the 2d day of performance than on the 1st (Figures 1 and 2). A negative difference (Δ_i) was demonstrated between parameters for the 2d and 1st experimental days only in unoperated control animals (VC_i). Performance

deteriorated the most on the 2d experimental day also in the FC_2 and C_2^0 groups of animals. The FW_3 group presented less worsening. The difference from the control (VC) in this criterion (Δ_i) was statistically unreliable (with the exception of the FC_2 group), but the above tendency was consistently manifested and very distinct.

Our findings warrant the statement that weightlessness and readaptation factors did not have an appreciable influence on performance in the Lachman maze and complex maze on the 18th-24th postflight day. There were very insignificant changes in the FW_3 group. We had already made a similar finding after flying rats with implanted foreign bodies aboard the Cosmos-782 biosatellite, where it was assessed as the result of the combined effect of flight factors and surgical intervention.

The difficulties that rats in the FC_2, C_2^0 and, in some cases, SC_2 groups experienced in the test indicate that centrifuging worsened their problem-solving capacity in such complex mazes. The adverse effect of the centrifuge was the most marked in the FC_2 group. Since the gravity experienced by animals submitted to centrifuging was close to that of earth, it may be assumed that angular velocity was the most active factor here. The presence of appreciable deviations in the C_2^0 group of animals confirms this assumption.

The most significant changes in behavioral reactions of the FC_2 group are probably attributable to the fact that the influence of angular velocity was not obscured in the set of flight factors, rather it was somewhat intensified. Apparently, it is for expressly this reason that we were unable to demonstrate a beneficial effect of artificial gravity, according to the criteria we scudied.

On the contrary, centrifuging animals aboard the spacecraft aggravated the adverse changes in their higher nervous activity (HNA).

The characteristics of behavioral reactions of animals in the SC_2 group differed when solving different problems. Some additional factors that appeared for technical reasons (greater alimentary motivation after a period of undereating, minimal burden referable to experimental examinations, etc.) distorted the effect of the factor. Nevertheless, here too, the adverse effect of angular velocity was distinctly evident in some tests.

Thus, it is apparently expressly angular velocity that determined the direction of changes in HNA parameters in our experiments. Studies of other authors also reported poorer HNA reactions with exposure to angular velocities [1, 3, 4, 6, 8].

Our findings warrant the statement that the effect of the above factor is more demonstrable when animals perform more difficult tasks which make greater demands of analytical and synthetic function of the brain.

When working in a simple maze, even at earlier postflight stages, HNA characteristics of centrifuged animals were not always manifest and to a lesser extent [5] than when working in complicated mazes at later stages.

Since the influence of angular velocity is implemented through the vestibular analyzer, it is also obvious that the greater the fine spatial orientation involved in solving the presented problem, the greater the difficulties the animals experienced.

Conclusions

1. Centrifuging rats aboard a spacecraft worsened their postflight capacity to learn new algorithms of behavior in mazes of the design used here.

2. The absence of beneficial effect of artificial gravity is apparently related to the fact that this effect is canceled out by the adverse effect on higher nervous activity of angular velocities during centrifuging.

BIBLIOGRAPHY

1. Vasil'yev, P. V. and Kotovskaya, A. R., "Prolonged Linear and Radial Accelerations," in "Osnovy kosmicheskoy biologii i meditsiny" [Fundamentals of Space Biology and Medicine], Moscow, Nauka, Vol 2, Bk 1, 1975, p 177.

2. Il'in, Ye. A., Korol'kov, V. I., Kotovskaya, A. R., Noskin, A. D., Kondrat'yeva, V. A., Shipov, A. A. and Britvan, I. I., "Objectives and Conditions of Physiological Experiments on Rats Aboard the Cosmos-936 Biosatellite," KOSMICH. BIOL. I AVIAKOSMICH. MED., Vol 13, No 6, 1979, p 18.

3. Kislyakov, V. A., "Effect of Rotation on Conditioned Food Reflexes of Dogs," TR. IN-TA FIZIOL. IM. I. P. PAVLOVA, Vol 5, 1956, p 156.

4. Klimovitskiy, V. Ya., Livshits, N. N. and Rodionov, M. I., "Systemic and Cerebral Hemodynamics and Central Nervous System Function Under the Effect of Accelerations. A Literature Survey," in "Nekotoryye voprosy kosmicheskoy neyrofiziologii" [Some Problems of Space Neurophysiology], Moscow, Nauka, 1967, p 57.

5. Livshits, N. N., Apanasenko, Z. I., Kuznetsova, M. A. and Meyzerov, Ye. S., "Effect of Artificial Gravity During Space Flight on Integrity of Motor Skills of Albino Rats," ZH. VYSSH. NERVN. DEYAT., Vol 31, No 2, 1981, p 261.

6. Nudman, S. I., "Effect of Rotation Conditioning on Conditioned Motor Reflexes of Rats," Ibid, Vol 14, No 5, 1964, p 885.

7. Plokhinskiy, N. A., "Biometry," Moscow, MGU [Moscow State University], 1970.

8. Savin, B. M., "Hypergravity and Nervous System Functions," Leningrad, Nauka, 1970.

9. Lachman, S. J., "Behavior in Complex Learning Situations Involving Three Levels of Difficulty," J. PSYCHOL., Vol 77, No 1, 1971, p 119.

10,657
CSO: 1840/200

UDC 629.78:612.398.145.1.014.24:576.315.42

INFLUENCE OF SPACE FLIGHT FACTORS ON STRESS REACTION OF NUCLEIC ACIDS IN RAT LIVER NUCLEI

Moscow DOKLADY AKADEMII NAUK SSSR in Russian Vol 260, No 1, Sep 81 (manuscript received 7 Apr 81) pp 236-239

[Article by G. S. Komolova and Ye. N. Troitskaya, Institute of Biochemistry imeni A. N. Bakh, USSR Academy of Sciences]

[Text] Prolonged chronic stress or injection of glucocorticoid hormones into the body elicits significant changes in the metabolism of target organs (lymphoid organs, liver, muscles). There are grounds for suggesting that changes in the nucleic acid system play an important role in these processes (1). In times of long space flight the animal body experiences both acute stresses (for example during launching and landing of the spacecraft) and chronic stress elicited primarily by weightlessness. Our objective was to study the stress reaction of nucleic acids in the animal liver following space flight. The experiments were conducted on Wistar line male rats weighing about 300 gm. The space flight lasted 18.5 days aboard the biosatellite Cosmos-1129. Animals maintained in a vivarium on the same diet as experimental animals served as the control. In a synchronous variant of the experiment we simulated the dynamic factors of space flight (except for weightlessness), and the animals were maintained in the same life support systems as in space flight.

In each variant of the experiment the animals were divided into three groups depending on the time of killing: 1--6 hours after termination of the experiment; 2--6 days after; 3--6 days after, but the rats were immobilized for 2.5 hours on days 0, 3, 4, 5 and 6. The reactivity of the analyzed nucleic acid systems was determined on the basis of the reaction to this additional stress. Nuclei were isolated from liver tissue by Chauveau's method (2). To determine the intensity of DNA biosynthesis, nuclei were incubated at 37°C for 15 minutes in a medium having the following ingredients: 47 mM tris-HCl (pH 8.0), 5 mM HCl_2, 15 mM KCl, 7.7 mM mercaptoethanol, 1.6 mM ATP, 0.08 mM each of deoxytriphosphates (dATP, dGTP, dCTP), 0.02 mM ^{3}H-TTP (specific activity following dilution with unlabeled TTP was 280 millicuries per millimole). The reaction was halted with perchloric acid. Following repeated washing, the obtained precipitate was hydrolyzed for 20 minutes at 90°C in 0.5 N $HClO_4$. The radioactivity of the hydrolyzates was analyzed using a toluol scintillation mixture containing triton X-100. The radioactivity of the samples was measured in an SL-400 liquid scintillation counter (made in France). Transcription in liver nuclei was studied by a method described earlier in (3). The unit radioactivity of nucleic acids was calculated (pulses per minute per microgram). The concentration of DNA and RNA in nuclei was determined spectrophotometrically. In all variants of the experiments the results obtained with animals in groups 2 and 3 were expressed as percentages of the results obtained for animals in group 1.

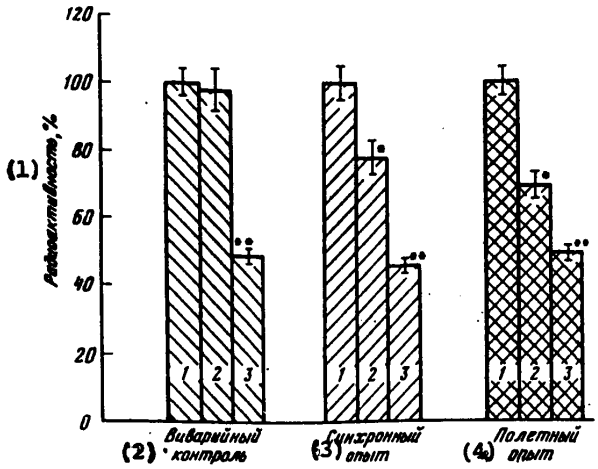

Figure 1. Intensity of DNA Biosynthesis in Isolated Liver Nuclei (*M±m*): Animal groups 1-3 (labeled correspondingly *1-3*). In variant *3* rats were immobilized for 2.5 hours on days 0, 3, 4, 5 and 6. A single asterisk indicates significant differences with respect to *1*; two asterisks indicate significant differences with respect to *2*

Key:
1. Radioactivity, %
2. Vivarium control
3. Synchronous experiment
4. Flight experiment

The results of our research on the intensity of DNA biosynthesis in isolated liver cells are shown in Figure 1. It follows from the obtained data that for vivarium control animals, DNA radioactivity decreased by about a factor of 2 in group 3 in comparison with group 1. Six days after the experiments the rate of nuclear DNA biosynthesis decreased by 22 and 31 percent for animals in the synchronous and flight experiments respectively. Immobilization caused an additional decline, with the final effect being practically the same as in the vivarium control. In the experimental variants, however, the additional stress was applied on the background of DNA biosynthesis that was already somewhat diminished, and therefore in this case the effect of immobilization was in fact lower than in the control. The possibility is not excluded that a slight decline in DNA-polymerase activity in liver nuclei 6 days after the experiments was elicited by stress developing in the animal body during the period of readaptation. Absence of differences in the reactivity of the nucleic acid system to additional stress among animals in the flight and synchronous experiments permits the conclusion that weightlessness does not have a significant influence on the stress reactivity of systems responsible for DNA biosynthesis.

Table 1 illustrates the intensity of RNA biosynthesis in isolated liver nuclei in the absence and presence of α-amanitin in the reaction medium. α-Amanitin is an inhibitor of RNA-polymerase II, responsible for biosynthesis of matrix RNA (mRNA). The enzyme RNA-polymerase I, which is synthesized by ribosomal RNA (rRNA), is not

Table 1. Intensity of RNA Biosynthesis in Isolated Liver Nuclei (Radioactivity, %)

(1) Вариант	(2) Без α-аманитина			С α-аманитином (3)		
	1	2	3	1	2	3
В	100 ± 20	88 ± 8	46 ± 26 $p_1 < 0,05$ $p_2 < 0,005$	100 ± 25	75 ± 15	63 ± 3 $p_1 > 0,05$ $p_2 > 0,05$
С	100 ± 23	54 ± 8 $p_1 < 0,05$	45 ± 9 $p_1 < 0,05$	100 ± 39	82 ± 8 $p_1 > 0,05$	67 ± 15 $p_1 > 0,05$ $p_2 > 0,05$
П	100 ± 16	72 ± 15 $p_1 > 0,05$	78 ± 13 $p_1 > 0,05$	100 ± 18	96 ± 15	70 ± 11 $p_1 > 0,05$ $p_2 > 0,05$

Note: В, С, П--Vivarium control, synchronous and flight experiments respectively. 1-3--variants of the experiment corresponding to different animal groups. Additional stress was applied in variant 3 on days 1, 4, 5 and 6. Significance indicators p_1 and p_2 were calculated in comparison with results obtained correspondingly for animal groups 1 and 2

Key:
1. Variant
2. Without α-amanitin
3. With α-amanitin

sensitive to α-amanitin. In the absence of additional stress, the inhibitor suppressed transcription in liver nuclei by a factor of about 2-2.5 in control and experimental animals.

In animals participating in the flight and in rats subjected to the synchronous experiment, 6 days after the end of the experiments the intensity of nuclear RNA biosynthesis in the liver in the absence of α-amanitin was found to be lower than 6 hours after the experiments. This decline was 28 and 46 percent for the flight and synchronous experiments respectively. Immobilization elicited inhibition of RNA-polymerase activity in nuclei of the liver of control animals; the effect was 54 percent if the intensity of RNA biosynthesis was determined in the absence of α-amanitin, and 37 percent in its presence.

Results of similar magnitude were also obtained in the synchronous experiment, while in the absence of α-amanitin the effect in animals participating in the flight experiment manifested itself more weakly. Thus animals in groups 2 and 3 exhibited only a tendency toward lower intensity of RNA biosynthesis (the differences with respect to control were statistically insignificant). Of interest is the fact that there are practically no differences between the results obtained for rats in groups 2 and 3. It may be suggested that during the readaptation period a stress reaction developed in the animal body, one which should be interpreted in our research as a stress load additional to that to which the body was subjected in the period before the end of the experiment. Obviously the decline in reactivity of the RNA biosynthesis system to additional stress was the product of exhaustion of molecular mechanisms responsible for adaptive processes in cells. The fact that

a decrease in the reactivity of this system was noted only after the flight and that it did not occur after the synchronous experiment implicates the weightlessness of space as a factor playing a role in this phenomenon.

Investigation of the intensity of nucleic RNA biosynthesis in the presence of α-amanitin did not reveal any noticeable changes in the reactivity to stress exhibited by the RNA biosynthesis system in the liver of animals participating in the flight experiment (Table 1). Consequently it is primarily the biosynthesis of mRNA that experiences stress in flight, while biosynthesis of rRNA was found to be more stable. Our data on the reactivity of the system responsible for biosynthesis of nucleic acids in rat liver nuclei to additional stresses permit classification of the stress factors operating in space flight as moderate.

The authors express their deep gratefulness to Prof R. A. Tigranyan for graciously providing liver tissue for analysis.

BIBLIOGRAPHY

1. Germanyuk, G. L., in "Novoye v gormonakh i mekhanizme ikh deystviya" [Advances in Research on Hormones and the Mechanisms of Their Action], Kiev, Naukova dumka, 1977, p 91.

2. Chauveau, J., and Moule, Y., EXP. CELL. RES., Vol 11, 1956, p 317.

3. Troitskaya, Ye. N., Komolova, G. S. et al., DAN, Vol 250, No 6, 1980, p 1,483.

4. Blobel, G., and Potter, V. R., BIOCHIM. ET BIOPHYS. ACTA, Vol 166, 1968, p 48.

11004
CSO: 1840/82

PSYCHOLOGICAL TRAINING--ONE OF THE MOST IMPORTANT FACTORS OF INCREASING SAFETY OF SPACE FLIGHTS

Moscow PSIKHOLOGICHESKIY ZHURNAL in Russian Vol 1, No 1, Jan-Feb 80 pp 104-107

[Article by G. T. Beregovoy]

[Text] The pace of exploration of outer space by manned spacecraft is increasing today. New spaceships supporting an extensive program of exploration in behalf of mankind are undergoing development and testing. The role of crew safety is growing disproportionately in this connection. This is why ensuring safety in lengthy space flights is one of the priority tasks.

While the possibilities of space exploration are broadening owing to the achievements of technical progress, man's reliable fulfillment of increasingly more complex tasks aboard spacecraft depends on prior professional and psychological training.

The reliability of the equipment is not absolute, and therefore an emergency situation may arise at practically any moment: when the crew takes its place within the spaceship prior to launching, in all phases of flight, and when the crew leaves the spaceship after landing.

Space flight safety depends not only on the reliability of the spaceship and the systems and gear it contains, but also on the quality of the crew's training and its ability to capitalize on its knowledge and endurance at the moment an emergency situation arises in the presence of the unfavorable factors of space flight.

Psychological training plays the most important role in solving the problems of space flight safety, and especially in emergency situations. The general psychological training a cosmonaut receives includes an entire intricate dynamic complex of pedagogical, methodological and psychological influences aimed at raising the quality of preparation for a space flight, with a consideration for the particular features of the flight program and the individual psychological characteristics of the persons participating in its implementation.

Psychological training must take sensible and maximal account of the individual psychological features of the cosmonaut's personality, and of the laws governing arisal and occurrence of mental processes, to include ones associated with his professional activity. These questions have been studied in ample detail by I. V. Davydov, N. V. Krylova and I. B. Solov'yeva.

Psychological training basically consists of purposeful pedagogical and psychological methods directed at mobilizing the mental functions needed of the cosmonaut, helping him to actively form a conceptual model of the forthcoming flight and teaching him to utilize his psychophysiological reserves with the greatest effectiveness.

As space flight programs grow more complex, psychological training becomes more extensive and diverse. Factors such as longer flight, inclusion of various cycles of scientific research and complex experiments into the program, and prolonged presence of the crew in an ecologically closed, restricted space causing deformation of the sensory field, are imposing new requirements on training.

Much attention must be devoted in professional training to measures having the purpose of forming and reinforcing the needed psychological qualities, ones which would ensure that the cosmonaut would act effectively in the complex conditions of space flight.

The effectiveness of a crew's actions in a complex flight situation depends on the capability the cosmonauts have for behaving actively in emotionally tense conditions. Therefore a certain system of psychological qualities must be shaped within the cosmonaut: emotional stability, the capability for self-regulation, and a preparedness for possible surprises and stressful effects.

All of this justifies maintaining a psychological approach to organizing the professional activity of cosmonauts--that is, concentrating on simulation of various mental states that would be typical of real activity in the flight. In other words preparation for flight must go beyond the limits of professional training with the existing training equipment, and it presupposes incorporation of special psychological methods and experimental procedures.

How productively we can develop professionally meaningful psychological qualities depends directly on how purposefully we employ effects in training that produce particular emotional responses.

Various so-called exogenous test fixtures, trainers, simulators and soundproof chambers used in the cosmonaut training system permit the individual to acquaint himself with individual factors of space flight, and they form certain professional habits. But this training, which is performed on the ground, does not proceed in real conditions. No matter how complex the emergency situation reproduced in a trainer is, it cannot elicit the same stress which would arise in a real situation, when the individual would know that his mistakes might cost him his health and, possibly, his life. Therefore despite the organizational difficulties that would be encountered, we feel it suitable to use real emotion-producing situations in cosmonaut training, ones which would cause reactions to real stressful effects (hydraulic laboratory, centrifuge, pressure chamber, aircraft simulator, parachute jumps, flying).

By analyzing professiograms of cosmonaut activity in real flight, we can distinguish the moments which are sufficiently complex from the standpoint of psychological effects upon the individual. The main time interval is the period of psychological adaptation to the unusual conditions of flight.

One prerequisite of maintaining the individual's ability to perform in this period is to preserve his operational stability. Hence one of the concrete tasks of psychological training is to teach the individual to purposefully perform his activities as an operator in unusual, emotionally saturated conditions.

The next category of complex flight situations that should be considered is various deviations from the normal situation. An emergency situation elicits two levels of responding reactions and actions: adaptive-protective (biological) and psychological, forming a behavior strategy and ensuring fulfillment of new actions not foreseen by the program. It is precisely the second level which must be developed during the cosmonaut's training. This can be done by simulating different mental states in trainers.

Flight training and parachute jumps provide effective training situations in support of these tasks.

An airplane is viewed as both an exogenous and a professional trainer, one creating a complex of influences upon the individual and causing him to experience unusual conditions, risk, responsibility, physiological stresses and conditions typical of an operator controlling a traveling vehicle.

Because parachute jumps (both parachute and free-fall) produce real stressful conditions that recreate the emotional background inherent to cosmonaut activity to a certain extent (unusual conditions, time deficit, sensory load, sensation of risk, responsibility and independence), and because they can be performed in conjunction with the primary objective--fulfilling the elements of professional activity, we can consider parachute training to be a necessary resource of cosmonaut psychological training.

Another merit of parachute and flight training is that they afford a possibility for teaching the cosmonaut to make optimum decisions on the background of rapidly changing processes.

The experience of flying aboard airborne platforms, to include spaceships, shows that situations may arise in which a flight would have to be aborted and a forced landing would have to be made outside the intended area.

In what way would such a situation be complex? It would be complex in that the crew will have experienced stress resulting from the particular mishap, and it would be landing immediately, having no prior knowledge of the nature of the landing procedure or the natural and weather conditions within the given region.

A number of experimental studies have shown that on occasion, stress arising during landing in extreme conditions in one of the critical zones of the earth (in a desert in the presence of high temperatures and strong winds, on the steppes in winter in the presence of winds and low temperatures, in high mountains offering hypoxic conditions, on a stormy sea) may disorganize the crew's activity to such an extent that it would not be able to complete its task.

There have been cases in which test pilots who had not been psychologically prepared for the possible influences of the external environment have had to abort an experiment early.

Psychological factors--confusion, passiveness, lack of will, fear, pain, loneliness and so on--may lead to illness among the crewmembers, or even to their death.

Cosmonauts are trained in various climatic and geographic zones with the purpose of surmounting these unfavorable factors and eliminating stress in the case of forced landing in extreme conditions. The main goal of such training is to psychologically prepare the crews of spaceships for possible hazardous influences, and to teach them the things they must do after landing.

The conditions of such training sessions are made as similar as those of real critical situations in order that the crewmembers would begin to feel that they could survive a complex situation owing to their knowledge, ability and endurance.

It should be noted that the experience of such training sessions has produced its fruits. Cosmonauts have had to utilize this experience several times in the final phase of space flight.

The clearest example of this can be found in what happened after cosmonauts V. G. Lazarev and O. G. Makarov made a forced landing on the steep slope of a snow-covered mountain. The stress of the emergency landing, which was compounded by the considerable G-forces experienced, was not made worse by the additional stress of being in uninhabited, inaccessible terrain, since the cosmonauts had undergone winter training in forested terrain. The crew displayed courage and steadfastness, and it was able to survive a very difficult situation.

No less endurance and steadfastness had to be displayed by V. D. Zudov and V. I. Rozhdestvenskiy, who made an unplanned night landing on a partially frozen bitter salt lake. Because they had been psychologically prepared by marine training the situation did not catch them unawares, and consequently they were able to act efficiently and correctly.

Thus psychological training, in the course of which professionally important qualities of the personality, the individual's capabilities and a system of certain knowledge, skills and habits are formed and reinforced (and all of this, taken together, makes the cosmonaut certain of his readiness to perform his missions), is the most important condition for raising space flight safety.

11004
CSO: 1866/25

SPACE ENGINEERING

UDC 629.78:621.396.624

LASER INFORMATION SYSTEMS FOR SPACECRAFT

Moscow LAZERNYYE INFORMATSIONNYYE SISTEMY KOSMICHESKIKH APPARATOV in Russian 1981 (signed to press 14 Sep 81) pp 2-5, 268-269

[Annotation, foreword and table of contents from book "Laser Information Systems for Spacecraft", by Igor' Viktorovich Minayev, Aleksandr Aleksandrovich Mordovin and Aleksey Grigor'yevich Sheremet'yev, Izdatel'stvo "Mashinostroyeniye", 1,900 copies, 272 pages]

[Text] ANNOTATION

The authors discuss the theoretical foundations and principles of the construction of laser information and measuring instruments and systems designed to operate on board spacecraft. They explain the principles of the construction of laser search, detection, tracking, communication and location systems.

This book is intended for specialists engaged in designing and operating laser instruments and information systems.

FOREWORD

Man's conquest of space is opening new areas for the use of laser information systems (LIS). Among these areas, the main ones are: studying the Earth's resources; investigating the movements of the continents; analyzing cloud cover and wind movement and velocity and, consequently, predicting Earth's weather; controlling the movements of artificial Earth satellites and spacecraft; communication between spacecraft and ground points; tracking meteorological rockets and satellites and so on. Laser information measurement, collection, processing and transmitting systems are already used extensively in these areas. Industry is developing laser short- and long-range communication systems, laser measuring systems for highly accurate measurements of the parameters of motion of objects and so forth. This is explained by the fundamental special feature of lasers: the capability of generating coherent optical radiation. This feature makes it possible for laser systems to have a huge information content, communication channels with high resistance to interference, instantaneous performance of the most complicated mathematical operations in the processing devices (integration, Fourier transformations and convolutions, spatial filtration, the finding of correlation functions, retention of large masses of information and so forth). The state of quantum electronics and laser technology makes it possible to solve scientific and technical problems that are of great importance to the national economy.

The result of the research and development work done in the last decade was the creation of various laser devices that confirmed the great prospects for the use of laser technology. However, along the way to the creation of laser information systems for use in space there still exist many difficulties. They include inadequate development of the element base technology, the complexity of the designing and building of opticoelectronic systems and instruments for spacecraft, and the lack of experience in designing and building laser information systems on the part of the engineers. In addition to this, the traditional scientific potential of radio engineers and the frequent inadequate understanding of the theoretical principles and possibilities of laser technology are retarding progress in this area. This book should, even if only to a small degree, contribute to an improvement in the level of scientific knowledge on the part of radio engineers. Its subject is the theoretical principles and possibilities for utilization in space of laser information systems. According to data published in the foreign press, the number of series-produced models of laser information systems for use in space is still relatively small, although there are some more being developed experimentally (data on some of them are presented in this book). In connection with this it is advisable to expand and extend the theoretical aspects of the space applications of laser information technology and equip engineers who are designing such equipment with techniques, algorithms, a calculative apparatus for evaluating efficiency and mathematical models of systems. The development of engineering methods for calculating the basic characteristics of laser technology systems is an extremely urgent and important matter. This book is devoted primarily to this end.

In this book we present a model of the optical field at the input of a receiving device that makes it possible to allow for its quantum-statistical properties in the simplest way possible. Using the entropy approach, we determine the density matrices that characterize the state of the optical field. There is an analysis of quantum measurements on the basis of which we determine the observed variables corresponding to coherent and noncoherent reception methods and find the statistics of the optical field observed for the different states.

On the basis of the statistical data, we analyze the resistance to interference of atmosphereless, digital, optical communication systems for different types of modulation and coherent and noncoherent reception methods. We also make a comparative analysis of different communication systems with respect to their resistance to interference and list the conditions under which quantum effects can be ignored.

We also investigate the resistance to interference of optical communication systems in which the radiation passing through a space channel is even partially propagated through the atmosphere. The atmosphere's effect on optical radiation is analyzed. There is a discussion of the resistance to interference of optical systems under conditions of fluctuations in the parameters of an optical system caused by turbulence in the atmosphere. There is an investigation of the effectiveness of several methods for weakening the effect of atmospheric turbulence, such as averaging with respect to the aperture, dispersed reception of optical signals, the use of corrective feedback in information systems with amplitude and polarization modulation and so on. There is a brief discussion of the basic features of a space communication system with a high information content and a traffic capacity of about 300 million binary units per second and optical locators for use in space.

We discuss the optimal measuring of the parameters of an optical signal that are related to corresponding parameters of spacecraft motion (distance, speed, angles).

We also list the special features of the construction of spatial opticoholographic systems for processing digital radio engineering information; derive analytical expressions for the average probability of incorrect reception of binary signals and encoded messages, as well as during the reception of messages in general. We discuss adaptive optical systems that make it possible to compensate for disturbances of the wave front of an optical beam propagating along a channel, as a result of which the intensity of the useful signal when it reaches the spacecraft's receiver is maximal. We also present mathematical models and efficiency indicators that are used to investigate the process of LIS control.

The special features of the support of the search mode of spacecraft (KA) LIS's are discussed in Chapter 6, where--on the basis of an analysis of the sources of the appearance of indeterminacy of the KA-subscriber positions at the moment of the beginning of a communication session--the statistical characteristics of the zone of determinacy are determined, as well as the parameters characterizing the subscribers' relative motion in the KA-observer search plane.

Chapter 7 is devoted to a discussion of automatic KA-subscriber tracking in the communication maintenance mode. Within the framework of a general mathematical model of the control process, there is an analysis of the accuracy characteristics of the basic methods of automatic tracking in the optical band, including allowing for the effect of a turbulent atmosphere in the "KA-Earth" communication link. The possibility of synthesizing a tracking system, according to the basic operating criteria, is also discussed.

Chapters 1 and 2 and Subsections 3.1-3.3 were written by A.A. Mordovin and A.G. Sheremet'yev, Subsections 3.4-3.6 and Chapter 4 (except for Subsection 4.4) by A.G. Sheremet'yev, Subsection 4.4 by A.T. Serobabin and A.G. Sheremet'yev, Chapters 5, 6 and 7 by I.V. Minayev.

TABLE OF CONTENTS

11746
CSO: 1866/66

UDC 629.78.05

BUILDING SCIENTIFIC INSTRUMENTS FOR USE IN SPACE

Moscow NAUCHNOYE KOSMICHESKOYE PRIBOROSTROYENIYE in Russian 1981 (signed to press 4 Sep 81) pp 2-3, 194-203

[Annotation, introduction, table of contents and abstracts from collection "Scientific Space Instruments", edited by V. I. Fuks (responsible editor) et al., Izdatel'stvo "Nauka", 1400 copies, 204 pages]

[Text] ANNOTATION

This collection of works is devoted to questions arising in the fields of planning, designing, systems analysis and production of instruments for space research. The subjects discussed include scanning devices, stringed position sensors, ground equipment units built according to the "Vektor" standard, and methods for designing printed-circuit boards.

This book is designed to be used by scientific, engineering and technical personnel.

INTRODUCTION

The planning, development and production of scientific instruments for the study of outer space has been developed considerably in recent years and is now distinguished as an independent branch of instrument building.

This book contains materials obtained as the result of work done by design offices and experimental production facilities. For the reader's convenience all the materials have been divided into four categories: "Organizing and Planning the Development of Scientific Instruments," "Planning and Designing Scientific Equipment," "Systems Analysis of Scientific Equipment" and "Equipment Production Technology."

The first section contains one article that is devoted to the problems involved in organizing and planning experimental design work with the help of a computer.

In the second section there is a discussion of the basic principles of the construction of a telescope for studying gamma radiation. There is a description of the individual assemblies of a multispectral scanning system that is used to investigate the Earth's natural resources. Questions on the thermal conditions of a system based on a specially developed program for calculating thermal fields are discussed. There is a description of methods for increasing the density of the layout of electronic radio parts on boards, as well as boards of an original curvilinear design.

The third section contains solutions to the problems involved in developing the basic electrical circuits of scientific instruments. As was the case with previous collections, there is a discussion of electrometic amplifiers and secondary power sources. A series of articles is devoted to describing blocs of ground monitoring and measuring equipment built according to the "Vektor" standard (KAMAK).

Individual questions of scientific equipment production technology are the subject of the articles in the fourth section.

Naturally, this collection of works does not encompass all the questions that have arisen in connection with the building of scientific instruments for use in space. Nevertheless, the editorial board hopes that the materials in it will be useful for engineering and technical personnel engaged in solving practical problems encountered in building scientific instruments for use in space.

TABLE OF CONTENTS

ABSTRACTS

UDC 001.89+681.3

ORGANIZING AND PLANNING EXPERIMENTAL DESIGN WORK ON THE BASIS OF A THIRD-GENERATION COMPUTER

[Abstract of article by Kurmanaliyev, T.I., Kuritskiy, A.B., Maksimenko, A.N., and Neyman, D.M.]

[Text] The authors discuss questions related to the planning and operational control of experimental design work (OKR) based on network planning methods. Special attention is given to the most important aspect of the use of network planning methods, which is related to the compilation of calendar work schedules on the basis of the solution of problems concerning the optimum distribution of resources among developers working in different areas. The authors explain their experience in solving these problems with the help of packages of applied programs for a third-generation computer. They also discuss organizational questions concerning the formulation of an OKR planning and control system based on the package of applied programs for the "Resursy" SMO [probably software system]. References 6.

UDC 529.1.07:629.78

POSSIBLE PRINCIPLES FOR THE CONSTRUCTION OF GAMMA-TELESCOPES AND LOGIC OF THE DISCRIMINATION OF REGISTERED PARTICLES

[Abstract of article by Akimov, V.V., Voronov, S.A., Gal'per, A.M., Grigor'yev, V.A., Dobriyan, M.B., Kalinkin, L.F., Kirillov-Ugryumov, V.G., Kurmanaliyev, T.I., Kurnosova, L.V., Luchkov, B.I., Melioranskiy, A.S., Nesterov, V.Ye., Tabaldyyev, S.R., and Chuykin, Ye.I.,]

[Text] The authors describe a gamma-radiation telescope and its individual systems, which must satisfy requirements emanating from the problems involved in recording very small flows gamma-quanta against a background of charged particles. They also describe the logic of the discrimination of the registered particles. Figures 3; references 3.

UDC 539.1.074.24

MULTILAYER, BROAD-GAP, SPARK CHAMBER-CONVERTER FOR RECORDING COSMIC GAMMA RADIATION

[Abstract of article by Belousov, A.S., Voronov, S.A., Gal'per, A.M., Kirillov-Ugryumov, V.G., Luchkov, B.I., Moiseyev, A.A., Ozerov, Yu.V., and Popov, A.V.]

[Text] The authors describe the design and power unit of a gamma-radiation telescope's basic detector, which is a broad-gap spark chamber. They present the results of an investigation of methods for reducing fluctuations in brightness and spark alignment, which have a significant effect on measurement accuracy during vidicon information output. Figures 4; references 2.

UDC 681.78

SPECTRAL, POLARIMETRIC AND MODULATION INSTRUMENTS FOR THE LONG-WAVE INFRARED BAND

[Abstract of article by Sholomitskiy, G.B., Maslov, I.A., Ignatenko, S.A., Namestnik, S.G., Soglasnova, V.A., and Gromov, V.D.]

[Text] The authors describe an adjustable Fabry-Perot interferometer and a polarimeter for extra-atmospheric astrophysical investigations in the long-wave infrared band with waves longer than 40 μm, as well as a focal infrared modulator with a swinging mirror. Figures 8; references 10.

UDC 535.8:681.7

LIGHT SOURCE FOR THE ABSOLUTE CALIBRATION OF UPPER ATMOSPHERE LUMINESCENCE PHOTOMETERS

[Abstract of article by Rabinkov, A.V.]

[Text] The author describes the design of a light source that is intended to be used for absolute calibration of upper atmosphere luminescence photometers. He also presents a technique for calibrating the light source and gives the power parameters of its emissions. Figures 2; references 6.

UDC 681.783.323.3

SCANNING DEVICE WITH A MAGNETOELECTRIC PROPELLING UNIT

[Abstract of article by Morozov, P.A., Grishin, I.A., and Namestnik, S.G.]

[Text] The authors describe the design of a scanning device with a magnetoelectric propelling unit. The device has a plane mirror that oscillates according to a saw-tooth rule, with a forward and backward motion ratio of 2:1 and a frequency of 12-15 Hz. Figures 2.

UDC 531.6:681.783.323.3

POWER CHARACTERISTICS OF A SCANNING MIRROR'S OSCILLATORY MOTION

[Abstract of article by Terent'yev, V.I.]

[Text] The author demonstrates how to calculate the parameters. The rules that he derives can be used as a basis for designing scanning devices that have (for example), a magnetoelectric motor. Figures 1.

UDC 535.312

LIGHTENED MIRRORS FOR THE SCANNING DEVICES OF SCIENTIFIC INSTRUMENTS

[Abstract of article by Polukhin, V.N., Podol'skaya, T.M., Gomel'skiy, M.S., Gryaznov, V.A., Namestnik, S.G., and Morozov, P.A.]

[Text] The authors describe the design of a lightened, metallic mirror backing, as well as the glass coatings used and the technology for applying them. The mirrors were developed at the USSR Academy of Sciences' Design Office. Figures 2.

UDC 531.749:621.396.965

THE UKS-1 SCANNING SYSTEM MONITORING UNIT

[Abstract of article by Busargin, V.A., Naumov, A.N., and Popkov, A.V.]

[Text] The authors describe the design of a unit that is used to measure the basic parameters of the oscillatory motion of a scanning system's mirror. They explain this unit's operating technique and present the results of tests with scanner models. Figures 2; references 2.

UDC 535.241.13:778.534.8

A RADIANT FLUX COMMUTATOR FOR ON-BOARD SPECTROMETERS

[Abstract of article by Derevyanchenko, A.S., Ignatenko, S.A., Namestnik, S.G., and Rozhavskiy, E.I.]

[Text] The authors describe a radiant flux commutator that is used for spatio-temporal separation of radiant energy flows striking the matrix of a fiber-optic

splitter and originating on the Earth's surface and in the internal calibration sources of a multispectral scanning system. Figures 1.

UDC 531.8

SYNTHESIS OF A SPATIAL TRANSFER DEVICE ACCORDING TO THE CONDITION OF AFFILIATION OF ITS POSITIONS TO A SINGLE ASSEMBLY

[Abstract of article by Ivanov, K.S., and Grishin, I.A.]

[Text] The authors set up the problem of formulating the geometric conditions for affiliation of the different positions of a spatial mechanism to one assembly and use these conditions to synthesize a crank-balance beam transfer mechanism with a given forward and backward motion ratio. Figures 4; references 4.

UDC 621.833.7:539.5

ON THE LOAD ON THE FLEXIBLE ELEMENT OF A SEALED TWO-WAVE TRANSMISSION FROM THE WAVE GENERATOR'S SIDE

[Abstract of article by Kozhakhmetov, K.Kh., and Klimov, A.M.]

[Text] The authors derive an analytical expression for the load on the flexible element of a sealed two-wave transmission that is imposed by the wave generator. The rigid ring's reaction is not taken into consideration. They use a computer to make the numerical calculations of the load and its resultant. Figures 2; references 1.

UDC 519.67:536+629.78

DETERMINING THE EXTERNAL THERMAL LOADS ON INSTRUMENTS MOUNTED ON THE OUTSIDE OF AN ARTIFICIAL EARTH SATELLITE, WITH DUE CONSIDERATION FOR SHADING

[Abstract of article by Andronnikov, B.I., Bruk, A.G., Dudeyev, A.A., and Maziya, L.V.]

[Text] The authors discuss numerical methods for determining the external thermal loads on externally mounted equipment, allowing for the mutual shadings of different parts of instruments. They analyze the accuracy of the results when the calculations are made on a computer. The algorithms and programs they have developed are suitable for calculating the thermal conditions for a multispectral scanning system. Figures 3; references 6.

UDC 629.78:536.24.08

EXPERIMENTAL INVESTIGATION OF PHASE-TRANSITION MATERIALS USED IN DEVICES FOR THE THERMAL REGULATION OF SPACECRAFT

[Abstract of article by Gudkova, N.D., and Petrov, A.I.]

[Text] The authors present experimental data during an investigation of two phase-transition materials--lithium trihydrate nitrate and disodium phosphate dodecahydrate--under a broad range of thermal loads. Figures 6; references 3.

UDC 681.51-529

RESEARCH AND DEVELOPMENT OF PROGRAMMED OPTIMUM CONTROL SYSTEMS

[Abstract of article by Sharshanaliyev, Zh., and Romashchenko, A.I.]

[Text] The authors present the full synthesis of an automatic control system (SAU) that is optimum with respect to energy consumption and is used, for example, to control the angular position of the shaft of a direct-current microelectric motor in the presence of a static reactive moment. They discuss the possibility of realizing the control algorithms for a programmed SAU that is optimum with respect to energy consumption and operating speed on the basis of monotypical analog computational elements. Figures 5; references 3.

UDC 681.322.002.2

INSURING DATA RELIABILITY IN INFORMATION SYSTEMS

[Abstract of article by Morozov, Ye.A.]

[Text] The author discusses the question of insuring intrasystem reliability, as well as the question of the functioning of an information system, and presents a model for determining the optimum interval between monitoring points. Figures 4; references 2.

UDC 531

STRINGED INFORMATION SENSORS BASED ON OPTICALLY PURE FUSED QUARTZ

[Abstract of article by Mel'nikov, V.Ye., Kim, A.I., Mel'nikova, Ye.N., Kurmanaliyev, T.I., and Tsyshnatiy, V.A.]

[Text] The authors discuss the possibility of improving the metrological accuracy and technological and operating characteristics of stringed information sensors made of optically pure fused quartz. They present some output characteristics of stringed sensors that have already been developed; these characteristics indicate that quartz stringed sensors are promising. Figures 3; references 4.

UDC 531.7+629.78

SPECIAL FEATURES OF THE METROLOGY OF LINEAR AND ANGULAR MOVEMENTS OF SPACE EQUIPMENT ASSEMBLIES BY STRINGED INFORMATION SENSORS

[Abstract of article by Mel'nikov, V.Ye., Volkov, N.V., Kim, A.I., and Zinov'yev, A.A.]

[Text] The authors discuss various types of stringed sensors for multipurpose use, determine the factors that affect the stability of a sensor's frequency, and make recommendations for the conditions under which several different element designs should be used. Figures 3; references 6.

UDC 531+539.67

ON THE POSSIBILITY OF CREATING A FREQUENCY-CONTROLLED CHARACTERISTIC OF A FLOATING-CORE SENSITIVE ELEMENT

[Abstract of article by Mel'nikov, V.Ye., Mel'nikova, Ye.N., Drobatukhin, V.Ch., Kurmanaliyev, T.I., and Kim, A.I.]

[Text] The authors discuss one of the possible versions of a controllable damping device that creates periodic braking forces along a sensor's measuring axis. They present calculating relationships, oscillograms of modeling performed on an MN-7M, and the results of an experimental test of the proposed damping device's basic parameters. Figures 3; references 2.

UDC 621.316.5+621.375

ELECTROMETRIC AMPLIFIER MEASUREMENT BAND AND OPERATING MODE SWITCHES

[Abstract of article by Sopin, P.G., and Nazarenko, A.F.]

[Text] The authors describe the designs of the measurement band and operating mode switches for electrometric amplifiers carried on board spacecraft. Figures 2; references 5.

UDC 621.3.049.75

INCREASING THE LAYOUT DENSITY OF MULTILAYER PRINTED-CIRCUIT BOARDS FOR ON-BOARD SCIENTIFIC EQUIPMENT

[Abstract of article by Panfilova, G.T., and Sadykov, K.S.]

[Text] The authors describe the design and technological improvements used in multilayer printed-circuit boards manufactured by the open contact area method, as a result of which it has been possible to reduce the unit's size and the number of layers in multilayer printed-circuit boards. Figures 2; references 3.

UDC 621.3.049.75

CURVILINEAR PRINTED-CIRCUIT BOARDS IN ON-BOARD SCIENTIFIC SPACE INSTRUMENT BUILDING

[Abstract of article by Velichko, G.I., Sadykov, K.S., Chernyshova, T.I., Gol'tsova, O.P., and Davlyatshina, N.V.]

[Text] The authors discuss the design and production technology for curvilinear printed-circuit boards. Figures 2.

UDC 681.5

SOME QUESTIONS ON THE CONSTRUCTION OF APERIODIC AUTOMATIC EQUIPMENT

[Abstract of article by Mayevskiy, O.V., and Mamrukov, Yu.V.]

[Text] The authors discuss questions concerning the element base of aperiodic devices and the construction of indicators of the completion of transient processes. They also substantiate a new approach to the synthesis of aperiodic devices based on arbitrary logic elements. Figures 4; references 4.

UDC 681.5

PLANNING AUTOMATIC ACTUATING UNITS FOR AUTOMATIC ON-BOARD SYSTEMS

[Abstract of article by Arsen'yev, Yu.N.]

[Text] The author investigates several questions concerning the rational construction of commutators from a given element base and questions on the encoding of internal states with due consideration for functional reliability and simplicity of control. He also presents a generalized technique for planning automatic actuating units. Figures 4; references 13.

UDC 621.374.32.037.372.2

COUNTERS WITH PRELIMINARY SCALING AND METHODS FOR BUILDING THEM

[Abstract of article by Shevchenko, D.G.]

[Text] The author presents a classification of counters with preliminary scaling and variants in the design of their electrical circuitry, as well as the basic methods for selecting these counters according to given parameters. Figures 3; references 2.

UDC 621.375:539.1.074

A SPECTROMETRIC AMPLIFIER WITH A BROAD DYNAMIC RANGE FOR SEMICONDUCTING DETECTORS

[Abstract of article by Kornev, Ye.A., Kulikov, A.T., and Lutsenko, V.N.]

[Text] The authors describe a spectrometric amplifier with automatic high-speed regulation of the amplification factor, which makes it possible to cover a broad dynamic range of signals from semiconducting detectors. Figures 3; references 3.

UDC 621.316.7

SELECTING THE RATIONAL ELECTRICAL CIRCUITRY FOR A SECONDARY POWER SOURCE WITH A BOOSTER UNIT

[Abstract of article by Osadchiy, V.I.]

[Text] The author presents an analysis of the known circuitry of secondary power sources with boosters, which sources are designed to provide the maximum possible efficiency from the smallest size. He makes recommendations for selecting circuits and presents an engineering method for calculating efficiency. He also describes a secondary power source with a booster that has increased efficiency and reduced dimensions in comparison with known systems. Figures 6; references 5.

UDC 621.316.7

A PRECISION, HIGH-VOLTAGE, STABILIZED POWER SOURCE

[Abstract of article by Burgeyev, D.A.]

[Text] The author describes a precision, high-voltage, stabilized power source, the special feature of which is the use of galvanically uncoupled feedback and a splitter with an increased transmission factor. Figures 1; references 2.

UDC 621.375.132

AN ELECTROMETRIC AMPLIFIER FOR MEASURING CURRENTS WITH DIFFERENT POLARITIES

[Abstract of article by Guseva, K.I., Notkin, V.A., Kozlov, B.G., and Gorbunova, I.S.]

[Text] The authors describe the layout of an electrometric amplifier with a piecewise-linear characteristic that is used to convert positively and negatively polarized direct current from high-resistance current sensors into an output voltage of 0.1-6.1 V. The range of measurable currents is from $-1 \cdot 10^{-9}$ to $+1 \cdot 10^{-8}$ A. The operating temperature range is from -20 to +50°C, while the power consumption is less than 300 mW. Automatic switching of the conversion conductance has been realized. The authors present the results of temporal drift measurements when MOP [metallic oxide semiconductor] transistors from different batches in a shipment are used. Figures 1; references 3.

UDC 681.3

THE BUK-52F COMPOSITE PROGRAMMED UNIT FOR CONTROLLING "VEKTOR"-STANDARD EQUIPMENT

[Abstract of article by Mayevskiy, O.V.]

[Text] The author describes a unit built according to the "Vektor" standard that makes it possible to organize program control of a branch in the "Vektor" standard with one additional frame. He suggests that the unit be used with a memory having a capacity of up to 4,096 x 18 words and the industrially produced BUM2-90 unit. Figures 3; references 2.

UDC 681.327.8

A "VEKTOR" SYSTEM COMMUNICATION UNIT WITH A 15VSM-5 KEYBOARD

[Abstract of article by Tsyganov, A.N., Yermolayev, Yu.F., Yefremkin, V.A., and Morozova, L.I.]

[Text] The authors describe the BUK-100 communication unit, which organizes the coupling of the standard data transmission channel of "Vektor" systems with a 15VSM-5 computer. The unit performs the following functions: reception of data and commands from the computer and transmission of them, in repackaged form, into the frame channel; reception of data and readiness patterns from the frame channel; organization of provisional UP1 and UP2 transitions in the computer's program. Figures 1.

UDC 681.327.8

A UNIT FOR COUPLING THE SMALL MPU16-3 PRINTER TO A CHANNEL IN A "VEKTOR" FRAME

[Abstract of article by Genvarev, A.A., and Yermolayev, Yu.F.]

[Text] The authors describe a module, built according to the "Vektor" standard, for coupling the small MPU16-3 printer to a frame channel. Figures 2.

UDC 681.327.8

A UNIT FOR COUPLING THE MT 1016 DIGITAL PRINTER TO A CHANNEL IN A "VEKTOR" FRAME

[Abstract of article by Genvarev, A.A., and Yermolayev, Yu.F.]

[Text] The authors describe a unit for coupling the MT 1016 digital printer with a "Vektor" frame channel. They discuss the coupling unit's functional diagram and temporal operating diagram. Figures 2.

UDC 621.317.004

AN INSTRUMENT FOR TESTING REMOTE SWITCHES

[Abstract of article by Kozlov, B.G.]

[Text] The authors describes an instrument for testing remote switches with a trip voltage of no more than 100 V. The input signal has positive polarity of any form and an amplitude of 3.5-7 V. The operating mode is automatic, and it can be set to operate either one time only or manually. Figures 1.

UDC 621.383.5

A PHOTOELECTRIC POSITION SENSOR

[Abstract of article by Bolbachan, V.V., and Izherovskiy, A.V.]

[Text] The authors describe a sensor that is used in a mobile mechanical system's monitoring system. The sensor forms a pulse, the forward front of which corresponds to the moving system's passage through a given point, with due consideration for the direction of movement with respect to a single coordinate. Figures 2; references 3.

UDC 681.322.51

AN ANALOG VOLTAGE-MULTIPLICATION CIRCUIT

[Abstract of article by Pankratov, N.N., and Romashchenko, A.I.]

[Text] The authors describe a circuit for the multiplication of alternating voltage into direct-current voltage. The circuit is based on two bipolar and one MOP [probably metallic oxide semiconductor] transistors, and its energy consumption is about 4 mW. Figures 2; references 4.

UDC 621.372.832.8

A DEVICE FOR GALVANIC UNCOUPLING

[Abstract of article by Logunov, A.V.]

[Text] The author describes the operating principle and technical characteristics of a device for galvanic uncoupling that is based on a modulator-demodulator system, with keys based on MOP [metallic oxide semiconductor] transistors. Figures 2.

UDC 681.586.38

PRODUCTION TECHNOLOGY FOR REFLECTING β-PARTICLE TARGETS

[Abstract of article by Sasov, A.M.]

[Text] The author discusses questions concerning the technology for producing reflecting β-particle targets based on bismuth. Figures 1; references 3.

UDC 53.082.54

OPTICAL TESTING OF THE PLANENESS OF THE GRID REFLECTORS OF A FABRY-PEROT INTERFEROMETER DURING OPERATION IN THE INFRARED BAND

[Abstract of article by Belorukov, A.N.]

[Text] The author describes a technique for the optical testing of the planeness of grid reflectors of a Fabry-Perot interferometer. Figures 5; references 1.

UDC 621.52

A VACUUM INSTALLATION FOR GROUND TESTING OF INSTRUMENTS THAT OPERATE UNDER OUTER SPACE CONDITIONS

[Abstract of article by Denisov, A.S., Velikasov, S.S., and Filatov, A.N.]

[Text] The authors describe an installation for ground testing of instruments that are intended to operate in outer space. A vibrationless evacuation system is achieved by replacing the mechanical pre-evacuation pump with an adsorption one. Figures 2; references 2.

11746
CSO: 1866/39

UDC 629.78

SYNTHESIS OF ALGORITHM FOR CONTROLLING MOTION IN VERTICAL PLANE OF TRANSPORT SPACECRAFT AT STAGE OF APPROACH FOR LANDING AND LEVELING

Moscow KOSMICHESKIYE ISSLEDOVANIYA in Russian Vol 20, No 2, Mar-Apr 82 (manuscript received 2 Jun 80) pp 206-210

[Article by A.A. Zhevnin and V.A. Strebkova]

[Text] The authors discuss questions related to the synthesis of laws, formulated in accordance to the feedback principle, for controlling the motion of a transport spacecraft. The synthesis is done on the basis of the inverse problem of dynamics. The values of the control effects are determined from the solution of a first-order differential equation.

This article is devoted to synthesizing a system for terminal control of the speed and altitude of a transport spacecraft (TKK) in the vertical plane. The basic difference between our results and those available in the literature [1] is that the algorithm for the formation of the control effects, as created by an aerodynamic elevator and thrust, is synthesized in accordance with a closed cycle.

The mathematical model of a TKK can be described by a system of nonlinear differential equations that allow for both the forward motion of the center of mass and rotation around it:

$$\dot{H}=V\sin\theta, \tag{1}$$

$$\dot{L}=V\cos\theta, \tag{2}$$

$$\dot{V}=(n_{xb}-\sin\vartheta)g, \tag{3}$$

$$\dot{\theta}=(n_{yb}-\cos\theta)g/V, \tag{4}$$

$$\dot{\vartheta}=\omega_z, \tag{5}$$

$$\dot{\omega}_z=(m_z+m_z^{\omega_z}b_A\omega_z/V_b+m_z^{\delta_b}\delta_b)b_AqS/I_z, \tag{6}$$

$$n_{xb}=(P\cos\alpha-(c_x(\alpha_b)\cos\Delta\alpha-c_y(\alpha_b)\sin\Delta\alpha)qS)/G,\quad q=\rho V_b^2/2,$$

$$n_{yb}=(P\sin\alpha+(c_y(\alpha_b)\cos\Delta\alpha+c_x(\alpha_b)\sin\Delta\alpha)qS)/G,\quad W=(W_x^2+W_y^2)^{1/2},$$

$$\Delta\alpha=\operatorname{arctg}\left((W_y\cos\theta-W_x\sin\theta)/(V-(W_x\cos\theta+W_y\sin\theta))\right),\quad \alpha=\alpha_b-\Delta\alpha,$$

$$V_b=(V^2+W^2-2V(W_x\cos\theta+W_y\sin\theta))^{1/2},\quad \vartheta=\theta+\alpha.$$

The dynamic properties of the autothrottle control are allowed for by the differential equation

$$\dot{P}=b_1P-b_2-b_3V_b+b_4\alpha_{c_{yb}}, \tag{7}$$

where H = vertical distance from the center of mass to the landing gear wheels' point of contact with the runway during a horizontal landing; L = horizontal

distance from the TKK's center of mass to the runway at the point of contact; θ = angle of inclination of the trajectory to the horizon; δ_b = angle of deflection of the elevator; G = weight of the TKK; I_z = moment of inertia; S = wing area; b_A = = aerodynamic mean chord of a wing; $m_z^{\bar{\omega}z}$, $m_z^{\delta b}$ = aerodynamic coefficients; ρ = density of the air; $c_x = c_x(\alpha_b)$, $c_y = c_y(\alpha_b)$ = prescribed functions; g = gravitational acceleration; W_x, W_y = effect of the medium (horizontal and vertical components of the wind); b_1, b_2, b_3, b_4 = constant coefficients; α_{cg} = deflection of the throttle quadrant; α = angle of attack. The change in the TKK's weight will be ignored.

We will consider the effect of the medium to be uncontrollable and assume that its effect on the flight up to current moment t is manifested in the state being realized at this moment:

$$\mathbf{X}(t)=\{V, \dot{V}, H, \dot{H}, \vartheta, \omega_z\}, \tag{8}$$

where V = ground speed; $\dot{V}$ = acceleration; $\dot{H}$ = vertical speed; ϑ = angle between the object's longitudinal axis and the horizon; ω_z = angular velocity.

For the sake of determinacy we will assume that the information about state (8) is both errorfree and timely.

Here we will understand synthesis of a system for controlling the TKK's vertical maneuvering to mean the construction of an algorithm for the formation of the control effects guiding the TKK from its current state to a given final state by a certain moment of time t_β. The flight begins from state (8) and should end with the TKK reaching the following state when $t = t_\beta$:

$$H(t_\beta)=H_\beta, \quad H^{(k)}(t_\beta)=H_\beta^{(k)}, \quad k=1,2,\ldots,4; \quad V(t_\beta)=V_\beta,$$
$$V^{(n)}(t_\beta)=V_\beta^{(n)}, \quad n=1,2,3. \tag{9}$$

In this article the control algorithm is constructed on the basis of the inverse problem of dynamics [2,3]. First, let us solve the problem of constructing the algorithm for the formation of control effects $\delta_b(t)$ and $\alpha_{cg}(t)$, which insures that the TKK goes from the initial state

$$\mathbf{X}(t_\alpha)=\mathbf{X}_\alpha \tag{10}$$

to the final state (9), with disturbing effects $W_x = W_y = 0$, it being the case that the motion should take place according to the known programs of motion H(t) and V(t), which connect the onset of motion (10) with its completion (9).

In order to find the control effects, let us formulate a system of differential equations [2], the order of which must coincide with the order of the original system of differential equations (1)-(7). This system can be derived by successive differentiation of equations (1) and (3):

$$\begin{aligned} H^{(4)}=&g/G(P^{(2)}\sin\vartheta+2\omega_z\dot{P}\cos\vartheta-P\omega_z^2\sin\vartheta)-4k_1V\dot{V}(\dot{\alpha}k_4+\dot{\vartheta}k_3)-\\ &-2k_1k_3(\dot{V}^2+V\dot{V}^{(2)})+\vartheta^{(2)}k_1V^2(k_4-k_3)-k_1V^2(2A(\dot{\alpha}c_y^\alpha)^2\sin\theta+\\ &+2\dot{\alpha}\dot{\vartheta}c_y^\alpha(2Ac_y\cos\theta+\sin\theta)-\dot{\vartheta}k_2)+\dot{\omega}_z(g/GP\cos\vartheta-k_1k_4V^2),\\ V^{(3)}=&P^{(2)}g/G\cos\alpha-\dot{\omega}_zk_5+\vartheta^{(2)}(k_5-g\cos\theta)-2k_1c_x(\dot{V}^2+V\dot{V}^{(2)})+g\dot{\vartheta}^2\sin\theta-\\ &-2\dot{\alpha}(\dot{P}g/G\sin\alpha+4Ak_1c_yc_y^\alpha V\dot{V})-\dot{\alpha}^2(g/GP\cos\alpha+2Ak_1(c_y^\alpha V)^2), \end{aligned} \tag{11}$$

where $\dot{\omega}_z=(m_z+m_z^{\omega_z}b_A\omega_z/V+m_z^{\delta_b}\delta_b)b_AqS/I_z$, $k_1=\rho gS/(2G)$, $c_y=c_{y0}+c_y^\alpha\alpha$, $c_x=$ $=c_{x0}+Ac_y^2$, $m_z=m_{z0}+m_z^\alpha\alpha$, $q=\rho V^2/2$, $k_2=c_x\sin\theta-c_y\cos 0$, $k_3=c_x\cos\theta+c_y\sin\theta$, $k_4=c_y^\alpha(2Ac_y\sin\theta-\cos\theta)$, $k_5=Pg/G\sin\alpha+2k_1c_yc_y^\alpha AV^2$, $P^{(2)}=b_1\dot{P}-b_3\dot{V}+b_4\dot{\alpha}_{cg}$.

. . . . . .

$$\theta^{(2)}=-\dot{V}\vartheta/V+(\dot{P}g/G\sin\alpha+\dot{\alpha}(Pg/G\cos\alpha+k_1V^2c_y^{\alpha})+2k_1c_yV\dot{V}+g\vartheta\sin\theta)/V,$$

where $\dot{\theta}$ and $\dot{P}$ are determined by expressions (4) and (7), respectively.

Let us rewrite system (11) in the following form:

$$P^{(2)}k_6+\dot{\omega}_zk_7=H^{(4)}+M_1,\quad P^{(2)}k_8-\dot{\omega}_zk_5=V^{(3)}+M_2, \tag{12}$$

where $k_6=g/G\sin\vartheta$, $k_7=(Pg/G\cos\vartheta-k_1k_4V^2)$, $k_8=g/G\cos\alpha$,

$$M_1=-g/G(2\dot{P}\omega_z\cos\vartheta-P\omega_z^2\sin\vartheta)+2k_1k_2(\dot{V}^2+V\dot{V}^{(2)})+4k_1V\dot{V}\times$$
$$\times(\dot{\alpha}k_4+\dot{\theta}k_3)+k_1V^2(\theta^{(2)}(k_3-k_4)+2A(c_y^{\alpha}\dot{\alpha})^2\sin\vartheta-\dot{\theta}^2k_2+2\dot{\alpha}\dot{\theta}c_y^{\alpha}\times$$
$$\times(2Ac_y\cos\theta+\sin\theta)),\ M_2=-\theta^{(2)}(k_5-g\cos\theta)+2\dot{\alpha}(\dot{P}g/G\sin\alpha+4Ak_1c_yc_y^{\alpha}V\dot{V})+$$
$$+\dot{\alpha}^2(Pg/G\cos\alpha+2k_1(c_y^{\alpha}V)^2+2k_1c_x(\dot{V}^2+V\dot{V}^{(2)})-g\dot{\theta}^2\sin\theta).$$

In system (12), let us replace $P^{(2)}$ and $\dot{\omega}_z$ with the expressions for them. Then, after transformation, system (12) will have the form

$$\begin{pmatrix} b_4k_6 & k_7k_9 \\ b_4k_8 & -k_5k_9 \end{pmatrix}\begin{pmatrix} \dot{\alpha}_{cg} \\ \delta_b \end{pmatrix}=\begin{pmatrix} E_1 \\ E_2 \end{pmatrix}, \tag{13}$$

where

$$E_1=H^{(4)}+M_1-k_6k_{10}-k_7k_{11},\ E_2=V^{(3)}+M_2-k_8k_{10}+k_5k_{11},$$
$$k_9=m_z^{\delta_b}b_AqS/I_z,\quad k_{10}=b_1\dot{P}+b_3\dot{V},\quad k_{11}=(m_z+m_z^{\omega_z}b_A\omega_z/V)b_AqS/I_z.$$

Having solved system (13), we have

$$\dot{\alpha}_{cg}=(E_1k_5+E_2k_7)/(b_4(k_5k_6+k_7k_8)), \tag{14}$$

$$\delta_b=(E_1k_8-E_2k_6)/(k_9(k_5k_6+k_7k_8)). \tag{15}$$

Solution (14), (15) exists if

$$b_4\neq0,\quad k_9\neq0,$$
$$k_5k_6+k_7k_8\neq0,\quad t\in[t_\alpha,\ t_\beta]. \tag{16}$$

From an analysis of equations (6) and (7), coefficients b_4 and k_9 determined the effectiveness of the control effects and cannot be zero. After transformation, the last relationship in system (16) is written in the following form:

$$P(\sin\alpha\sin\vartheta+\cos\vartheta\cos\alpha)+c_y^{\alpha}\rho SV^2(c_yA(\sin\vartheta-$$
$$-\cos\alpha\sin\theta)+0{,}5\cos\theta\cos\alpha)\neq0. \tag{17}$$

An analysis of (17) shows that relationship is fulfilled. For real modes and aerodynamic aircraft layouts,

$$\cos\theta\neq\pm\pi/2,\quad c_yA\sin\alpha+0{,}5\cos\alpha>0, \tag{18}$$

then, having transformed (17), we obtain the inequality

$$\cos\theta(P+c_y^{\alpha}\rho SV^2(c_yA\alpha+0{,}5))\neq0, \tag{19}$$

which is always correct when conditions (18) exist.

Thus, we can conclude that system (13) is solvable.

Further, by giving the motion programs H(t) and V(t) in the form of polynomials [3]

$$H(t)=H_\alpha+\sum_{k=1}^{3}H_\alpha^{(k)}(t-t_\alpha)^k/k!+\sum_{k=1}^{5}C_k'(t-t_\alpha)^{k+3}, \tag{20}$$

$$V(t)=V_\alpha+\sum_{k=1}^{2} V_\alpha^{(k)}(t-t_\alpha)^k/k!+\sum_{k=1}^{4} B_k'(t-t_\alpha)^{k+2} \tag{21}$$

and substituting them into (14), (15), we obtain expressions that will be used to determine the control effects δ_b and α_{cg}. Coefficients C_i' (i = 1,...,5) and B_j (j = 1,...,4) in (20) and (21) are determined from the conditions of the passage of programs (20) and (21) through their final states.

In order to fulfill the condition of monotonicity of the trajectory H(t), we have derived the following relationship for selecting time t_β:

$$-\frac{210(H_\alpha-H_\beta)}{120\dot{H}_\beta+90\dot{H}_\alpha}+t_\alpha<t_\beta<-\frac{840(H_\alpha-H_\beta)}{504\dot{H}_\beta+336\dot{H}_\alpha}+t_\alpha. \tag{22}$$

Now, in order to formulate control in accordance with a closed cycle, we make the following substitutions [2,3] in equations (14) and (15):

$$\begin{gathered} t_\alpha=t,\quad H_\alpha=H(t),\quad \dot{H}_\alpha=\dot{H}(t),\quad H_\alpha^{(2)}=H^{(2)}(t),\quad H_\alpha^{(3)}=H^{(3)}(t),\\ V_\alpha=V(t),\quad \dot{V}_\alpha=\dot{V}(t),\quad V_\alpha^{(2)}=V^{(2)}(t). \end{gathered} \tag{23}$$

We then obtain the system of equations

$$\dot{\alpha}_{cg}=(E_1'k_5+E_2'k_7)/(b_4(k_5k_6+k_7k_8)), \tag{24}$$

$$\delta_b=(E_1'k_8-E_2'k_6)/(k_9(k_5k_6+k_7k_8)), \tag{25}$$

where

$$E_1'=4!c_1'M_1'-k_6k_{10}-k_7k_{11},\ E_2'=3!B_1'+M_2-k_8k_{10}+k_5k_{11},$$

$$C_1'=-(1680(H-H_\beta)+840(\dot{H}+\dot{H}_\beta)(t_\beta-t)+180(H^{(2)}-H_\beta^{(2)})(t_\beta-t)^2+$$

$$+20(H^{(3)}+H_\beta^{(3)})(t_\beta-t)^3+H_\beta^{(4)}(t_\beta-t)^4)/(4!(t_\beta-t)^4),\quad B_1'=-(120(V-V_\beta)+$$

$$+60(\dot{V}+\dot{V}_\beta)(t_\beta-t)+12(V^{(2)}-V_\beta^{(2)})(t_\beta-t)^2+V_\beta^{(3)}(t_\beta-t)^3)/(3!(t_\beta-t)^3),$$

$$H^{(2)}=\dot{V}\sin\theta+V\dot{\theta}\cos\theta,\quad H^{(3)}=g/GP\sin\vartheta+g/GP\omega_z\cos\vartheta-2k_1k_2V\dot{V}-$$

$$-k_1V^2(\dot{\alpha}k_4+\dot{\vartheta}k_3),\quad V^{(2)}=\dot{P}g/G\cos\alpha-\dot{\alpha}k_3-2k_1c_xV\dot{V}-g\dot{\theta}\cos\theta,$$

$H_\beta^{(2)}$, $H_\beta^{(3)}$, $H_\beta^{(4)}$ and $V_\beta^{(2)}$, $V_\beta^{(3)}$ can be chosen on the basis of the condition of monotonicity of the process by zero-order points and defined more precisely during the modeling.

Equation (25), for δ_b, is computed at each step of the integration of equation (24), for the initial condition $\alpha_{cg}(t_\alpha) = \alpha_{cg\ \alpha}$, the right side of which is a nonlinear combination of phase coordinates. The coefficients of the nonlinear combination are functions of the TKK's aerodynamic, geometric and weight parameters. Besides this, they include time t and terminal state (9).

Thus, we have derived the law for controlling a TKK's motion in the vertical plane, with both altitude and velocity control, as formulated in accordance with a closed cycle.

The proposed algorithm for the formulation of control effects (24) and (25) can be used for stabilization purposes if H_β = const, V_β = const, $t_\beta - t = \Delta t$ = const, and for tracking purposes if $H_\beta = f_1(t)$, $V_\beta = f_2(t)$, $t_\beta - t = \Delta t$ = const. In this case, $\lim_{t\to\infty}(f_1(t) - H(t)) \to 0$.

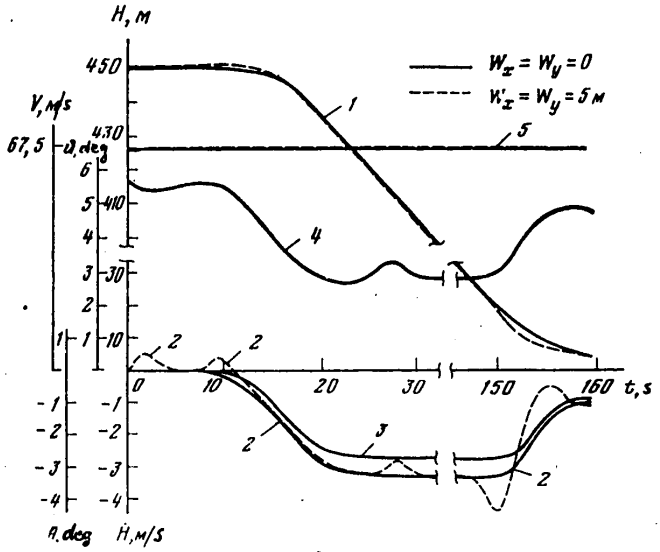

Figure 1. Dependence of H, $\dot{H}$, θ, , V on time. Curves: 1 = = H(t), 2 = $\dot{H}$(t), 3 = θ(t), 4 = (t), 5 = V(t).

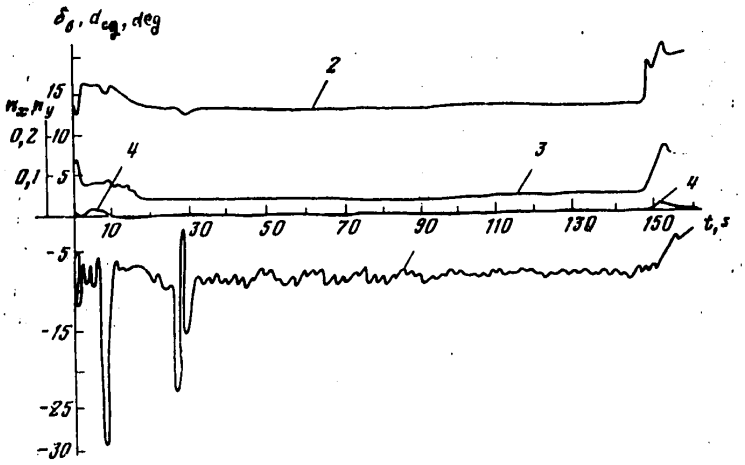

Figure 2. Dependence of δ_b, α_{cg} and overloads n_x, n_y on time. Curves: 1 = δ_b(t), 2 = α_{cg}(t), 3 = n_x(t), 4 = n_y(t).

We carried out digital modeling of the closed system of an equation including the object itself (1)-(7) and control algorithm (24), (25). The following maneuver was examined. The first section consists of horizontal flight at an altitude of 450 m for a period of 8 s. In this case, in algorithm (24), (25), it was assumed that $t_\beta - t = \Delta t$ in coefficient C_1'. In the second section, there was a descent from altitude H_α = 450 m to H_β = 414 m. Here the TKK's motion was formulated according to the tracking principle. Function $f_1(t)$ is given as

$$f_1(t) = H_\alpha + \dot{H}_\alpha T + \frac{1}{2!} H_\alpha^{(2)} T^2 + \frac{1}{3!} H_\alpha^{(3)} T^3 + \sum_{k=1}^{5} d_k T^{k+3},$$

where d_i ($i = 1,\ldots,5$) is calculated from the condition of the fulfillment of the final state, $T = t_\beta - t + \Delta T$, and $t_\beta - t = \Delta t$ in coefficient C_1'.

The next section consists of rectilinear motion along the glide path to an altitude of 24 m, with a vertical descent rate H(t) of 3.2 m/s. Here function $f_1(t)$ is given in the form $f_1(t) = H_\alpha + (H_\beta - H_\alpha)(t + \Delta t)/t_\beta$.

The maneuver is completed with a leveling-off section and descent until the landing gear wheels come in contact with the runway. Here we examined the bringing of the TKK to the point $H(t_\beta) = 4m$, $\dot{H}(t_\beta) = -0.7$ m/s by moment $t_\beta = 10.2$ s, as computed from monotonicity condition (22). The speed was regulated during all sections of the maneuver, and kept constant at V = 67.5 m/s. For this purpose, in coefficient B_1' it is necessary have the difference $t_\beta - t = \Delta t_1$. From the results of the modeling, the values $\Delta t = 1$, $\Delta t_1 = 0.5$ were chosen. The modeling was carried out with due consideration for disturbing effects $W_x = W_y = 5$ m/s, with a wind shear at altitude H = 24 m.

The results of the modeling are presented in Figures 1 and 2. They confirm the effectiveness of the algorithm for controlling altitude and speed that was obtained. An analysis of control algorithm (24), (25) showed that it can also be used as an on-board one.

BIBLIOGRAPHY

1. Zhevnin, A.A., Toloknov, V.I., and Shevyakov, O.V., "Programmed Control of Transport Spacecraft Landings on Earth," KOSMICH. ISSLED., Vol 13, No 6, 1975, p 935.

2. Zhevnin, A.A., and Glushko, Yu.V., "Synthesis of an Algorithm for Controlling Nonlinear, Nonstationary Objects on the Basis of the Inverse Problem of Dynamics," DAN, Vol 256, No 5, 1981, p 1057

3. Zhevnin, A.A., and Krishchenko, A.P., "Controllability of Nonlinear Systems and Synthesis of Control Algorithms," DAN, Vol 258, No 4, 1981, p 805.

11746
CSO: 1866/86

UDC 629.783.064: 519.863

SYNTHESIZING PLANNING PARAMETERS FOR ARTIFICIAL EARTH SATELLITE'S POWER SYSTEM

Moscow KOSMICHESKIYE ISSLEDOVANIYA in Russian Vol 19, No 6, Nov-Dec 81
(manuscript received 9 Apr 80) pp 845-854

[Article by Yu. N. Chilin and M. A. Kuz'min]

[Text] The authors explain a technique for determining the optimum planning parameters for an ISZ's [artificial Earth satellite] power system. As the optimization parameter they use the minimum total mass of the solar and storage batteries and propulsion system used to compensate for aerodynamic resistance. They analyze the effect of several operating conditions on the choice of the solar batteries' planned electric capacity, the storage batteries' capacity, and the specific impulse of the electric-heating reaction engine.

Propulsion systems based on low-thrust, electric-heating reaction engines (END) that receive electricity from orientable solar batteries (SB) are extremely promising as a means for maintaining an ISZ's orbital parameters [1]. At the same time, these batteries can supply electricity to other equipment installed in the ISZ.

The existence of shaded sections in an orbit results in the necessity of using storage batteries (AB) in combination with the SB's; under conditions of irregular power consumption, the AB's can also be used to cover electrical load peaks in illuminated sections of the orbit.

Thus, the power system (ES) for covering irregular on-board equipment load schedules and to compensate for an ISZ's aerodynamic resistance consists of sets of SB's and AB's and a propulsion system.

An analysis of the ES shows that among the masses of the SB's, AB's and propulsion system there exists an optimum relationship that corresponds to their minimum total mass [2].

Consequently, in the initial stages of preliminary planning, the choice of the planning parameters should be made with due consideration for the mutual effects of the SB', AB's and propulsion system. In connection with this, the development of the appropriate techniques is an important problem.

The purpose of this article is to explain one of the possible ways of determining the optimum values of the SB's planned electric capacity, the AB's planned capacity and the END's specific impulse, as well as to analyze the effect of the operating conditions on these parameters.

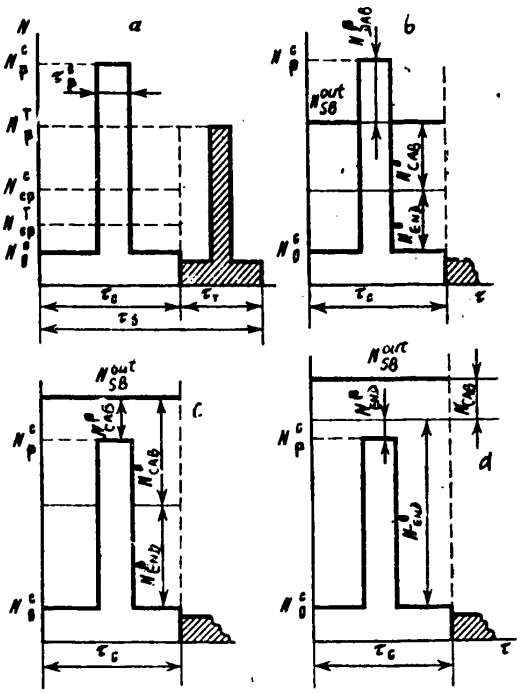

Figure 1. Variants of power system operation.

The problem is formulated in the following manner. The basic indicator of the effectiveness of the fulfillment of its assignments by the ES is an indirect economic criterion: the ES's flight weight, which--if the weight of the correction engine itself is ignored--is determined by the expression

$$m_{ES} = m_{SB} + m_{AB} + m_{PT}, \qquad (1)$$

where m_{SB} = weight of the SB's, along with their panel orientation and deployment system; m_{AB} = weight of the AB's and their thermal regulation system; m_{PT} = weight of the tanks and the working body.

All the factors affecting the ES's mass are provisionally divided into external and internal ones. The external factors include the set of conditions under which the system must operate. These include the characteristics of the ISZ's orbit (density ρ of the surrounding medium, the solar constant E_C, the modulus of velocity vector v, duration τ_B of a single ISZ orbit, illuminated τ_C and shaded τ_T periods in the orbit and so on), duration t of active functioning, and the ISZ's aerodynamic characteristics (resistance coefficient C_X^{ISZ} and area of the maximum cross-section S_M^{ISZ}), as well as the characteristics of the on-board equipment's load schedule. It is assumed that the resulting load schedule consists of identical orbital schedules (Figure 1a) corresponding to the most loaded (from the viewpoint of irregular power consumption) case and characterized by "duty" N_0^c, average N_{cp}^c and peak N_p^c electric capacities required during the illuminated section of the orbit and the average N_{cp}^t and peak N_p^t capacities required during the shaded section of the orbit.

The internal factors characterize the component parts of the system and consist of two groups. The first consists of the parameters that are fixed in a given problem. They include: the subsystems' efficiency (η_{SB}, η_{AB}, η_{END}); specific masses of the solar batteries μ_{SB}, storage batteries μ_{AB} and AB thermal regulation system μ_{CTP}^{AB}; the relative mass of the engine's tanks K_b; the planned electric capacity's utilization factor a_{SB} and the SB's coefficient of aerodynamic resistance C_x^{SB}; the AB's charge U_{AB}^c and discharge U_{AB}^d voltage; the maximum allowable charging I_c^{max} and discharging I_d^{max} currents and rated capacity q_r of an individual AB unit; the maximum possible specific END impulse I_{sp}^{max}.

The second group of internal factors consists of control parameters: the SB's planned electric capacity N_{SB}, the AB's planned capacity Q_{AB} and the END's specific impulse I_{sp}. A change in these parameters in a certain direction results in the achievement of the minimum value for the ES's mass.

Technological, operational and other limitations are placed on the values of the control parameters.

The AB's planned capacity is selected on the basis of the following conditions: 1) not exceeding the maximum allowable charging and discharging currents of the individual storage batteries; 2) observation of the the maximum (for considerations of reliability) depth of AB discharge ξ_{AB}.

These limitations are taken into consideration by the relationship

$$Q_{AB}=\max\left\{\frac{q_r N_{CAB}^{max}}{U_{AB}^{c} I_{c}^{max}};\ \frac{q_r N_{DAB}^{max}}{U_{AB}^{p} I_{p}^{max}};\ \frac{N_{ep}^{\tau}\tau_{\tau}}{\xi_{AB} U_{AB}^{p}}\right\}, \tag{2}$$

where N_{CAB}^{max} and N_{DAB}^{max} are the AB's maximum charging and discharging capacities.

The AB's maximum depth of discharge is determined as a function of the required number of charge-discharge cycles, in accordance with the empirical characteristics of the cycling that are inherent in the given type of storage battery.

A limitation is imposed on the END's specific impulse, based on considerations (for example) of not melting the heating chamber:

$$I_{sp}\leq I_{sp}^{max}. \tag{3}$$

The SB's planned electrical capacity is selected with due consideration for redundancy of the photoelements for the purpose of insuring the given level of reliability, as well as with due consideration for the losses caused by an increase in the photoelements' temperature, the effect of numerous factors encountered in outer space, the transmission and conversion of electrical energy, and the amount of power used to power the electric panel orientation motors:

$$N_{SB}=N_{SB}^{out}/a_{SB}, \tag{4}$$

where N_{SB}^{out} = the SB's electric power output; a_{SB} = a coefficient allowing for the factors listed above.

The SB's electric power output is determined on the basis of satisfying the on-board equipment's electricity requirements, providing the END with electricity, and observing the AB power charge and discharge balance during a single ISZ orbit. It is obvious that it is rational to use the END during the illuminated section of the orbit, when electricity is supplied to the motor directly from the SB's. In the general case, therefore (when the question of using the AB's to cover electrical load peaks in illuminated sections of the orbit is not answered), these conditions have the form

$$\begin{gathered} N_{SB}^{out}=N_{CAB}^{0}+N_{END}^{0}+N_{0}^{c},\quad N_{SB}^{out}+N_{DAB}^{p}=N_{CAB}^{p}+N_{END}^{p}+N_{p}^{c}, \\ \eta_{AB}(N_{CAB}^{0}\tau_{0}^{c}+N_{CAB}^{p}\tau_{p}^{c})=N_{DAB}^{p}\tau_{p}^{c}+N_{ep}^{\tau}\tau_{\tau}, \end{gathered} \tag{5}$$

where N_{CAB}^{0}, N_{CAB}^{p} = charge capacities of the AB's in the "duty" and peak modes in the illuminated section of the orbit; N_{DAB}^{p} = discharge capacity of the AB's when covering the peak electrical load during the illuminated section of the orbit; N_{END}^{0}, N_{END}^{p} = electricity required by the END in the duty and peak modes during the illuminated section of the orbit; τ_{0}^{c}, τ_{p}^{c} = durations of the duty and peak modes, as

determined by the expressions

$$\tau_0^c = \frac{N_\beta^c - N_{0\beta}^c}{N_\beta^c - N_0^c}\tau_0, \quad \tau_\beta^c = \frac{N_{0\beta}^c - N_0^c}{N_\beta^c - N_0^c}\tau_0. \tag{6}$$

In the general case, the AB's maximum charge and discharge capacities are found from the conditions

$$N_{CAB}^{max} = \max\{N_{CAB}^0;\ N_{CAB}^\beta\}, \quad N_{DAB}^{max} = \max\{N_{DAB}^\beta;\ N_\beta^\tau\}. \tag{7}$$

The dependence of the ES's mass on the parameters characterizing the external and internal factors enumerated above is represented, in accordance with expression (1), in the following form:

$$m_{ES} = \mu_{SB}N_{SB} + \mu_{AB}Q_{AB} + \mu_{CTP}^{AB}(1-\eta_{AB})N_{CAB}^{max} + (1+K_b)\frac{I_{END}}{I_{sp}}\frac{t}{\tau_n}. \tag{8}$$

The END's single-orbit thrust pulse I_{END} must the sum of the pulses of the aerodynamic resistance of the ISZ's hull I_{ISZ} and the SB panels I_{SB} for one ISZ orbit:

$$I_{END} = I_{ISZ} + I_{SB}, \tag{9}$$

where

$$I_{ISZ} = \int_0^{\tau_n} C_x^{ISZ}(\tau)\frac{\rho(\tau)v^2(\tau)}{2}S_M^{ISZ}(\tau)d\tau, \tag{10}$$

$$I_{SB} = \int_0^{\tau_n} C_x^{SB}\frac{\rho(\tau)v^2(\tau)}{2}S_{SB}\cos\beta(\tau)d\tau, \tag{11}$$

$S_{SB} = N_{SB}/\eta_{SB}E_C$ = area of the SB panels; $\beta(\tau)$ = angle between the ISZ's velocity vector and the normal to the SB's surface, the law governing the change of which is determined by the SB orientation method.

In order to reduce I_{SB}, when the ISZ is in the shade it is advisable to arrange the SB panels parallel to the ISZ's velocity vector. In this case, $\beta(\tau) = \lambda/2$ in the shade and expression (11) acquires the form

$$I_{SB} = \frac{\tau_0 \bar{b}_{SB}}{\eta_{SB}E_0}N_{SB}, \quad \bar{b}_{SB} = \int_0^1 C_x^{SB}\frac{\rho(\bar{\tau})v^2(\bar{\tau})}{2}\cos\beta(\bar{\tau})d\bar{\tau}, \quad \bar{\tau} = \frac{\tau}{\tau_0}, \tag{12}$$

where $\bar{b}_{SB}$ = average (during the illuminated period) pressure of the aerodynamic resistance forces on the SB panels.

The END's specific impulse can be expressed by the well-known formula

$$I_{sp} = 2\eta_{END}\frac{E_{END}}{I_{END}}, \tag{13}$$

where E_{END} = electricity used by the END during one ISZ orbit:

$$E_{END} = N_{END}^0\tau_0^c + N_{END}^\beta\tau_\beta^c. \tag{14}$$

The problem is formulated in the following manner: for given values of the parameters characterizing the external factors and the group of fixed internal factors,

and allowing for the negative nature of all the ES's characteristics and limitations (2)-(5), (7), (9) and (12)-(14), find the values of the control parameters (N_{SB}, Q_{AB}, I_{sp}) that provide the minimum value of purpose function (8).

An analysis of the purpose function and the limitations shows that this problem belongs to the class of nonlinear programming problems. There exists no general method of for soling problems in this class, so it is necessary to develop a specific optimization algorithm, based on allowing for the special features of the system being modeled.

An analysis of the interaction of the ES's elements makes it possible to reduce the problem of multiparametric optimization to several simpler problems of minimizing the function of a single control variable in the presence of additional limitations on the range of the change in it.

It is not difficult to show that it is sufficient to examine three competing variants of ES operation (a graphic interpretation of them is presented in Figure 1b-d) that are realized in connection with the following additional conditions:

$$\text{Variant I: } N_{sб}^{out} \leqslant N_{р}^{c}, \quad N_{CAB}^{р}=N_{ENЗ}^{р}=0; \tag{15.1}$$

$$\text{Variant II: } N_{р}^{c}<N_{sб}^{out} \leqslant N_{р}^{c}+\frac{N_{CP}{}^{т}\tau_{т}}{\eta_{AB}\tau_{c}}, \quad N_{ЗAB}^{р}=N_{ENЗ}^{р}=0; \tag{15.2}$$

$$\text{Variant III: } N_{sб}^{out}>N_{р}^{c}+\frac{N_{CP}{}^{т}\tau_{т}}{\eta_{AB}\tau_{c}}, \quad N_{ЗAB}^{р}=0, \quad N_{CAB}^{0}=N_{CAB}^{р}=N_{CAB}. \tag{15.3}$$

Since the algorithms for finding the optimum solution are analogous for all the variants, we will examine in detail only the first one, which is the most typical from methodological viewpoint.

Having combined expressions (2)-(9), (12)-(14) and (15.1), with due consideration for the condition of non-negativeness of all the variables in them, after making some transformations we obtain

$$m_{ES}=\mu_{sб}N_{sб}+\mu_{CTP}^{AB}(1-\eta_{AB})(A-BN_{sб})+\mu_{kэш}\frac{(N_{sб}+S)^{2}}{CN_{sб}-D}+$$

$$+\mu_{AB}\max\left\{\begin{array}{l} Q_{AB_1}=\dfrac{q_{т}}{U_{AB}^{c}I_{c}^{max}}(A-BN_{sб}); \\ Q_{AB_2}=\dfrac{q_{т}}{U_{AB}^{Д}I_{Д}^{max}}(N_{р}^{c}-a_{sб}N_{sб}); \\ Q_{AB_3}=\max\left\{\dfrac{N_{р}{}^{т}q_{т}}{\eta_{AB}^{Д}I_{Д}^{max}};\ \dfrac{N_{cp}{}^{т}\tau_{т}}{\xi_{AB}U_{AB}^{Д}}\right\} \end{array}\right\}, \tag{16}$$

$$\frac{D}{C}=N_{sб}^{min}<N_{sб}\leqslant\frac{N_{р}^{c}}{a_{sб}}=(N_{sб}^{max})_{1}, \tag{17}$$

$$N_{sб}\leqslant\frac{2\eta_{ENЗ}D+\dfrac{I_{1ЗZ}}{\tau_{c}}I_{sр}^{max}}{2\eta_{ENЗ}C-\dfrac{b_{sб}}{\eta_{sб}E_{c}}I_{sр}^{max}}=(N_{sб}^{max})_{2}, \tag{18}$$

where

$$S=\frac{\eta_{SB}E_c I_{1SP}}{\tau_c b_{SB}};\quad \mu_{KBM}=\frac{(1+K_b)}{2\eta_{END}}\tau_c t\left(\frac{b_{SB}}{\eta_{SB}E_c}\right)^2;$$
$$A=\frac{N_P^c(N_{cp}^c-N_c^c)+N_{cp}^T(N_P^c-N_c^c)(1/\bar{\tau}_c-1)}{\eta_{AB}(N_P^c-N_{cp}^c)}.$$
$$B=\frac{a_{SB}(N_{cp}^c-N_c^c)}{\eta_{AB}(N_P^c-N_{cp}^c)};\quad C=\frac{a_{SB}}{(N_P^c-N_c^c)}\left[(N_P^c-N_{cp}^c)+\frac{(N_{cp}^c-N_c^c)}{\eta_{AB}}\right]; \tag{19}$$
$$D=\frac{N_{cp}^T}{\eta_{AB}}\left(\frac{1}{\bar{\tau}_c}-1\right)+\frac{N_P^c(N_{cp}^c-N_c^c)+N_c^c(N_P^c-N_{cp}^c)\eta_{AB}}{\eta_{AB}(N_P^c-N_c^c)}.$$

$\bar{\tau}_C = \tau_C/\tau_B$ = relative duration of the illuminated portion of the orbit.

Let us mention here that inequality (17) follows from the condition of nonnegativeness of variables N^0_{END} and N^P_{DAB}, while inequality (18), which expresses the limitation on the END's maximum possible specific impulse (3), makes sense only when

$$b_{SB}<b_{SB}^{np}=2\eta_{END}\eta_{SB}CE_c/I_{SP}^{max}. \tag{20}$$

Otherwise, limitation (3) is immaterial, since it is observed even when $N_{SB\to\infty}$, which is explained by the proportional increase in the SB's aerodynamic resistance impulse as their planned capacity is increased.

Let us also note here that the set of allowed values of N_{SB} (17) is not empty only when

$$N_P^c>N_{cp}^c+\frac{N_{cp}^T}{\eta_{AB}}\left(\frac{1}{\bar{\tau}_c}-1\right). \tag{21}$$

Thus, the first variant of the ES's operation can be realized only when there is a certain relationship of the load schedule's characteristics (clearly expressed unevenness in power consumption).

In the case where condition (21) is fulfilled, optimization of the variant under discussion consists of minimizing purpose function (16) in the presence of the bilateral limitation

$$N_{SB}^{min}<N_{SB}\leqslant N_{SB}^{max}, \tag{22}$$

where

$$N_{SB}^{max}=\begin{cases}(N_{SB}^{max})_1, & b_{SB}\geqslant b_{SB}^{np},\\ \min\{(N_{SB}^{max})_1;\ (N_{SB}^{max})_2\}, & b_{SB}<b_{SB}^{np}.\end{cases}$$

It is not difficult to demonstrate that function (16) over interval (22) is unimodal and, by using any of the well-known methods for finding the extremum of functions of this class [3], to determine the optimum value of N_{SB} with the required degree of accuracy.

At the same time, there exists the possibility of finding an exact numerical solution.

From function (16) let us form three auxiliary functions that differ from each other by the following components:

$$m_{ES_i} = \mu_{SB} + N_{SB} + \mu_{CTP}^{AB}(1-\eta_{AB})(A - BN_{SB}) + \\ + \mu_{KDU}\frac{(N_{SB}+S)^2}{CN_{SB}-D} + \mu_{AB}Q_{AB_i}; \quad i=1, 2, 3. \tag{23}$$

After reducing the similar terms, auxiliary functions (23) acquire the form

$$m_{ES_i} = E_i + F_i N_{SB} + \mu_{KDU}\frac{(N_{SB}+S)^2}{CN_{SB}-D}, \quad i=1, 2, 3, \tag{24}$$

where

$$E_1 = A\left[\frac{\mu_{AB}q_r}{u_{AB}{}^c I_c^{max}} + \mu_{CTP}^{AB}(1-\eta_{AB})\right]; \quad F_1 = \mu_{SB} - B\left[\frac{\mu_{AB}q_r}{U_{AB}{}^c I_c^{max}} + \mu_{CTP}^{AB}(1-\eta_{AB})\right];$$

$$E_2 = \frac{\mu_{AB}q_r}{U_{AB}{}^p I_p^{max}} N_p{}^o + A\mu_{CTP}^{AB}(1-\eta_{AB});$$

$$F_2 = \mu_{SB} - \left[\frac{\mu_{AB}q_r}{U_{AB}{}^p I_p^{max}} a_{SB} + B\mu_{CTP}^{AB}(1-\eta_{AB})\right];$$

$$E_3 = \mu_{AB}Q_{AB_3} + A\mu_{CTP}^{AB}(1-\eta_{AB}); \quad F_3 = \mu_{SB} - B\mu_{CTP}^{AB}(1-\eta_{AB}).$$

It is obvious that

$$m_{ES}(N_{SB}) = \max_{i=1, 2, 3} m_{ES_i}(N_{SB}). \tag{25}$$

An analysis of the auxiliary functions shows that they are all convex in the downward direction. For $F_iC + \mu_{KDU} \leq 0$, the function $m_{ES_i}(N_{SB})$ decreases monotonically over the interval $D/C < N_{SB} < \infty$, while for $F_iC + \mu_{KDU} > 0$ it has a minimum that is reached at the point

$$N_{SB_i} = \frac{D}{C} + \left(\frac{D}{C} + S\right)\sqrt{\frac{\mu_{KDU}}{(CF_i + \mu_{KDU})}}. \tag{26}$$

The abscissas of the auxiliary functions' points of intersection

$$N_{SB_1} = \frac{AU_{AB}{}^p I_p^{max} - N_p{}^o U_{AB}{}^c I_c^{max}}{BU_{AB}{}^p I_p^{max} - a_{SB}U_{AB}{}^c I_c^{max}};$$

$$N_{SB_2} = \frac{1}{a_{SB}}\left(N_p{}^o - \frac{U_{AB}{}^p I_p^{max}}{q_r}Q_{AB_2}\right); \tag{27}$$

$$N_{SB_3} = \frac{1}{B}\left(A - \frac{U_{AB}{}^c I_c^{max}}{q_r}Q_{AB_3}\right)$$

are determined from the conditions $Q_{AB1} = Q_{AB2}$; $Q_{AB2} = Q_{AB3}$; $Q_{AB3} = Q_{AB1}$, and the abscissas of the possible minimums (26), belongong to interval (22), divide the latter into intervals inside which each auxiliary function is monotonic and does not intersect the other two. This means that the unknown minimum of function (25) is reached at one of the division points or on the right boundary of interval (22).

Thus,

$$N_{SB}^{opt} \in R = \{N_{SB_j}\}_{j=1,\ldots,6} \cap (N_{SB}^{min}, N_{SB}^{max}) \cup \{N_{SB}^{max}\}$$

and

$$m_{ES}^{min} = m_{ES}(N_{SB}^{opt}) = \min_{N_{SB} \in R} \max_{i=1,2,3} m_{ES_i}(N_{SB}) = \min_{N_{SB} \in R} m_{ES}(N_{SB}).$$

Fixing the optimum value of the planned electrical capacity for the first variant is the only thing remaining to be done.

Optimization of the second and third ES operation variants is done analogously. We will mention here only the fact that for clearly expressed unevenness of power consumption by the on-board equipment, inequality (3) and the inequality from condition (15) for the corresponding variant can prove to be contradictory. This means that it is technically impossible to realize the given ES operation variant, it being the case that from nonrealizability of the second variant naturally follows the conclusion that the third variant is unrealizable. Thus, as the result of the preliminary analysis the number of optimizable ES operation variants can be reduced.

The solution of the problem is completed by comparing the optimized variants. As the final optimum value of the SB's planned electrical capacity we select the value N_{SB}^{opt} that corresponds to the variant with the smallest m_{ES}^{min}, after which the ES's other planning parameters (Q_{AB} and I_{sp}) are determined unambiguously.

In accordance with the technique that has been developed, a program for the solution of a specific problem on a computer was compiled. It was assumed that the ISZ's orbit is circular and is located in the plane of the ecliptic and that the SB's orientation is biaxial.

In this case, parameters $\bar{b}_{SB}$, $\bar{\tau}_c$ and τ_B are functions of a single orbital characteristic--its altitude h:

$$\bar{b}_{SB} = \frac{C_x^{SB} \rho(h) v^2(h)}{2} \cdot \frac{1+\cos\varphi_T(h)}{\pi - \varphi_T(h)}; \quad \bar{\tau}_c = \frac{\pi - \varphi_T(h)}{\pi}; \quad \tau_B = \frac{2\pi(R_3+h)}{v(h)},$$

where $\rho(h)$ is tabulated in [4]; $v(h) = R_E\sqrt{g_0/(R_E + h)}$; $\varphi_T(h) = \arcsin(R_E/(R_E + h)) =$ = half the angle of shading of the orbit; R_E = radius of the Earth; g_0 = free fall acceleration at the Earth's surface. The expressions for the single-orbit aerodynamic resistance impulse of the ISZ's hull (10) and parameter S (19) have the form

$$I_{ISZ} = \overline{C_x^{ISZ} S_M^{ISZ}} \frac{\rho(h) v^2(h)}{2} \tau_B; \quad S = \frac{\pi \overline{C_x^{ISZ} S_M^{ISZ}} \eta_{SB} E_c}{C_x^{SB} [1+\cos\varphi_T(h)]},$$

where

$$\overline{C_x^{ISZ} S_M^{ISZ}} = \int_0^1 C_x^{ISZ}(\bar{\tau}) S_M^{ISZ}(\bar{\tau}) d\bar{\tau}, \quad \bar{\tau} = \tau/\tau_B.$$

As our initial information we used data from the literature [1,2,4-6] on nickel-cadmium AB's, silicon SB's, radiative heat discharge systems and electric-heating engines. The relationship between the dimensions of the ISZ's hull and the amount of power consumed by the on-board equipment was characterized by the provisional parameter $\overline{C_x^{ISZ} S_m^{ISZ}}/N_p^C$ = 2m^2/kW.

The characteristics of the on-board equipment's energy consumption were represented by the following values of the load schedule's dimensionless parameters:

$$N_{cp}^{c}/N_{p}^{c}=0,5; \quad N_{0}^{c}/N_{p}^{c}=0,25; \quad N_{cp}^{r}/N_{p}^{c}=0,4; \quad N_{p}^{r}/N_{p}^{c}=0,8.$$

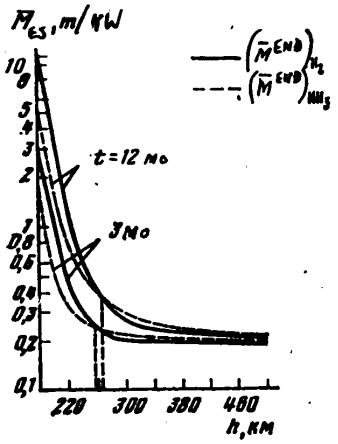

Figure 2. Dependence of minimized provisional power system mass on orbital altitude and duration of ISZ functioning.

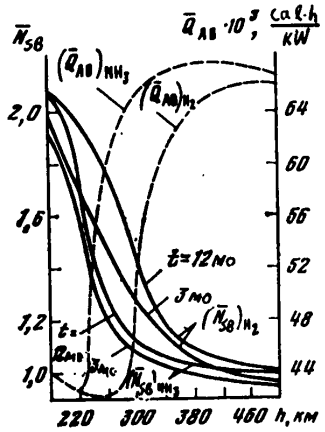

Figure 3. Dependence of optimum power system planning parameters on orbital altitude and duration of ISZ functioning.

Two types of END working body--hydrogen and ammonia--were discussed. Cryogenic storage of them on board the ISZ was assumed.

The altitude of the orbit varied from 180 to 500 km. The duration of the system's functioning ranged from 3 to 12 months.

As a result of the calculations, we obtained values for the power system's minimum mass and the optimum values of the planning parameters for the indicated range of changes in the initial data.

Figures 2 and 3 show the effect of orbital altitude, duration of operation and type of END working body (hydrogen or ammonia) on the minimized provisional (with respect to the maximum required power capacity N_p^c) mass M and the optimum values of the provisional power system planning parameters.

From an analysis of the graphs (Figure 2) it follows that preference can be given to either of the working bodies under discussion.

For orbits at altitudes of less than 260 km, it is advisable to use ammonia as the END's working body. At higher altitudes (h > 260 km), hydrogen works better. The duration of the ISZ's functioning has no practical effect on the boundary for the rational use of the given working bodies.

The preferential use of ammonia in low orbits is the result of the lower (in comparison with hydrogen) relative mass of its tanks (the optimum value of the END's specific impulse is still far from the maximum possible one (see Figure 4)). In higher orbits the possibility of selecting the maximum specific impulse takes precedence (the mass of the tanks is an insignificant percentage of the entire power system's mass) and it becomes advisable to use hydrogen.

An analysis of the graphs in Figure 3 shows that the strongest effect on the choice of the planned electrical capacity of the SB's and the capacity of the AB's is exerted by orbital altitude.

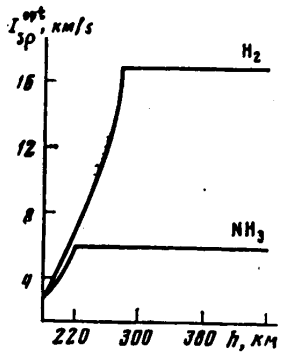

Figure 4. Dependence of optimum specific END impulse on ISZ orbital altitude.

As the orbital altitude increases, the optimum value of the SB's planned capacity decreases because of the reduction in the percentage of the electricity needed to power the END.

The optimum value for the planned capacity of the AB's first decreases as the orbital altitude increases, because of the reduction in the relative duration of the shaded period, and then increases. The latter fact is explained by the need for an increase in Q_{AB} for the purpose of observing the limitation on the maximally allowable charging current (AB charging for this band of altitudes is carried out only in the intervals between power consumption peaks and, consequently, the charging current is a high one.

The increase in planned SB capacity as duration of functioning increases (see Figure 3) is caused both by the need for photoelement redundancy for the purpose of insuring a given level of SB reliability and (in low orbits) the increase in electricity needed to power the END as the result of the increase in the optimum value of the END's specific impulse as t increases.

Figure 4 depicts the graphs of the dependence of the END's optimum specific impulse on orbital altitude and the type of working body used.

From an analysis of these graphs it follows that each orbital altitude value has its own optimum END specific impulse value I_{sp}^{opt}. As the altitude increases so does I_{sp}^{opt}, moving toward some limit I_{sp}^{max} imposed by the type of working body used and operational, structural and other limitations. For low-orbit ISZ's with power systems based on orientable SB's, it is necessary to select specific END impulse values that are lower than those maximally possible. This is explained by the fact that in low-altitude orbits, an insignificant increase in the END's specific impulse for the purpose of reducing the working body reserve requires a large increase in the SB's rated power, since increasing the amount of electricity used to power the END for the purpose of compensating for a braking impulse results, at the same time, in an increase in this impulse because of the increase in the area of the SB panels.

Conclusion

1. A technique for selecting the optimum planning parameters for an ISZ power system has been developed. This technique makes it possible to allow for the mutual effect of its most important subsystems. The discrimination and analysis of a finite number of variants for the power system's operation makes it possible to reduce the solution of the formulated problem to the minimization of a function with one variable and to the coordination of the obtained solutions, which makes it possible to formulate rather simple calculation algorithms.

2. An analysis was made of the effect of orbital altitude, the duration of an ISZ's active functioning and the type of END working body on the choice of the planned

electrical capacity of orientable SB's, the planned capacity of the AB's and the optimum specific impulse of the END.

3. The technique which has been developed and the recommendations that have been made can be used in the initial stages of the preliminary planning of prospective ISZ power systems.

BIBLIOGRAPHY

1. Mikelsen, "Present and Future Auxiliary and Service Propulsion Electric Reaction Engines," RAKETNAYA TEKHNIKA I KOSMONAVTIKA, No 12, 1967, p 181.

2. Grodzovskiy, G.L., Ivanov, Yu.N., and Tokarev, V.V., "Mekhanika kosmicheskogo poleta" [Mechanics of Spaceflight], Moscow, Izdatel'stvo "Nauka", 1975.

3. Yayld, D.Dzh., "Metody poiska ekstremuma" [Methods for Finding an Extreme], Moscow, Izdatel'stvo "Nauka", 1967.

4. Solodov, A.V., editor, "Inzhenernyy spravochnik po kosmicheskoy tekhnike" [Engineering Handbook for Space Technology], Moscow, Izdatel'stvo "Voyenizdat", 2nd edition, 1977.

5. Vasil'yev, A.M., and Landsman, A.P., "Poluprovodnikovyye fotopreobrazovateli" [Semiconducting Photoconverters], Moscow, Izdatel'stvo "Sovetskoye radio", 1971.

6. Kulandin, A.A., and Timashev, S.V., editors, "Voprosy kosmicheskoy energetiki" [Questions on Space Power Engineering], Moscow, Izdatel'stvo "Mir", 1971.

11746
CSO: 1866/44

UDC 681.3.01:629.7

AUTOMATING PROCESSING OF SCIENTIFIC EXPERIMENT RESULTS DURING OPERATIONAL CONTROL OF EXPERIMENTS CONDUCTED WITH SPACECRAFT

Moscow IZMERENIYA, KONTROL', AVTOMATIZATSIYA in Russian No 6, Nov-Dec 81 pp 43-47

[Article by M.Yu. Belyayev, candidate of technical sciences]

[Text] In both our country and abroad, much scientific research and many experiments are being conducted with the help of spacecraft (KLA), with a multitude of different measurements being made by instruments installed in these KLA's that, in particular, operate under extremely favorable conditions because of the lack of atmosphere at the altitudes at which spacecraft fly. Experience has shown that for the efficient execution of a program of scientific investigations with a KLA, it is necessary to exercise operational control over an experiment during spaceflight. The concept of controlling an experiment in space includes the problems of evaluating the status of the scientific research systems and working out control laws that insure the realization of an investigative program's goals with simultaneous minimization of the criterion of loss of control quality.

Information arriving at the flight control center (TsUP) from the scientific equipment can be categorized as service or scientific information. The problems involved in automating the operational analysis of service information have been discussed in detail in [1]. At the present time, methods for the automated processing of the results of scientific measurements in connection with operational control during spaceflight are being developed intensively. The purpose of this article is to elucidate on the experience gained in developing these methods.

In space, research is being done in different areas of science and technology: astronomy, geophysics, technology and so on. Rockets, manned spacecraft and orbital stations (OS), artificial Earth satellites (ISZ) and automatic interplanetary stations are used for the realization of scientific programs. As a rule, the creation of specialized KLA's (technological, astronomical, geophysical and so on) is preceded by the development of the investigative techniques and equipment on board spacecraft and orbital stations. For example, the development of methods for the practical investigation of the Earth's surface was based on scientific and applied experiments conducted with the help of cosmonauts [2].

Since the first investigations in space lasted a comparatively brief amount of time and the techniques used in them were relatively simple, the scientific information was, as a rule, processed after the flight. With the development of methods for space research on long-term KLA's, the problem of the operational processing of

scientific information arriving at the TsUP during a flight has become an urgent one. The basic purpose of this processing is to obtain objective data for the purpose of working out recommendations for the further conduct of the scientific experiment; that is, to control the experiment [1,3]. At the same time, a number of other problems that facilitate the postflight analysis of the scientific information are also solved. Large flows of information (up to 10^{12} bits per day) are generated during the conduct of astronomical and geophysical experiments. Comparatively complex algorithms must be used for the operational processing of this information.

Let us discuss questions concerning the automation of the operational analysis of scientific information obtained during the conduct of the most complicated experiments on board spacecraft and orbital stations. First, however, we will give a brief description of the methods and equipment used in geophysical and astronomical investigations.

Geophysical Research. When our planet is studied from a KLA, observations are made in the most variegated bands of the Earth's spectrum of electromagnetic radiation. The following are typical of geophysical investigations [2]: visual observations (in the 0.40-0.64 μm band of wavelengths); photography (0.40-0.92 μm); television surveying (0.45-0.75 μm); infrared surveying (0.72-14.0 μm); microwave surveying (0.5-8.5 cm and longer); multizonal photography (0.40-0.92 μm); multispectral surveying (0.3-14 μm); spectrography (0.4-0.7 μm). Initially, investigations from space involved primarily visual observations and photography. After that, other and better remote sensing methods began to be used.

It should be mentioned here that only simultaneous surveying of the Earth's natural formations in different and quite narrow spectral intervals is capable of producing reliable and versatile information about the natural medium. Therefore, multispectral systems based on photomultipliers are used extensively to carry out geophysical investigations. The first multispectral space survey in the United States was conducted in 1969, with the "Nimbus-3" ISZ, in five spectral intervals, using a medium-resolution camera. An improved multispectral scanning system was installed in the ERTS-1 artificial satellite (United States), which was to investigate the Earth's natural resources after being launched into orbit on 23 July 1972. During the year the system was in operation, variegated data on the structure, composition and dynamics of the natural medium were obtained. At the same time, there arose difficulties in the processing of the information because of the extraordinarily large number of measurements that were made. These difficulties, in particular, delayed the launching of the ERTS-B ISZ by 2 years. In the USSR, multispectral surveys (on wavelength intervals of 0.5-0.6, 0.6-0.7, 0.7-0.8 and 0.8-1.1 μm) were carried out with the help of a four-channel system and a "Meteor"-series ISZ launched on 9 July 1974.

The great promise of space surveying of the Earth's natural resources is related to the possibility of measuring the intrinsic radiothermal radiation of its surface in the microwave band (0.3-30 cm). The basic advantage of microwave surveying is that it makes it possible to obtain information about the Earth's surface almost without regard to the presence of cloud cover. In the USSR, microwave surveying has been conducted with "Cosmos"-series ISZ's, while in the United States it has been done with the "Nimbus-5" ISZ, the "Skylab" OS and other KLA's.

Astronomical Research. Astronomical experiments are conducted on KLA's over almost the entire spectrum of electromagnetic radiation. X- and gamma-rays are recorded

by counters that register the arrival of photons within the instrument's field of view. Because of the high energy of photons, when they interact with a special substance--such as argon in X-ray instruments--charged particles are formed: electrons in X-ray telescopes and electron-positron pairs in the crystal scintillator of an gamma-ray detector. A Geiger-Müller counter filled with gas is the counter most often used in X-ray telescopes. Photons enter the counter's chamber through a special port covered with beryllium foil or capron. When the operating gas mixture is ionized by a rapidly moving photon, a current pulse is generated and registered by the counter; after conversion, it is then sent into the telemetry system.

Investigations of X-ray radiation are sometimes conducted with the help of mirror telescopes with glancing incidence of the rays For instance, X-ray sources have been investigated by the American "Uhuru" ISZ, the "Salyut-4" station and other KLA's [4-6]. The RT-4 equipment, developed by FIAN [Physics Institute imeni P.N. Lebedev, USSR Academy of Sciences], and the "Filin" installation, developed by IKI AN SSSR [Institute of Space Research, USSR Academy of Sciences] and GAISh [State Astronomical Institute imeni P.K. Shternberg], were used for this purpose on the "Salyut-4" station [4,5]. Gamma-rays were registered by the American "Explorer-11" satellite.

The Earth's atmosphere is almost completely opaque to ultraviolet radiation (30-300 nm; electromagnetic rays with wavelength $\lambda < 300$ nm are absorbed by the ozone layer), so the observation of ultraviolet sources must be done at altitudes of more than 60 km. As a rule, KLA's are used for this, although--generally speaking--rockets can also be used. Ultraviolet radiation receivers consist of photoelements, ultraviolet photon counters and photomultipliers.

As is the case with emissions in the ultraviolet and visible bands, investigative techniques for the infrared band (1-100 μm) differ little from the techniques used in terrestrial observations. Infrared radiation receivers are usually subdivided into photoelectric and thermal types, depending on their operating principle. Thermal receivers, which measure the increase in temperature of sensitive elements acted upon by infrared rays, can function over the entire band of investigated wavelengths, whereas photoelectric receivers register only radiation with a wavelength less than some critical value. When measurements are made in the infrared band, there arises the problem of distinguishing the useful signal against the background of noise caused by the emissions of the KLA itself. In some cases this problem is a serious engineering problem. The submillimeter (far-infrared) band from 100 μm to 3 mm has been studied the least, although the investigation of radiation in this band is a matter of considerable scientific interest. Radiation sources in the ultraviolet, infrared and submillimeter bands have been investigated with the help of a BST-1M telescope, from on board the "Salyut-6" station.

For investigations in the radio band ($\lambda < 10$ mm) it is also advisable to lift the radiotelescope into space, because radio waves with $\lambda \lesssim 2$ cm are absorbed in the Earth's atmosphere and those with $\lambda \gtrsim 30$ cm are reflected by the ionosphere. Radio research conducted on KLA's differs little in its techniques from research done by ground stations. The only differences are in aiming technique, telescope antenna stabilization and the method for transmitting the measured information to the consumer. The first such investigations were carried out from the "Salyut-6" station in the summer of 1979, using the KRT-10 telescope. In connection with this, in addition to the study of astronomical sources, the cosmonauts did radio mapping of the Earth's surface [7].

In all of the experiments that have been mentioned, radiation is the source of the information characterizing the physical processes taking place in the objects under investigation. The making of scientific measurements is accompanied by the appearance of analog and pulse signals. The former come from radiometers, photometers and other instruments; the latter appear during the registration of particles different types (electrons, protons and so on), as well as gamma quanta and X-ray radiation. In connection with this, pulse signals cannot be transmitted directly to Earth, since a very high request frequency would be required in the telemetry system in order to transmit them. As a rule, modern scientific instruments used for the registration of pulse signals contain special devices for the preliminary processing of them [8]. The method used most frequently is pulse selection according to certain criteria and calculation of the number of events accompanied by the appearance of pulses with given characteristics over some given amount of time (in such cases the signals appearing at the output are called digital-counting signals). Signals recorded during scientific experiments are transmitted to the TsUP over radiotelemetry equipment and there undergo statistical processing [9,10].

Let us examine several general principles of the design of a system for processing scientific information for the purpose of operational analysis during a flight in space. A preliminary program for the conduct of the scientific experiments is developed before the flight. However, since it is based on elementary and frequently inaccurate ideas about the phenomena to be studied, operational analysis of the scientific data is necessary in order to evaluate the adequacy of the measurements being made, test the principles on which the investigative technique is based and so on. The algorithms and programs for the operational processing of scientific telemetric information (TMI) can differ considerably from those used during postflight processing (the latter are usually determined completely by the experimenter). At the same time, some of the results obtained during the analysis of the information in the TsUP can also be used profitably during the detailed postflight processing. The need for an operational solution during an experiment of several problems that were previously solved only after the flight was over dictates the rapid growth of information flows. For instance, for KLA's that have been analyzed, information flows of 10^7-10^9 bits per day are typical.

Most continuous signals from scientific equipment on board a KLA can be regarded as random processes, while each specific result of a measurement is a realization of the random process being investigated. Although the random functions reflecting the physical processes being studied are transient ones, many real signals can be represented as being nontransient over some interval of time. Actually, a real signal F(t) from a scientific instrument can be written as

$$F(t) = M(t) + f(t),$$

where M(t) = mathematical expectation, which changes slowly with time in the general case; f(t) = the centered random process, which is also transient in the general case (dispersion, the form of the spectrum and so forth change with time). In sections of the process's realization, however, after preliminary processing of the information it can be assumed that M(t) = const, the transience of f(t) can be ignored, and the algorithm for processing the signals from the scientific equipment can be simplified. However, if the assumption about the nontransience of a signal cannot be made, it is subject to special processing.

A general diagram of the processing of scientific information during the operational analysis of the results of experiments is depicted in Figure 1. After reception and

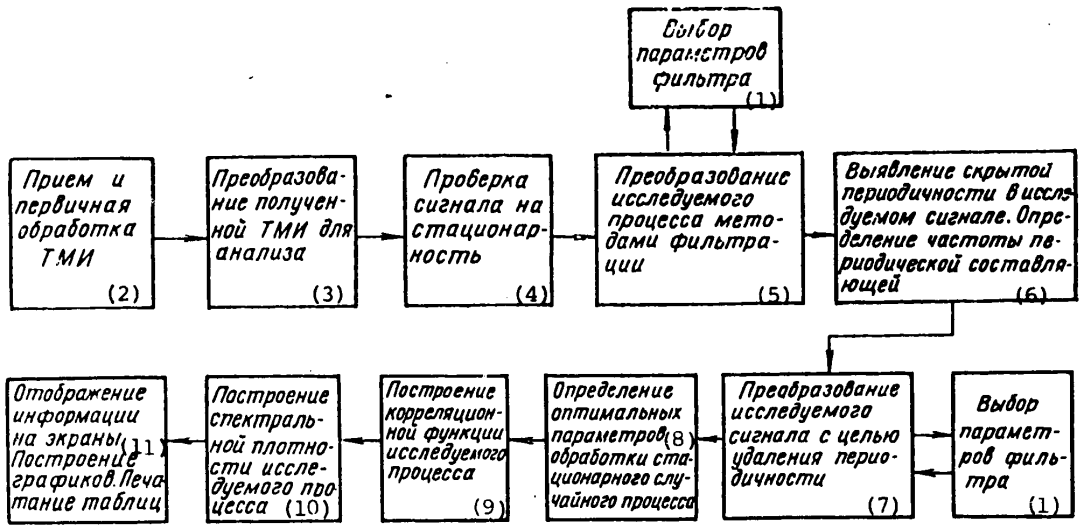

Figure 1. General diagram of automated processing of scientific information.

Key:
1. Selection of filter parameters
2. Reception and primary processing of TMI
3. Conversion of obtained TMI for analysis
4. Checking of signal for nontransience
5. Conversion of investigated process by filtration methods
6. Detection of hidden periodicity in investigated signal; determination of frequency of periodic component
7. Conversion of investigated signal for the purpose of removing periodicity
8. Determination of optimum parameters for processing steady-state random process
9. Construction of investigated process's correlation function
10. Plotting of spectral density of investigated process
11. Depiction of information on screens; plotting of graphs; printing of tables

primary processing, the TMI is presented in a form that is convenient for automated analysis; that is, it is enscribed in masses of a given form and volume on a carrier that can be used by a computer. The following processing phases are carried out preliminarily: data array redundance that appears as the result of the simultaneous reception of the TMI by several measuring points is eliminated, and unreliable information on the carrier is detected and marked by a special service character.

It should be mentioned here that during a KLA flight, operational processing of the telemetric information in the TsUP according to this system can be accomplished only when the information's qualitative level is quite high. The presence of intermittent failures lowers the probability of a correct interpretation of measurement results. In the case of the obtaining of TMI with intermittent failures and impossibility of its operational processing in the TsUP, either the experiment is repeated or the accumulated data are retransmitted from the KLA. The quality of TMI depends on a number of factors, including the organization of the process of transmitting and receiving it. The information is transmitted to the TsUP through measuring points [1]. It can be received and processed during a communication session with a KLA or with some temporal delay. During processing with a delay, there may appear additional interference caused by the preliminary recording and storage of

the information flows by the measuring points' facilities. TMI quality also depends on the method used to transmit it to the TsUP (broad-band and telephone channels and satellite communication are used for transmission), the time the KLA is in the measuring point's zone, the number of simultaneously transmitted TMI flows and so forth. Thus, TMI quality and, consequently, the quality of its subsequent processing are more or less determined during the stage when the flight and experimental programs are being planned.

In order to increase the accuracy of the determination of measurement times, special precision on-board clocks are used; their readings are registered simultaneously with the scientific measurements. After the unreliable TMI is determined, signals carrying additional information (about the orientation sensors, overloads and so on) for the analysis of an experiment's results are processed. Since we are specifying the automated processing of nontransient signals, they are first tested for nontransience (see Figure 1). If a signal is transient, it is subjected to filtration. The filtration methods and filter parameters are selected automatically or are entered in the processing program from the computer's console. Hidden periodicity in the investigated signal is then detected.

All conversions of the obtained scientific information should be approached cautiously, and at each stage of the processing it should be shown on display facilities for visual monitoring and analysis by the experimenter. There should also be a capability for changing the processing parameters according to instructions from the specialist who is analyzing the TMI. After signal filtration, the function characterizing the physical process can be regarded as random and the average and correlation functions, as well as the spectral density function, can be constructed. The optimum values of the statistical processing parameters are found by a dialogue process. The constructed functions are entered in a printer in the form of a graph and are used for the operational analysis of the results of the scientific experiments.

The system depicted in Figure 1 reflects only very general principles for the processing of scientific information during a KLA flight. In order to make a number of its aspects more specific, let us discuss how the automated operational analysis of TMI obtained from the equipment during the conduct of astronomical experiments is carried out. In accordance with the general principles for the automated analysis of scientific TMI when controlling a flight, the processing of information from astronomical equipment is carried out in two stages. In the first stage, the processing proceeds at the speed of TMI reception. The equipment's fitness for operation is determined, the correctness of the transmission of the control commands is confirmed, the degree of execution of the planned program and intensity of the observed sources are evaluated, and events corresponding to a change in intensity are registered. In the second stage, after the communication session with the KLA, the statistical characteristics of the obtained measurement results are determined and the spatial orientation of the KLA is refined.

Astronomical observations are made by aiming at the source or by surveying the celestial sphere. In the aiming mode, the KLA is stabilized in inertial space in such a fashion that the telescope's sensitive axis is directed at the object being investigated; in the survey mode, the spacecraft is oriented relative to the Earth according to the observation program (in connection with this, either triaxial or uniaxial orientation can be realized). The celestial sphere is surveyed because of the spacecraft's orbital motion. In connection with this, one effective method is

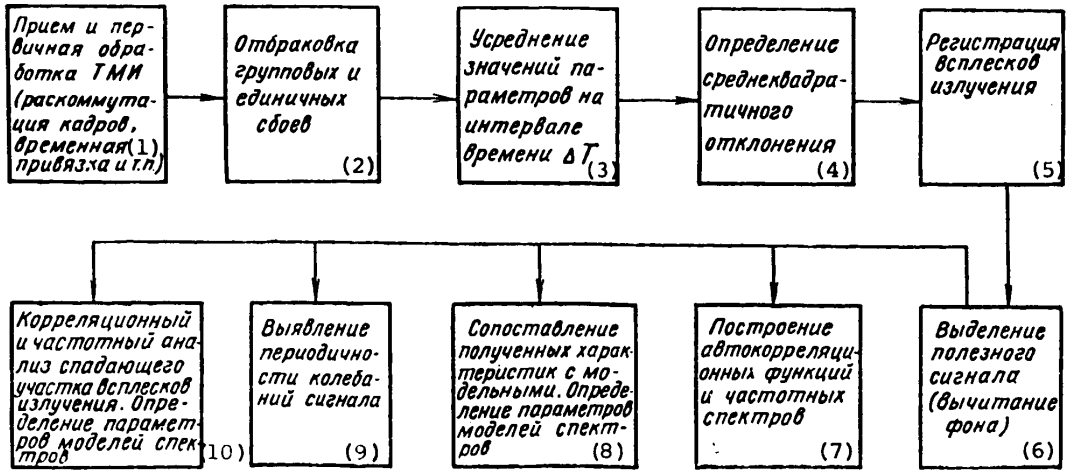

Figure 2. Diagram of automated TMI analysis when aiming mode is used.

Key:

1. Reception and primary processing of TMI (decommutation of frames, temporal correlation and so on)
2. Rejection of group and solitary intermittent failures
3. Averaging of values of parameters over time interval ΔT
4. Determination of root-mean-square deviation
5. Registration of radiation surges
6. Useful signal discrimination (subtraction of background)
7. Construction of autocorrelation functions and frequency spectra
8. Comparison of obtained and model characteristics; determination of parameters of spectra models
9. Detection of periodic signal fluctuations
10. Correlation and frequency analysis of diminishing section of radiation surges; determination of parameters of spectra models

torsion or controlled rotation of the KLA around an axis perpendicular to the telescope's sensitivity axis. When the passive torsion mode is used, it is necessary to allow for the KLA's angular position in the telemeasurement data.

Let us trace the organization of the operational processing of TMI during a flight, using the interesting example of experiments with X-ray equipment (in the case, the processing of the information reflects most fully the principles described in this article). Let us examine a system for the automated operational analysis of TMI obtained from an X-ray telescope in the aiming mode (Figure 2). In the X-ray equipment, the telemetry encompasses the outputs of differential discriminators in all the energy bands of a spectrometer, the output of an integral channel, service parameters and so forth [4]. After reception and primary processing of the TMI, group and isolated intermittent failures are discarded. Rejection of group intermittent failures is accomplished most frequently with the help of 0 and 100 percent levels transmitted from the spacecraft, while rejection of the isolated ones is carried out when the condition limiting the relative increase in reading speed is not fulfilled.

In the computer complex, the parameters' values are averaged over a given time interval ΔT and the root-mean-square deviation $\sigma_{\Delta T}$ is determined. If the reading

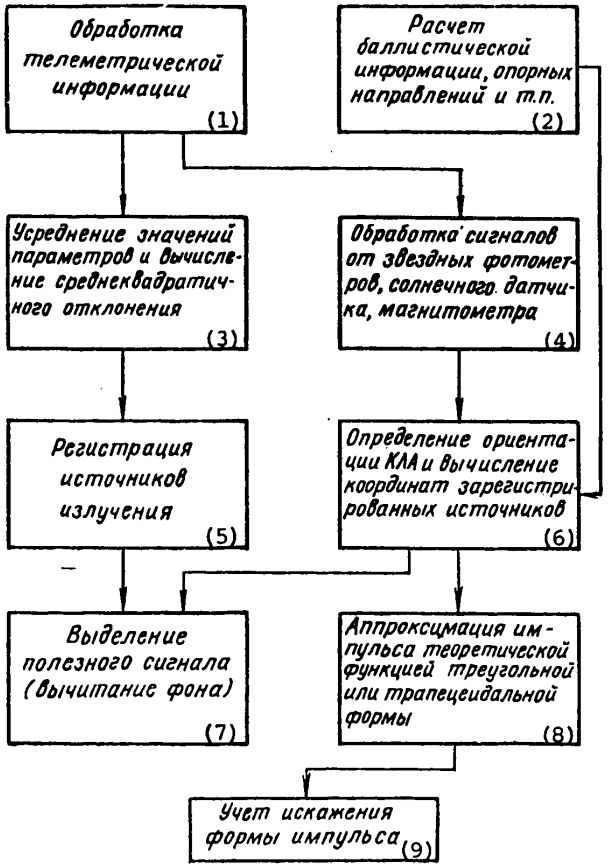

Figure 3. Diagram of automation of operational TMI analysis when survey mode is used.

Key:

1. Processing of telemetric information
2. Calculation of ballistic information, reference directions and so on
3. Averaging of values of parameters and computation of root-mean-square deviation
4. Processing of signals of stellar photometers, solar sensor, magnetometer
5. Registration of radiation sources
6. Determination of KLA orientation and calculation of coordinates of registered sources
7. Useful signal discrimination (subtraction of backgrouns)
8. Approximation of pulse by a theoretical function in triangular or trapezoidal form
9. Allowance for distortion in shape of pulse

speed deviates from that of the neighboring points by more than a given value ($x_i - x_{i+1} \geqslant 3\sigma_{\Delta T}$, for example), information on the presence of a surge of X-ray radiation is printed out. The true speed of reading from the observed sources is determined by subtracting the background reading speed. Information processed in this manner is displayed on television screens and printed out.

After the results of the preliminary processing are analyzed, autocorrelation functions and frequency spectra are constructed. The observed characteristics of the processed information are compared with model spectra and the parameters of the models of the spectra are determined (exponential and power dependences of the flow on the energy of the quanta are used as models [4,5]). In addition to this, any periodicity in the fluctuations of the signal being studied are detected. The results of the analysis carried out during the second stage of TMI processing are used in the operational planning of the program of experiments. The characteristics found after processing are compared with those obtained earlier and a conclusion is reached on the value of the information obtained, after which recommendations on further implementation of the program are made.

An algorithm for the operational processing of information during astronomical observations in the survey mode is presented in Figure 3. After primary TMI processing and computation of the statistical characteristics, the observed sources that came into the telescope's viewing field are registered. Information on the possible registration of a source is displayed when the reading speed deviates from that for the neighboring points by more than a given value ($3\sigma_{\Delta T}$, for example). The background (particularly that measured before and after registration of the source) is then substracted from the signal in order to determine its true intensity.

When making observations in the survey mode, it is important to determine the registered sources' coordinates accurately. This problem is solved by determining the spatial orientation of the KLA's axes, given the known orientation of the telescope's axis of sensitivity relative to the KLA's axes. The KLA's angular position is calculated on the basis of information from orientation sensors (solar sensor, magnetometer, stellar photometer and so on). Algorithms for determining KLA orientation according to measurement results, with due consideration for the specifics of operational information processing in a TsUP, are explained in [11,12]. A signal from an X-ray source that is registered in the survey mode is approximated by a theoretical function of triangular or trapezoidal form. The method of least squares is used to find the numerical values of the parameters (base of the trapezoid, height and so forth). Distortion of the shape of the pulse is also taken into consideration when processing a signal registered in the celestial sphere survey mode.

BIBLIOGRAPHY

1. Belyayev, M.Yu., "Automation of the Operational Analysis of Telemetric Information During the Conduct of Scientific Research on Board Spacecraft," IZMERENIYA, KONTROL', AVTOMATIZATSIYA, No 6, 1979, pp 57-63.

2. Vinogradov, B.V., "Kosmicheskiye metody izucheniya prirodnoy sredy" [Space Methods for Studying the Environment," Moscow, Izdatel'stvo "Mysl'", 1976, 287 pp.

3. Gernet, Ye.D., Zabiyakin, G.I., et al., "Rapid Processing of Information From Scientific Experiments on the 'Venera-11' and 'Venera-12' Automatic Interplanetary Stations," KOSMICHESKIYE ISSLEDOVANIYA, Vol 17, No 5, 1976, pp 686-689.

4. Babichenko, S.I., Goganov, D.A., Grechko, G.M., et al., "Some Results of Investigations of Cosmic X-Ray Radiation on Board the 'Salyut-4' Orbital Station," KOSMICHESKIYE ISSLEDOVANIYA, Vol 14, No 6, 1976, pp 878-891.

5. Novikova, G.V., Yerokhina, Ye.V., Kurt, V.G., et al., "Observations of X-Ray Sources in the Area of the Galactic Center and the Constellation Cygnus," KOSMICHESKIYE ISSLEDOVANIYA, Vol 15, No 2, 1977, pp 321-323.

6. Giacconi, R., Murray, S., et al., "The Uhuru Catalog of X-Ray Sources," THE ASTR. JOURNAL, Vol 178, 1 December 1972, pp 281-308.

7. Belyayev, M.Yu., and Tyan, T.N., "Research and Development of Economical Methods for Conducting Geophysical Experiments," ISSLEDOVANIYE ZEMLI IZ KOSMOSA, No 1, 1981, pp 90-95.

8. Yevdokimov, V.P., and Pokras, V.M., "Metody obrabotki dannykh v nauchnykh kosmicheskikh eksperimentakh" [Methods for Processing Data in Scientific Experiments Conducted in Space], Moscow, Izdatel'stvo "Nauka", 1977, 176 pp.

9. Boks, Dzh., and Dzhenkins, G., "Analiz vremennykh ryadov: Prognoz i upravleniye" [Analyzing Time Series: Prediction and Control], Moscow, Izdatel'stvo "Mir", 1st edition, 1974, 406 pp.

10. Anderson, T., "Statisticheskiy analiz vremennykh ryadov" [Statistical Analysis of Time Series], Moscow, Izdatel'stvo "Mir", 1976, 758 pp.

11. Belyayev, M.Yu., "Determining the Angular Position of a Spacecraft According to Telemetric Measurement Data," UCH. ZAP. TSAGI, Vol 9, No 4, 1978, pp 115-121.

13. Belyayev, M.Yu., "Determining Spacecraft Orientation According to Measurement Data," "Tr. pyatykh chteniy F.A. Tsandera. Sektsiya 'Astrodinamika'" [F.A. Tsander's Fifth Lecture Series: "Astrodynamics" Section], Moscow, 1978, pp 116-129.

11746
CSO: 1866/43

UDC 543.876

ANALYSIS OF EFFECT OF SEVERAL PARAMETERS OF LANDING VEHICLE OF 'VENERA-9'-'VENERA-12' AUTOMATIC INTERPLANETARY STATIONS ON STABILITY DURING LANDING

Moscow KOSMICHESKIYE ISSLEDOVANIYA in Russian Vol 19, No 6, Nov-Dec 81 (manuscript received 25 Jun 80) pp 913-918

[Article by P.P. Karyayev, Ye.I. Grigor'yev and S.N. Yermakov]

[Text] The authors use mathematical modeling of the performance of an automatic interplanetary station's landing vehicle during a landing on a planet's surface to find several design cases for the development of landing gear. The results of their calculations coincide quite well with the results of experiments.

One important characteristic that determines the fulfillment of its task by the landing vehicle (PA) of an automatic interplanetary station (AMS) when landing on the surface of a planet is the PA's stability when landing on a surface about which little is known. Initially, experimental methods of investigating the landing characteristics of a vehicle were used to evaluate PA stability during landing. These methods were frequently based on scale modeling [1,2]. The inadequacies of these methods were the impossibility of modeling several PA characteristics, such as the characteristics of the landing gear, and the complexity involved in modeling the characteristics of the planet being studied under terrestrial conditions. Later, methods for the mathematical modeling of the landing process with subsequent experimental testing of the results obtained [3,4] were developed and realized during the planning of a number of Soviet and American AMS's. In this article we explain a method for evaluating PA stability during landing that utilizes mathematical modeling of the landing process with correction on the basis of test data, as a result of which we were able to define several design cases for the development of PA stability. This method was used during the planning of the Soviet "Venera-9"-"Venera-12" AMS's.

In order to define a design case for the development of PA stability by mathematical modeling of the process of a PA landing on the surface of a planet, we determined the effect of parameters characterizing the PA and the conditions on the planet. We will understand "design case for stability" to mean that landing situation in which is achieved the maximum value of the angle between the PA's longitudinal axis and the local gravitational vertical, which determines the PA's limiting state in accordance with the chosen criterion for stability during landing Φ.

Structurally, the landing gear of the "Venera-9"-"Venera-12" AMS's consisted of a toroidal shell that was deformed during landing and absorbed the PA's energy at

the moment of impact, a shell attachment frame and a rigid truss by means of which the frame is attached to the PA's hull.

In order to formulate the mathematical model of the PA landing process, we used the equations of motion of a perfectly rigid body with attached, deformable landing gear; in connection with this, the toroidal shock absorption was represented by 10 separate legs. The experimentally obtained elastoplastic force-displacement diagram for each leg, which represents the dependence of the compressive force on the path of the compression, was approximated by a parabola. The flat, perfectly rigid landing surface was modeled by a set of planes in which each of the 10 landing gear legs had its own plane. The landing gear legs' coefficient of sliding friction on the surface was assumed to the constant for leg speeds not equal to zero and zero for zero velocities.

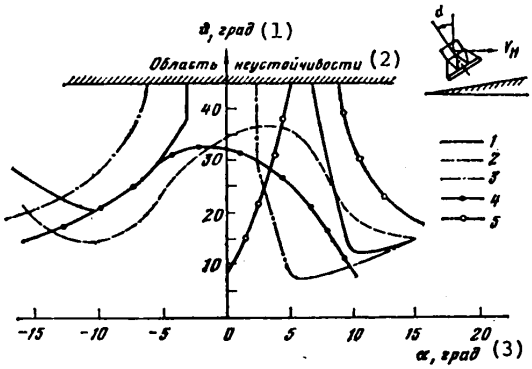

Figure 1. Effect of PA's initial angle of inclination α on stability: H = 0.1; μ = 0.3; V_B = 8.4 m·s^{-1}; I = = I_0 (2, 4); I = 1.1·I_0 (1, 3, 5); ϕ = 10° (1, 2); ϕ = 5° (3, 4); ϕ = 0° (5); V_H = 0 m·s^{-1} (1, 2): V_H = = -1 m·s^{-1} (3, 4); V_H = 1 m·s^{-1} (5).
Key: 1. ϑ, deg
2. Area of instability
3. α, deg

Using theoretical calculations only, it proved to be impossible to determine the force-displacement diagram of the landing gear because of the elastoplastic shock absorption characteristics and the elasticity of its design, which has a considerable effect on the amount of recoil H (here we will understand recoil H to mean the ratio of the elastic part of the landing gear's deformation under standard compression to the magnitude of this compression). At the same time, experimentally obtained shock absorption force-displacement diagrams cannot, in principle, allow for the dynamic nature of the landing process. Calculations showed that the shape of the force-displacement diagram for direct compression has little effect on PA stability when it changes within reasonable limits, so for a good approximation it is possible to use a static compression diagram by correcting the shock absorption recoil. Besides this, for all practical purposes the recoil defines unambiguously the height of the PA's rebound after the first impact; that is, the time between the first and second impacts. Thus, by knowing the calculative relationship and using bounce test data it is possible to determine the unknown shock absorption recoil.

The parameters affecting PA stability during landing were divided into several groups. Consideration was also given to the effect on PA stability of the following parameters, which characterize the physical properties of planets: angle of inclination ϕ of the planet's surface to the PU's [landing gear] base, the load-bearing capacity of the planet's soil, gravitational acceleration, atmospheric density.

Calculations showed that, within given limits, the landing area's angle of inclination is not definitive from the viewpoint of PA stability. The angle between the

slope and the PU's plane (see Figure 1) turns out to have a much greater effect on stability.

Bounce tests using an area of porous agglomerate sand (similar to yielding soil), with the angles of inclination to the horizon substantially exceeding the given ones, demonstrated the PA's stability. Thus, the worst case from the viewpoint of stability is a landing on hard ground, which is why a model of this type was used in the calculations. As an analog of perfectly hard ground we used cellular concrete. The calculated value of the shock absorption pressure on the area was 26 kg/cm^2. In the jump tests it was possible to achieve some increase in the calculated pressure by uneven distribution of the pressure forces over the contact area. Nevertheless, the deformations of the area were insignificant when compared with the deformations of the landing gear. Thus, cellular concrete with a load-bearing capacity of 30-40 kg/cm^2 differs little from perfectly hard ground as far as its effect on the stability of a given PU design.

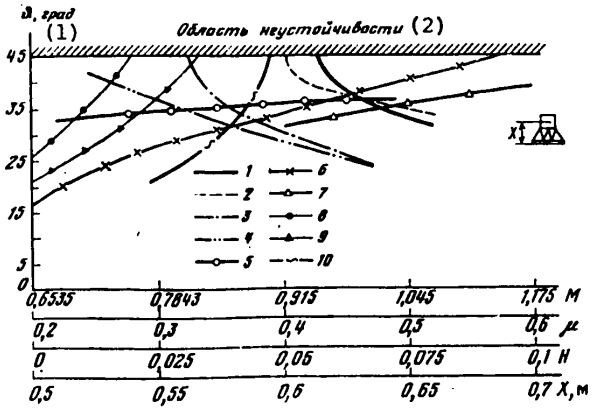

Figure 2. Effect of PA mass (M (1-4)), position of center of PA mass (X (5)), shock absorption recoil (H (6, 7)) and coefficient of friction (μ (8-10)) on stability: $\alpha = 5°$; $\phi = 10°$; H = 0.05 (5, 9); H = 0.1 (1-4, 10); H = 0.2 (8); μ = 0.3 (1-4, 6); μ = 0.5 (5, 7); $I = I_0$ (1, 2, 9); $I = 0.735 \cdot I_0$ (10); $I = 0.85 \cdot I_0$ (3, 4); $I = 1.06 \cdot I_0$ (6, 7); $I = 1.1 \cdot I_0$ (5, 8); $M = 0.836 \cdot M_0$ (10); M = $= 0.989 \cdot M_0$ (6-8); $M = M_0$ (5, 9); $V_B = 8.4$ m·s^{-1} (1, 3, 5-10); $V_B = V_B(M)$ (2, 4); $\overline{M} = MM_0^{-1}$.
Key: 1. ϑ, deg 2. Area of instability

An increase in gravitational acceleration is analogous to an increase in the PA's mass and results in improved PA stability (Figures 2 and 3).

A planet's atmosphere has a complicated effect on the dynamics of PA landing. In the first place, a buoyancy force acts on a PA, causing its stability to deteriorate; in the second place, the presence of an atmosphere results in the appearance of associated masses that are comparable to a PA's mass-inertial characteristics. The accurate determination of the elements of the associated masses' tensor for a PA of such a complex shape proved to be a practically unsolvable problem. On the one hand, the associated masses caused an increase in the PA's moments of inertia and caused its stability to deteriorate (Figure 3), while on the other, an increase in PA mass within certain limits caused it to improve.

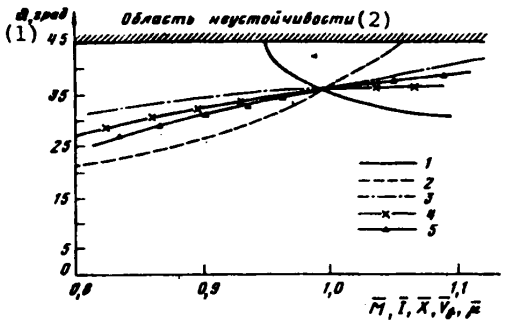

Figure 3. Comparative analysis of the effect of PA mass (M (1)), the PA's transverse moment of inertia (I (2)), the height of the PA's center of mass (X (3)), the PA's vertical landing velocity (V_B (4) and the PA's coefficient of friction on the surface (μ (5)) on stability: $\overline{M} = MM_0^{-1}$; $\overline{I} = II_0^{-1}$; $\overline{X} = XX_0^{-1}$; $\overline{V}_B = V_B V_{B_0}^{-1}$; $\overline{\mu} = \mu\mu_0^{-1}$; $X_0 = 0.611$ m; $V_{B_0} = 8.4$ m·s^{-1}; $\mu_0 = 0.3$.

Key: 1. ψ, deg
2. Area of instability

In our analysis of PA stability, as the PU's structural characteristics we used the following parameters (Figures 2 and 3): coefficient of completeness K of the shock absorption force-displacement diagram; shock absorption recoil H; the landing gear's coefficient of friction on the ground μ.

The coefficient of completeness K of the shock absorption force-displacement diagram equals the ratio of the shock absorption work on some compression path to the work that would have been done by the maximum force on the same path. As has already been mentioned, the shape of the force-displacement diagram and, consequently, its coefficient of completeness K have little effect on stability. The insignificant deterioration in stability when K increases is within the limits of accuracy of the initial data, such as the coefficient of friction μ or recoil H.

Recoil H has a substantial effect on PA stability (Figure 2). For a certain combination of PA parameters, even an insignificant increase in recoil can lead to a sharp deterioration in stability. For the PA under discussion, the recoil was within 10 percent limits and was basically rebound of the truss and the landing gear frame, so the problem of reducing the recoil was an extremely complicated one.

The coefficient of friction also has a considerable effect on stability. From Figures 2 and 3 it is obvious that the effect of coefficient of friction μ increases as the zone of instability is neared. The value of coefficient of friction μ is determined by the "shock absorption shell-ground" pair, and when material samples were dragged along the ground analog, values $\mu = 0.4$-0.6 were noted. However, tests showed that a coefficient of sliding friction of the landing gear on the ground of about 0.3 is realized. This is explained by shock absorption deformation in the direction of the slope when there are insignificant movements of the landing gear over the surface. Thus, replacement of the force of tangential shock absorption deformation by the force of friction is an adequate approximation, as demonstrated by a comparison with the experimental results, for engineering calculations; and, by reducing the rigidity of the landing gear's shock absorption in this direction it would be possible to reduce the effective coefficient, thereby improving stability.

As our calculations showed, the value of the maximum coefficient of friction--that is, that value for which the PA is still stable--increases as the angle between the landing area and the landing gear's plane of shock absorption does. This can be explained by the increase in shock absorption compression as the "scissors" grow larger and, as a result, the arm of friction forces relative to the PA's center of mass is reduced.

In our analysis of PA stability we discussed the effect of the following inertial characteristics of a PA: its inertia tensor, its mass M_0 and the position of the center of mass along the longitudinal axis X.

Since a plane situation was used as the design case for stability during landing, we examined the effect of the greatest (relative to the transverse axis) PA moment of inertia I. From Figure 3 it is obvious that when the moment of inertia increases, stability deteriorates considerably, which is particularly noticeable on the edge of the area of stability.

When the other parameters remain unchanged and the PA's mass is increased, there is an improvement in PA stability. However, the positive effect of an increase in mass is reduced substantially because of the simultaneous increase in vertical landing velocity (Figure 2). At the same time, the force that the PA's shock absorption apparatus has to absorb increases proportionally to the square of the mass. For low PA shock absorption energy reserves, an increase in its mass could result in a sharp deterioration in the landing gear's shock absorption characteristics and the PA's stability.

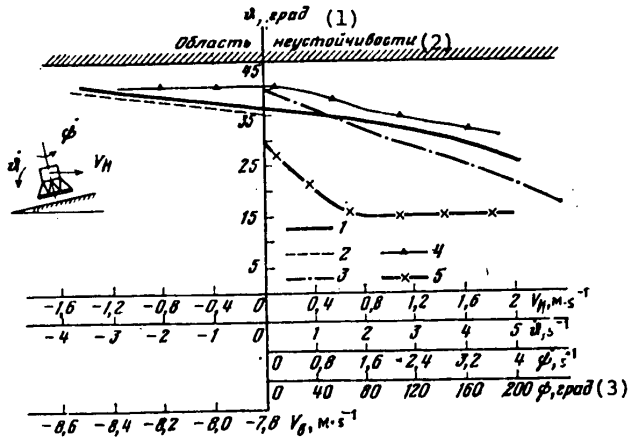

Figure 4. Effect of original horizontal (V_H (1)) and vertical (V_B (2)) components of the velocity of the PA's center of mass, the components of the PA's angular velocity ($\dot{\psi}$ (3)) and ((4)) and the PA's original angular position (ψ (5)) on stability: $\alpha = 5°$ (1-4); $\alpha = -15°$ (5); H = 0.05 (2, 5, 4); H = 0.1 (1, 3); $\mu = 0.3$ (1, 3, 5); $\mu = 0.5$ (2, 4); $I = 1.065 \cdot I_0$ (3); $I = 1.07 \cdot I_0$ (1); $I = 1.097 \cdot I_0$ (5); $I = 1.1 \cdot I_0$ (2, 4); $M = 0.989 \cdot M_0$ (3); $M = M_0$ (1, 2, 4, 5).
Key: 1. ϑ, deg 2. Area of instability 3. ψ, deg

Given a constant landing gear base, the location of the PA's center of mass determines its static angle of stability. It is obvious that as the height of the PA's center of mass increases, this angle decreases and stability deteriorates, which is confirmed by the graphs in Figures 2 and 3. It should be mentioned here that in the calculations we discovered an angle of dynamic stability that was less than the first angle by 10-15°.

In our calculations we also took into consideration the effect of kinematic characteristics on PA stability during landing: the velocity of the PA's center of mass, the PA's angular velocity relative to the center of mass.

As our design case we took the case of a plane landing, so we examined the effect on stability of the vertical and horizontal components of the velocity of the PA's center of mass. In the area of stability (Figure 4) there existed a practically linear dependence of stability on the vertical component of the velocity of the PA's center of mass (V_B), but it existed only when shock absorption was carried out correctly.

From Figure 4 it is obvious that it is possible for the PA to overturn for some horzontal velocity V_H value if it is negative. However, according to data gathered on preceding flights the horizontal component of the velocity of the PA's center of mass should be no more than 1 m/s and its effect on PA stability can be ignored.

The calculations showed that the components of the PA's angular velocity, which result in its movement through space, have little effect on stability when landing on a flat surface (Figure 4). Overturning of the PA is possible for some negative value of the component of angular velocity that is parallel to the PA's transverse axis ($\dot{\vartheta}$).

The calculations also showed that the PA's initial angular position, which leads to its spatial motion during the landing process, does not cause its stability to deteriorate (Figure 4). Some deterioration in stability was observed when the PA's longitudinal axis was tilted downward along the slope (Figure 1), with two-dimensional motion of the PA. Given a certain combination of PA and shock absorption parameters, the appearance of areas of instability determined by the initial angular position of the craft (angle α) is possible.

Thus, a comparison of the results of the mathematical modeling and experiments with flight results confirms:
1) the suitability of our method for investigating the stability of an AMS's PA during landing, which reduces considerably the amount of experimental development work needed for landing gear;
2) our conclusions on the effect of parameters characterizing the landing process on PA stability during landing.

BIBLIOGRAPHY

1. Herr, Robert W., "Outriggers as a Means of Improving Landing Stability of Legged Vehicles," NASA, Langley Research Center, Hampton, Virginia; AIAA Paper, No 68-307, 1968.

2. Bazhenov, V.I., and Osin, M.I., "Posadka kosmicheskikh apparatov na planety" [Spacecraft Landings on the Planets], Moscow, Izdatel'stvo "Mashinostroyeniye", 1978.

3. Polhen, J.C., "Planetary Lander Concepts Dictated by Touchdown Parameters," Martin Marietta Corporation, Denver Colorado; AIAA Paper, No 68-306, 1968.

4. Jones, R.H., and Hinchey, J.D., editors, "Some Basic Guidelines for Establishing Structural Design Parameters for the Landing Gear of Stable, Soft-Landing Spacecraft," Hughes Aircraft Company, El Segundo, California; AIAA Paper, No 68-345, 1968.

11746
CSO: 1866/44

SPACE APPLICATIONS

UDC 525:551:629.78

EARTH OBSERVATION BY FIRST-CREW COSMONAUTS OF SALYUT-6 ORBITAL STATION

Moscow ISSLEDOVANIYE ZEMLI IZ KOSMOSA in Russian No 1, Jan-Feb 82 (manuscript received 19 Mar 80, after revision 19 Mar 81) pp 5-13

[Article by G. M. Grechko, USSR cosmonaut, Yu. V. Romanenko, USSR cosmonaut, I. K. Abrosimov, L. V. Desinov, A. D. Koval', G. A. Nosenko, V. Ye. Permitin and V. V. Kozlov, "Priroda" State Scientific Research and Production Center; "Aerogeologiya" Geological Production Association for Regional Study of Geological Structure of the USSR, Moscow]

[Text] During recent flights of Soviet manned spaceships and obrital stations, broad studies have been made of the geological and geographic peculiarities of the earth's surface by visual-instrument observations. The possibilities of this method were manifested especially clearly during the long expeditions by cosmonauts such as the long phases of manned operation of the "Salyut-6" orbital station. High resolution of the visual analyzer of man and the capacity of the cosmonaut to solve complex logical problems offer the possibility of assigning the crew of an orbital station the duties of observing natural objects and analyzing their state under conditions of dynamic variability of the landscape. These observations can be made both by using the naked eye and using various instruments: binoculars, optical range finders, colorimeters, and so on. Cameras, television and spectrometric systems can be used to document the observation results. We call such observations visual-instrument studies of the natural environment.

When preparing for the flight of the "Salyut-6" orbital station on the basis of reports of Soviet cosmonauts in space in 1961 to 1977 [1-9], a program was developed for visual surveying of the land masses and bodies of water of the world ocean. A characteristic feature of this program was the fact that planned observation problems could be more precisely defined by the specialists and the cosmonauts themselves in flight. In addition to traditional operations of controlling the remote sensing equipment, this program assigned the crew the duty of more precise definition of the objects of investigation and selection of the time to study them as a function of illumination conditions, meteorological situations and other factors. Thus, the success of the entire experiment was determined by the creative capabilities of the crew, their training and fitness, and also the level of operative consultations between the cosmonauts and the assigners of the individual missions.

A characteristic feature of the "Salyut-6" orbital station is flight in the drift mode accompanied by arbitrary rocking of it and rotation around the center of masses. In order to survey the earth's surface by camera or spectrometers, usually active stabilization of the station by low-thrust motors is used. In this case the longitudinal axis of the "Salyut-6"-"Soyuz" complex is maintained perpendicular to the local vertical, for which an economical orientation and stabilization system is used, but it still consumes fuel. During the operations of photographing the earth by the stationary cameras, both crew members were heavily loaded with operations of servicing of the photographic and spectral equipment and monitoring the stabilization of the complex. The necessity for studying operative surveying assignments, recording the results on the on-board documents and preparation of reports for the Flight Control Center also require defined time from the time allotted for the experiments.

The crew was actually granted the possibility of visual-instrument observations of the earth only when the station was in the drift mode. At the same time, in a number of cases when approaching the research area where the cosmonauts, having prepared binoculars and cameras, took their places at the windows, the station was turned so that its solar cells cut off the view of the earth.

Quite quickly the crew became aware of the obvious law that the station always rocked around the transverse axes, on the average maintaining orientation with the solar cells down or up, and sometimes it did not move quickly from one orientation to the other. This fact gave the cosmonauts the idea of orienting the station by the longitudinal axis with respect to the local vertical and giving it an angular velocity in the plane of the orbit equal to the velocity of orbital rotation around the earth, extinguishing all other orthogonal components of the angular velocity. In other words, the cosmonauts decided to realize in practice the theoretically well known possibility of gravitational stabilization. Since the station had no special dampers to extinguish the natural oscillations in the orbital coordinate system, the required initial conditions were obtained by manual control of the micromotors, using a wide-angle viewer.

The effect from such dynamics as rotational motion of the station turned out to be excellent. The image of the earth in the viewer was almost stationary, and the rocking around the given position was minimally noticeable. There were periods when the station was in a state of gravitational stabilization up to 7 days, from one dynamic condition to the other. The crew was able to have an almost panoramic view from the station's transfer compartment, which had five windows. Creating a type of visual-instrument observation post of the natural environment here, the crew transmitted several hundreds of reports on the objects of investigation, accompanying many of them by pictures taken by a portable on-board camera.

In the future it is possible to imagine a station in which the remote sensing instruments are aimed at the earth along the longitudinal axis of the orbital complex, and pictures will be taken in the gravitational stabilization mode. Of course, such a station will be distinguished by an increased ballistic coefficient, increasing the rate at which it drops into the dense layers of the atmosphere. This effect reduced the lifetime of the American "Skylab" orbital station. However, in contrast to "Skylab," automatic refuelers can be regularly docked with the "Salyut-6" type stations, in practice sustaining them indefinitely.

A characteristic feature of the flight of the "Salyut-6" station is the fact that its path passes every two days over the same regions of the earth. Therefore, even during a prolonged expedition using stationary equipment it is not possible to make a continuous survey of broad regions or significant areas of the ocean. The use of manual cameras in many cases offers the possibility of filling this gap. The results of such work are determined by the actions taken by the crew. As a result of analyzing various visual experiment control systems, preference was given to the version in which the cosmonauts are given the authority to select the objects of observation in flight from a large number of previously planned assignments. For example, in order to estimate the possibility of observation of glacier pulsations from orbit, it was recommended that attention be paid to the mountainous regions of Pamir, Karakorum, the western part of the Himalayas and the ice fields of Patagonia. Considering the season of the observations (summer in the southern hemisphere), the orbital peculiarities and meteorological conditions, the most successful region turned out to be the last-mentioned one.

All of the flight assignments with respect to observations of the natural environment were grouped into six sections: geology, geography, oceanology, glaciology, meteorology and environmental control. Beginning with ballistic data, the specialists calculated the time of passage of the station over each object of observation and reported this time and the distance of the object from the path to the crew. It turned out that such information helps the cosmonauts to plan visual observations of the earth efficiently and accent attention on the key objects of the flight assignments.

The first weeks of on-board work demonstrated that in a large number of cases the mission of the specialists could not be carried out as a result of cloud cover over the selected part of the earth's surface. By the suggestion of the cosmonauts, they were granted the possibility of altering the choice of observation time. This solution was quickly felt, and positive results were recorded not only by those setting up the visual experiments, but also the medical flight support group, noting positive emotions in the crew caused by performing the visual-instrument observations.

The mission of the crew included evaluation of several types of different-scale topographic and geographic maps in order to select the most convenient of them for location and fixing of the objects of visual observations. It was established that the stated requirements are most completely satisfied by a 1:2,500,000 scale map. The crew poposed that the image of the earth's surface be brought into accordance with the true color of different landscape zones on the maps. Binoculars were delivered to support the on-board experiment. Trying them out, the cosmonauts found that six and twelve power binoculars are the most convenient. When observing bodies of water, a multicolor atlas was tried out. The experiment demonstrated that in order to obtain objective color indices of various parts of the dry land and water, it is necessary to use colorimeters. The same conclusion was also drawn during the 140-day flight of the second expedition when the number of shades of color on the atlas was increased to 196.

Attention should be given to the conclusion of the important role of standard objects well known to the cosmonauts from demonstration training flights on aircraft. Thus, when detecting linear geological structures the cosmonauts compared their observations with images of the Talaso-Fergan fault in Central Asia, the Dzhalair-Nayman fault and the Glavnyy Karatauskiy fault in Kazakhstan. When studying the hydrogeological peculiarities of arid regions the standards were the indicators connected with the development of vegetation, various types of sand or ancient river valleys within the territory of Turkmenia and Uzbekistan. Observing familiar natural training areas in the southern part of the USSR, the cosmonauts made recommendations to improve the theoretical training and the preliminary aerovisual observation programs for subsequent crews.

During the 96-day stay on board, the influence of weightlessness on the results of visual examination of the earth's surface was evaluated. It was noted that during the first days of the flight the sharpness of vision decreased insignificantly, and after adaptation to weightlessness, it remained almost unchanged. The general indices of the incoming scientific information about the natural environment are increased as a result of the observers' acquiring experience in visual study of the earth's surface. This is taken into account when planning the visual-instrument observation programs for the crews making short visits, including international crews. The basic crews are assigned the duties of preliminary examination of the objects of observation in order to estimate the optimal surveying conditions and to accumulate experience in quick detection of them by landmarks which can be seen well from orbital altitude. The main crew assists the visiting cosmonauts on short expeditions in implementing the programs for studying the natural environment.

Among the new organizational forms, attention must be given to the operative report to the crew prepared in the form of an express report about the course of the performance of the visual-instrument experiments and the first results from analyzing them. This type of report was delivered for the first time on board the "Salyut-6" station on the first expeditionary visit. The report contained a survey of the completed steps of the studies and focused attention of the cosmonauts on the primary goals of the upcoming period.

On completion of the 96-day flight of the first basic expedition, it became possible to develop recommendations with respect to the procedure for visual studies of the natural environment which included the following operations:

The study of the flight assignment by the on-board documents and operative supplements to it, preparation of observation and recording means;

Checking the stability of the position of the station with respect to the velocity vector of it in orbit and the performance of dynamic operations when necessary;

Detection of the object of observation on the terrain, using the cartographic material available on board and space photographs (SP) with respect to characteristic landmarks, in particular, fluctuations of the shorelines of the seas, large lakes, the drainage system, and with respect to segregated forms of relief;

The discovery of peculiarities of the object in accordance with the assignment;

Photographing the observation areas by an on-board manual camera;

Plotting the object on the map, schematic or SP in the flight log;

Recording of the observation and survey results (filling in the corresponding tables) and making drawings when necessary;

Reporting to the Flight Control Center about work performed, consultation with specialists who set up the experiments;

Additional study or photographing of the object upon receiving new recommendations from the specialists.

Let us discuss some of the examples of visual observations of the earth's surface from on-board the "Salyut-6" station. Here an important role has been attached to studying various geological objects. The performed experiments demonstrated that even by the naked eye numerous faults, folds, ring structures, volcanic systems, forms of relief of different genesis, areas of propagation of various types of surface deposits are clearly observed. With respect to their scope and direction, the geological problems which were solved by the crew can be divided into global, regional and local. The operative observations of certain geological phenomena made up a special group.

The global problems included, for example, the problem connected with determining the significance of ring structures in the earth's crust. Such structures were already known to geologists of the last century, but the development of cosmo-geological methods has attracted special attention to them. Therefore the mission was stated to observe the known structures and discover new ones. As a result of the studies, broad material was gathered on the possibilities of orbital study of ring formations. From an altitude of about 350 km individual unique ring structures such as Rishat in Mauritania, the El-Uveynat group in the Eastern Sahara, Konder in the USSR Far East are especially clearly visible. However, the number of such exceptionally clearly segregated ring structures of exceptionally regular shape is comparatively small. Much more frequently sections with concentric structure of the hydrogeological network, mountain ridges and other forms of relief, rock massifs of circular and oval shape are observed from orbit. Such structures are noted in large number, in particular, in the mountainous southern part of the USSR where their role in the structure of the earth's crust has still been far from completely established.

For subsequent orbital flights the goal can be stated of fixing all the observed large ring structures, giving a brief description of them. The result of such work (combined with deciphering the SP) can become a map of ring formations of the earth's surface, the scientific and practical significance of which is difficult to overestimate.

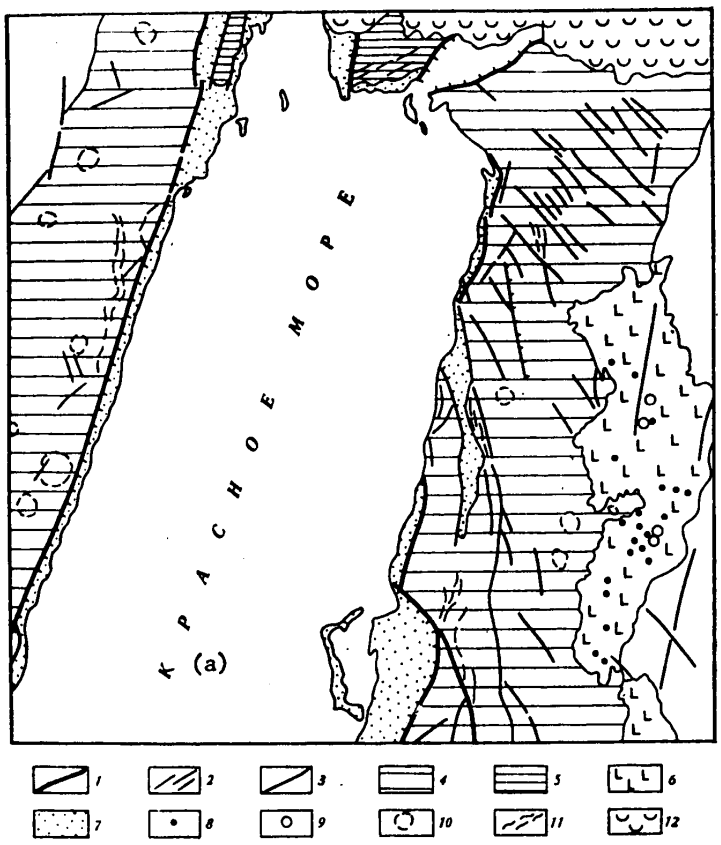

Figure 1. Diagram of deciphering the geological structure of the northern part of the Red Sea Rift by a space photograph taken by the KATE-140 camera from the "Salyut-6" DOS [permanent orbital station]: 1 -- regional faults along the outlines of a rift basin; 2 -- other dislocations with a break in continuity; 3 -- tectonic scarps along the faults; 4 -- halfarches along the outline of a rift valley (the arms of the rift); 5 -- horsts inside the rift system; 6 -- volcanic plateaus made up of Quaternary basalts; 7 -- depressions made up of Quaternary deposit; 8 -- volcanoes; 9 -- caldera; 10 -- tectonic-plutonic ring structures; 11 -- structural lines corresponding to bedding; 12 -- sections covered with clouds

Key:

a. Red Sea

Another goal of global order was connected with studying the largest faults in the earth's crust. The Yuzhno-Atlasskiy, Glavnyy Karatauskiy and many other faults extending hundreds and even a few thousands of kilometers were clearly visible from orbit. For example, the fault zone along the Himalayas was traced for almost 2000 km. Since such tectonic lines were observed in very high relief, an entirely defined mission has been planned with respect to discovering the principal faults of the earth. Such lines have been shown by different researchers far from unambiguously. Visual-instrument observations combined with interpretation of SP can provide the basis for making a more precisely defined map of the chief faults of the earth's crust. Making such map will promote the solution of a number of problems of geotectonics and more precise definition of the concepts of the seismogenic structures of the earth.

The regional problems of orbital geological observations are highly varied and consist in fixing various geological structures within the limits of a defined region and discovering the specific problems of the geological structure. For example, an orbital study was made of the Red Sea rift system to discover the role of transform faults in its structure and to discover other structural peculiarities (see Figure 1). Visual observations were accompanied by purposeful photography using stationary and hand cameras. The materials obtained demonstrate that genuine transform faults that clearly completely intersect the entire Red Sea rift as shown on some tectonic schemes are not detected here. At the same time, numerous transverse fractures and secondary dislocations with a break in continuity are obvious in the Red Sea mountains and Khidzhaze. On the northern end of the rift system, the transverse Wadi-Araba graben is noted, the fault boundaries of which are clearly visible on prospective photographs of this region, although they usually do not show up on geological maps.

Large faults which form the boundaries of the rift basin are especially clearly distinguishable. They are emphasized by straight or geniculate scarps running along the coasts. On the Arabian side a basalt plateau is distinguished with rows of well expressed volcanic systems, the high degree of preservation of which indicates recent, possibly Late Pleistocene or even Holocene age of the volcanic eruptions. It is remarkable that the basalt fields as a whole extend in the direction coinciding with orientation of the Red Sea rift. Therefore from the geodynamic points of view not only the rift basin, but the entire Red Sea system as a whole must be considered as a broad region of crustal tension with creviced rifts and additional jointing with volcanic systems spread over them.

The regional problems were connected with studying the structural pattern of the dislocations with a break in continuity or folded forms. A characteristic fracture pattern was observed, for example, in the southern part of the Patagonean Andes where the system of fjords in the form of rectilinear segments forms a complex network. The dislocations with a break in continuity and fracture zones are emphasized here as a result of activity of the ancient glacial cover. The reticular pattern of the faults is especially characteristic of regions of widespread magmatic or metamorphic rock, in sections with relatively shallow occurrence of the consolidated base. The discovery of such sections is important to the solution of many regional tectonic problems.

The problems of orbital geological observations of local order are connected with the solution of specific problems of discovering certain geological structures, including those that play an important role in the location of ore regions and zones of oil and gas accumulation. In particular, this pertains to individual ring structures which are noted when deciphering the SP. The study of them by traditional methods encounters great difficulties. Observation experience shows that here it is efficient to state missions to study ring structures no less than a few tens of kilometers in diameter.

Examples of such problems of local order which are accessible to study from orbit include the following:

Tracing individual large faults in sections where they are masked by surface deposits, for example, the northwestern continuation of the Glavnyy Karatauskiy or Dzhalair-Naymanskiy faults in Kazakhstan;

Confirmation of the possibilities of visual segregation and determination of the structural peculiarities of large arched uplifts (for example, the Astrakhan and Severo-Buzachinskiy arches in the Caspian region);

Discovery and fixing of dislocations with a break in continuity of defined rank within the limits of a given region;

Discovery of fragments of the ancient drainage system, for example, a regions prospective for finding placers;

Confirmation of individual local structures segregated on the basis of deciphering SP and which are favorable for planning oil and gas exploration.

Operative geological observations from space offer the possibility of tracing the processes of an elemental nature, for example, volcanic activity. Volcanoes are sharply distinguished among other mountain structures from orbit. The crew observed such large volcanoes as Aetna, Fujiama, Klyuchevskaya Sopka, ancient volcanic structures of the type of the Emi-Kusi caldera of the Central Sahara (Figure 2) and many others many times. The visual observation program of the crew included following the state of all the volcanoes of Kamchatka and the Kuril Islands. During the work period of the cosmonauts in orbit, no shows of volcanic activity were noted, which agrees with the ground data. At the same time eruptions of an explosive nature were recorded at Aetna and an entire series of volcanoes in Central and South America. Gas and ash plumes were noted at the volcanic peaks, gas flames were noted above the craters and traces of fresh discharges were seen at the feet of the volcanoes.

A significant role in the flight program was given to observations of the snow cover, mountain glaciers, and the ice situation at sea. A survey of these studies is presented in reference [10].

The geographic peculiarities of the natural environment and results of anthropogenic activity were periodically traced from on board the station. Hence we have

observations of the sharpness of the limits of propagation of vegetation, wind and sand flows, water percolation out of canals, atmospheric and sea water pollution, and fires. Especially serious forest fires were noted in Australia.

Studying wind and sand movements, the crew eatablished that the most favorable conditions for observing such phenomena exist when the sun is low above the horizon. The dimensions of wind and sand movements, their color and structure, the direction of transport of the dust were noted. The crew gave attention to the characteristic striated pattern of the landscape in the vicinity of Lake Eyre in Australia, in the southern part of Angola and near Lake Chad in Africa. This pattern was formed by alternating strips of stabilized sands, lakes and elongated solonchaks. Analogs of this pattern can be seen near the Volga River delta. The origin of such relief has still not been exactly established. Future orbital studies can provide data for solving this problem.

The cosmonauts observed the Nasca plateau in South American near the Pacific coast many times. No traces of so-called extraterrestrial civilization were detected from orbital altitude here. To counterbalance this, the cosmonauts saw the Pyramids quite clearly in the vicinity of Cairo.

Observing the ocean, the cosmonauts turned attention to the fact that as a rule, the currents are distinguished by color from the color of the water surface surrounding them. A series of color photographs obtained after short, approximately equal time intervals offer the possibility of estimating the space-time variability of the water masses. The ocean currents and eddies were observed by the crew in close connection with the meteorological situation. The cosmonauts noted the interrelation of the hydrographic map with clouds many times. This was especially clearly obvious at points of appearance of mesoscale eddies which serve as one of the basic mechanisms of heat transfer.

The experience in purposeful visual-instrument observations made by the cosmonauts in close contact with specialists in different earth sciences gave results which serve as the basis for statement of a broad complex of experiments to study the lithosphere, hydrosphere and atmosphere of our planet from space.

PHOTO CAPTION

1. p 12. The Emi-Kusi shield volcano in the Tibesti Mountains in the Central Sahara. The caldera with a white spot, the incrustations on the bottom of the crater where fumarole activity was manifested, is clearly distinguishable. In appearance, this volcanic structure is very similar to Mount Olympus on Mars, which indicates the possibility of using the materials from orbital observations for comparative planetology.

BIBLIOGRAPHY

1. Beregovoy, G. T., et al., ISSLEDOVANIYA PRIRODNOY SREDY S PILOTIRUYEMYKH ORBITAL'NYKH STANTSIY [Studies of the Natural Environment from Manned Orbital Stations], Leningrad, Gidrometeoizdat, 1972, 399 pages.

2. Desinov, L. V. and Kozlov, V. V., "Visual Observations of the Natural Environment from the 'Salyut-5' Orbital Station," PRIRODA [Nature], No 12, 1977, pp 56-61.

3. Koval', A. D. and Uspenskiy, G. R., KOSMOS - CHELOVEKU [Space for Man], Moscow, Mashinostroyeniye, 1974, p 200.

4. Nikolayev, A. G. and Popovich, P. R., "How Does the Earth Look from Outer Space?" PRIRODA, No 1, 1963, pp 1-4.

5. Rukavishnikov, N. N., "Role of the Cosmonaut in Scientific Experiments in Space," PRIRODA, No 10, 1977, pp 137-141.

6. Sevast'yanov, V. I., "Scientific and Technical Experiments on Board 'Soyuz-9'," VESTNIK AN SSSR [News of the USSR Academy of Sciences], No 11, 1970, pp 31-39.

7. Khrunov, Ye. V., Observations from Orbit," AVIATSIYA I KOSMONAVTIKA [Aviation and Cosmonautics], No 8, 1971, pp 38-39.

8. Kurdinovskiy, O. Yu., "A Program of Scientific Experiments to Study the Earth's Resources Using the 'Skylab' Manned Orbital Station," IZV. VUZOV. GEOLOGIYA I RAZVEDKA [News of the Institutions of Higher Learning. Geology and Exploration], No 2, 1974, pp 131-133.

9. El-Baz, F., "Astronaut Observation from the Apollo-Soyuz Mission," SMITHSONIAN STUD. AIR AND SPACE, Vol IX, No 1, 1977, p 400.

10. Desinov, L. V., Nosenko, G. A., Grechko, G. M., Ivanchenkov, A. S. and Kotlyakov, V. M., "Glaciological Studies and Experiments on Board the 'Salyut-6' Orbital Station," ISSLED. ZEMLI IZ KOSMOSA [Studies of the Earth from Space], No 1, 1980, pp 25-34.

10845
CSO: 1866/48

UDC 542.65:629.786.2

'KHALONG' TECHNOLOGICAL EXPERIMENT IN GROWING CRYSTALS OF SEMICONDUCTING COMPOUNDS AND 'IMITATOR' EXPERIMENT FOR MEASURING TEMPERATURE PROFILES OF 'KRISTALL' FURNACE ON 'SALYUT-6' ORBITAL STATION

Moscow KOSMICHESKIYE ISSLEDOVANIYA in Russian Vol 20, No 2, Mar-Apr 82 (manuscript received 24 Dec 81) pp 310-312

[Article by V.V. Gorbatko, A.A. Il'in, I.P. Kazakov, A.V. Korovin, L.I. Popov, V.V. Ryumin, S.P. Tikhomirova, V.M. Truzhenikov, M.B. Shcherbina-Samoylova, Nguyen Van Vyong, Nguyen Van Sung, Nguyen Tkhan' Ngi, Nguyen Khong Khuyen, Fam Tuan, Chan Suan Khoay, V. Aykhler, Kh. Zyusmann, Kh. Kvaas, R. Kul', Kh. Langer, S. Langkhammer and K. Shtekker]

[Text] Six technological experiments in growing crystals of semiconducting compounds in "Kristall" and "Splav-01" units and two "Imitator" experiments in measuring the temperature fields in a "Kristall" unit were developed and conducted in accordance with the "Khalog" and "Imitator" programs, with the participation of USSR and SRV [Socialist Republic of Vietnam] specialists ("Khalong-1, -4, -5, -6" experiments) and USSR, SRV and GDR specialists ("Khalong-2, -3" and "Imitator-1, -2").

1. The subject of the "Khalong-1, -2, -3" experiments was the production of semiconducting compounds, by the directed crystallization method, in a "Kristall" unit. The solid solution $Bi_2Te_{2.7}Se_{0.3}$ was investigated in "Khalong-1," the solid solution $BiSbTe_3$ in "Khalong-2" and the solid solution $Bi_{0.5}Sb_{1.5}Te_3$ in "Khalong-3." The "Khalong-4, -5" experiments were also conducted with the "Kristall" unit and concerned the growing of semiconducting GaP crystals from a melt bath by the moving solvent method (MDR) (the "Khalong-4" experiment) and the growing of GaP crystals alloyed with zinc and oxygen from a melt bath (by the MDR method). In the "Khalong-6" experiment, which was conducted with a "Splav-01" unit, PbTe and $Bi_2Te_{2.7}Se_{0.3}$ crystals, with an excess of tellurium, were grown in two separate ampules in a single capsule.

The "Imitator-1" experiment involved measuring the axial temperature fields of the "Kristall" furnace by the method of shaped, meltable wires with different melting temperatures, for given control panel modes. In the "Imitator-2" experiment, the "Kristall" furnace's temperature profiles were measured in both steady-state and dynamic modes, using 10 Ni-CrNi microthermocouples in a shell; the microthermocouples were firmly attached at different points in a simulating ampule place in a container. The thermoelectromotive forces were measured with the help of a special electronic digital voltmeter.

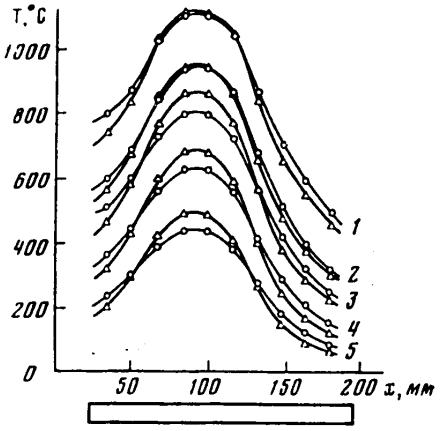

Figure 1. Steady-state axial temperature profiles of "Kristall" furnace obtained in "Imitator-2" experiment. The location of the container is indicated in the figure. The plunger is to the right. Circles = average values of two measurement cycles made on 28 July 1980; triangles = values obtained in experiment on 17 September 1980; the temperature, as set on the control panel, was: 1. 1,100°C; 2. 900°C; 3. 800°C; 4. 600°C; 5. 400°C.

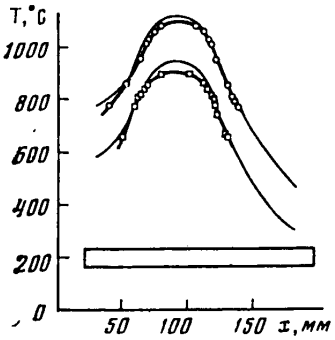

Figure 2. Steady-state temperature profiles of "Kristall" furnace obtained in "Imitator-2" (fine curve) and "Imitator-1" experiments for T_z = = 1,100°C (circles) and T_z = 900°C (squares). The location of the container is indicated in the figure. The plunger is to the right.

2. The purpose of the experiments in growing crystals of semiconducting compounds of GaP and PbTe and solid solutions of Bi_2Te_3-Bi_2Se_3 and Bi_2Te_3-Sb_2Te_3 under conditions of microgravitation was to study the process of crystallization of these binary and ternary semiconducting systems under space conditions and to determine the effect of the crystallization and the thermal-mass-transfer conditions on the growth kinetics, impurity segregation and physicochemical properties of the materials that were obtained.

3. The GaP and PbTe semiconducting compounds and the Bi_2Te_3-Bi_2Se_3 and Bi_2Te_3-Sb_2Te_3 solid solutions were selected on the basis of the following considerations:
a) these materials have been studied quite thoroughly on Earth and it is known that their many electrophysical properties are extremely structurally sensitive and depend on the growth conditions;
b) these materials are used extensively in electronics technology and instrument building, and the improvement of their properties would be of great practical value;
c) the technological parameters of the processes involved in growing these crystals correspond to the operating characteristics of the "Kristall" and "Splav-01" units.

4. All the experiments in the planned program were conducted, according to the staff cyclograms, in July-September 1980. As far as the technological ampules delivered from Earth were concerned, the cosmonauts discovered no mechanical damage and no unforeseen shifts in the locations of the crystals inside them, which indicates the suitability of the ampules' design and production process for similar types of experiments with substances that undergo a considerable increase in volume when melted.

Morphological investigations were conducted for all the samples that were obtained. The results of the "Imitator-1, -2" experiments have been processed. Figure 1

depicts the "Kristall" furnace's steady-state temperature profiles that were obtained during the "Imitator-2" experiment. In Figure 2, for the purpose of comparison, we show the average values of the steady-state temperature profiles obtained in the "Imitator-2" experiment and the values obtained in the "Imitator-1" experiment.

The structural and electrophysical properties of the materials that were obtained are being investigated at the present time. The results that have already been obtained enable us to reach some conclusions about the special features of the crystallization process in space and their effect on the quality of the crystals produced, as well as the feasibility of conducting further, analogous experiments in space.

11746
CSO: 1866/86

UDC 528:629.195

ORBITAL METHODS IN SPACE GEODESY

Moscow ORBITAL'NYYE METODY KOSMICHESKOY GEODEZII in Russian 1981 (signed to press 12 Aug 81) pp 2, 255-256

[Annotation and table of contents from monograph "Orbital Methods in Space Geodesy", by Mikhail Sergeyevich Urmayev, Izdatel'stvo "Nedra", 2250 copies, 256 pages]

[Text] Annotation. The monograph deals with the problems involved in the use of orbital methods in determining the coordinates of artificial earth satellite observation stations and also in the coordinate-time tie-in of the results of space surveys of the earth's surface. The monograph gives the reading systems, necessary information from the theory of motion of artificial earth satellites, methods for computing the matrices of isochronal derivatives and problems in the numerical integration of the differential equations of artificial earth satellite motion in application to space geodesy. The book is intended for scientific specialists and engineers in the field of geodesy, geophysics, practical astronomy and geology who in their activities must use orbital measurements for determining orbits and coordinates of stations. It was written with the intent of use as a study aid for students in advanced courses at geodetic colleges and universities studying space geodesy. Tables 11, figures 19, references 74.

Contents

5303
CSO: 1866/57

- END -